

สารยับยั้งแอลฟาไกลูโคซิเดสจากใบมะตูม *Aegle marmelos* และปอกระเจา *Corchorus olitorius*



นางสาวธัญชนก ปักษาสุข

สถาบันวิทยบริการ
วิทยานิพนธ์นี้เป็นส่วนหนึ่งของการศึกษาตามหลักสูตรปริญญาวิทยาศาสตรมหาบัณฑิต
จุฬาลงกรณ์มหาวิทยาลัย
สาขาวิชาเทคโนโลยีชีวภาพ

คณะวิทยาศาสตร์ จุฬาลงกรณ์มหาวิทยาลัย

ปีการศึกษา 2551

ลิขสิทธิ์ของจุฬาลงกรณ์มหาวิทยาลัย

**α -GLUCOSIDASE INHIBITORS FROM BAEI *Aegle marmelos* AND
JEW'S MALLOW *Corchorus olitorius* LEAVES**

Miss Thanchanok Puksasook

สถาบันวิทยบริการ

A Thesis Submitted in Partial Fulfillment of the Requirements
for the Degree of Master of Science Program in Biotechnology

Faculty of Science

Chulalongkorn University

Academic Year 2008

Copyright of Chulalongkorn University

Thesis Title **α -GLUCOSIDASE INHIBITORS FROM BAEL *Aegle marmelos* AND JEW'S MALLOW *Corchorus olitorius* LEAVES**


By Miss Thanchanok Puksasook

Field of Study Biotechnology


Advisor Assistant Professor Preecha Phuwapraisirisan, Ph.D.

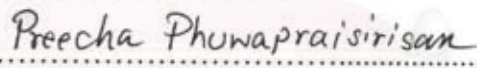
Co-Advisor Jongkolnee Jongaramruong, Ph.D.

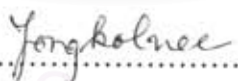
Accepted by the Faculty of Science, Chulalongkorn University in Partial Fulfillment of the Requirements for the Master's Degree

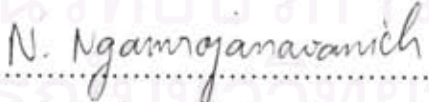

.....Dean of the Faculty of Science
(Professor Supot Hannongbua, Dr. rer. nat.)

THESIS COMMITTEE


.....Chairman
(Associate Professor Sirirat Kokpol, Ph.D.)


.....Advisor
(Assistant Professor Preecha Phuwapraisirisan, Ph.D.)


.....Co-Advisor
(Jongkolnee Jongaramruong, Ph.D.)


.....Examiner
(Associate Professor Nattaya Ngamrojanavanich, Ph.D.)


.....External Examiner
(Assistant Professor Wimolpun Rungprom, Ph.D.)

ธัญชนก ปักษาสุข : สารยับยั้งแอลฟาไกลูโคซิเดสจากใบมะตูม *Aegle marmelos* และ
 ปอกระเจา *Corchorus olitorius*. (α -GLUCOSIDASE INHIBITORS FROM BAE
Aegle marmelos AND JEW'S MALLOW *Corchorus olitorius* LEAVES) อ. ที่ปรึกษา
 วิทยานิพนธ์หลัก: ผศ. ดร.ปรีชา ภูวไพโรศิรศาล, อ. ที่ปรึกษาวิทยานิพนธ์ร่วม:
 อ. ดร. จงกลณี จงอร่ามเรือง, 93 หน้า

การค้นพบสารยับยั้งเอนไซม์ α -glucosidase จะสามารถนำไปสู่การพัฒนาการรักษา
 โรคเบาหวานชนิดที่ 2 ได้ เราจึงพยายามค้นหาสารยับยั้งเอนไซม์ α -glucosidase จากพืช
 สมุนไพรไทย ในงานวิจัยนี้ได้เลือกศึกษาใบมะตูมและใบปอกระเจาโดยการทดสอบฤทธิ์ทาง
 ชีวภาพนำไปสู่การแยกสารบริสุทธิ์ที่มีฤทธิ์ยับยั้งเอนไซม์ α -glucosidase การแยกส่วนสกัดได
 คลอโรมีเทนและส่วนสกัดเมทานอลจากใบมะตูมได้สารฟีนิลเอทิลซินนามายด์ใหม่ 3 ชนิด คือ
 anhydromarmeline (1), aegelinosides A (7) และ aegelinosides B (8) รวมทั้งสารฟีนิลเอทิล
 ซินนามายด์ที่มีรายงานแล้ว 8 ชนิด คือ anhydroaegeline (2), (-)-tembamide (3)
 dehydroaegeline (4), (-)-aegeline (5), (-)-O-methylether aegeline (6), alangionosides L
 (9), N-2-ethoxy-2-(4-methoxyphenyl)ethyl-cinnamide (10) และ N-(2-(4-hydroxyphenyl)
 ethyl)-cinnamide (11) และอีก 4 ชนิดเป็นสารในกลุ่มฟลาโวนอยด์ไกลโคไซด์ (12-15) ที่มี
 รายงานมาแล้ว เมื่อนำสารทั้งหมดที่แยกได้จากใบมะตูมมาทดสอบฤทธิ์ยับยั้งเอนไซม์ α -
 glucosidase พบว่าสารหลักที่ออกฤทธิ์ยับยั้งเอนไซม์ α -glucosidase ได้สูงสุดคือ สาร 14 และ
 15 ที่ IC_{50} เท่ากับ 0.34 และ 0.46 mM ตามลำดับ นอกจากนี้มีสารฟลาโวนอยด์ไกลโคไซด์ใหม่ 2
 ชนิด คือ corchoruside A (16) และ corchoruside B (17) รวมทั้งสารประเภทไตรเทอร์พีนอยด์
 ไกลโคไซด์ที่มีรายงานแล้ว 1 ชนิด คือ capsugenin-25,30-O- β -diglucopyranoside (18) แยกได้
 จากส่วนสกัดเมทานอลของใบปอกระเจา corchoruside A (16) ออกฤทธิ์ยับยั้งเอนไซม์ α -
 glucosidase สูงสุดที่ IC_{50} เท่ากับ 0.18 mM

สาขาวิชา... เทคโนโลยีชีวภาพ.....ลายมือชื่อนิสิต.....ธัญชนก ปักษาสุข.....
 ปีการศึกษา.....2551.....ลายมือชื่ออ.ที่ปรึกษาวิทยานิพนธ์หลัก.....ปรีชา ภูวไพโรศิรศาล
 ลายมือชื่ออ.ที่ปรึกษาวิทยานิพนธ์ร่วม.....จงกลณี

##4972323523: MAJOR BIOTECHNOLOGY

KEYWORDS: α -GLUCOSIDASE INHIBITORS / *Aegle marmelos* / *Corchorus olitorius* / DIABETES

THANCHANOK PUKSASOOK: α -GLUCOSIDASE INHIBITORS FROM BAELE *Aegle marmelos* AND JEW'S MALLOW *Corchorus olitorius* LEAVES. ADVISOR: ASST. PROF. PREECHA PHUWAPRAISIRISAN, Ph.D., CO-ADVISOR: JONGKOLNEE JONGARAMRUONG, Ph.D., 93 pp.

Discovery of α -glucosidase inhibitors has been actively pursued with the aim of developing therapeutics for the treatment of type 2 diabetes. We have examined the inhibitory effect of Thai medicinal plants against α -glucosidase. The leaves of *Aegle marmelos* and *Corchorus olitorius* were selected for this investigation. Bioassay-guided fractionation led to the isolation of active principles. The isolation of dichloromethane and methanol crude extracts from leaves of *Aegle marmelos* afford three novel phenylethyl cinnamides named anhydromarmeline (**1**), aegelinosides A (**7**) and B (**8**) along with eight known compounds, anhydroaegeline (**2**), (-)-tembamide (**3**) dehydroaegeline (**4**), (-)-aegeline (**5**), (-)-*O*-methylether aegeline (**6**), alangionosides L (**9**), *N*-2-ethoxy-2-(4-methoxyphenyl)ethyl-cinnamide (**10**) and *N*-(2-(4-hydroxyphenyl) ethyl)-cinnamide (**11**) as well as four known flavonoid glycosides (**12-15**). All the isolated compounds from this plant were tested for inhibitory activity against α -glucosidase. The most active principles against α -glucosidase were **14** (IC₅₀ 0.34 mM) and **15** (IC₅₀ 0.46 mM). In addition, two new flavonoid glycosides named corchorosides A (**16**) and B (**17**) together with a known triterpenoid glycoside named capsugenin-25,30-*O*- β -diglucoopyranoside (**18**) were isolated from methanolic extract of *Corchorus olitorius* leaves. Corchorosides A (**16**) showed the most inhibitory effect with IC₅₀ value of 0.18 mM.

Field of Study:.....Biotechnology..... Student's Signature:.....Thanchanok P.....
 Academic Year:.....2008..... Advisor's Signature:.....Preecha.....
 Co-advisor's Signature:.....Jongkolnee.....

ACKNOWLEDGEMENTS

I would like to express my deepest appreciation to my advisor, Assistant Professor Preecha Phuwapraisirisan and co-advisor, Dr. Jongkolnee Jongaramruong for the advice, encouragement and supporting at all time of this research.

I would like to gratefully acknowledge the members of the thesis committees, Associate Professor Sirirat Kokpol, Associate Professor Nattaya Ngamrojanavanich and Assistant Professor Wimolpun Rungprom for discussion, guidance and extending cooperation over my presentation.

I would like to express my gratitude to Natural Products Research Unit, Department of Chemistry, Faculty of Science, Chulalongkorn University for supporting of chemicals and laboratory facilities throughout the course of study and Program of Biotechnology, Faculty of Science, Chulalongkorn University for giving me a chance to study here.

I would also like to express my appreciation to my family and Assistant Professor Malee Srisotsuk for their great support and encouragement throughout the course of my education and I special thank to Ms. Kamjira Saisin and Ms. Chalouyluk Phoopichayanun for their technical assistance. Furthermore, all of my friends in the laboratory for their friendships and help during the course of my graduate research.

Finally, I would like to thank 90th Anniversary of Chulalongkorn University Fund and TRF-Master (MAG Window II) Research Grants of Thailand Research Fund for the financial supports.

สถาบันวิทยบริการ
จุฬาลงกรณ์มหาวิทยาลัย

CONTENTS

	Page
ABSTRACT (IN THAI).....	iv
ABSTRACT (IN ENGLISH).....	v
ACKNOWLEDGEMENTS.....	vi
CONTENTS.....	vii
LIST OF TABLES.....	x
LIST OF FIGURES.....	xi
LIST OF SCHEMES.....	xiv
LIST OF ABBREVIATIONS.....	xv
CHAPTER	
I INTRODUCTION.....	1
II PHENYLETHYL CINNAMIDES: A NEW SERIES OF	
α-GLUCOSIDASE INHIBITOR FROM THE LEAVES OF	
<i>Aegle marmelos</i>	15
2.1 Introduction.....	15
2.1.1 Botanical aspect and distribution of <i>Aegle marmelos</i>	15
2.1.2 Phytochemical and pharmacological investigation of <i>Aegle</i>	
<i>Marmelos</i>	16
2.2 Results and discussion.....	19
2.2.1 Isolation	19
2.2.2 Structure elucidation of Anhydromarmeline (1).....	22
2.2.3 Structure elucidation of Aegelinoside A and B (7-8).....	23
2.2.4 α -Glucosidase inhibitory activity of the isolated compounds..	27
2.3 Experiment section.....	29
2.3.1 General experimental procedures	29
2.3.2 Plant material.....	29
2.3.3 Extraction and isolation	29
2.3.4 α -Glucosidase inhibitory assay	32

	Page
III FLAVONOID GLYCOSIDES: α-GLUCOSIDASE INHIBITORS	
FROM THE LEAVES OF <i>Aegle marmelos</i>.....	44
3.1 Introduction.....	44
3.2 Results and discussion.....	44
3.2.1 Structure elucidation of kaempferol-3- <i>O</i> -(6''- <i>O</i> - α -rhamosyl) - β -glucoside (12).....	47
3.2.2 Structure elucidation of kaempferol-3,7- <i>O</i> - α - dirhamnopyranoside (13).....	48
3.2.3 Structure elucidation of quercetin-3- <i>O</i> -(6''- <i>O</i> - α -rhamosyl) - β -glucoside (14).....	49
3.2.4 Structure elucidation of quercetin 3,7- <i>O</i> - α - dirhamnopyranoside (15).....	50
3.2.5 α -Glucosidase inhibitory activity of the isolated compounds	51
3.3 Experiment section.....	53
3.3.1 General experimental procedures	53
3.3.2 Plant material.....	53
3.3.3 Extraction and isolation	53
3.3.4 α -Glucosidase inhibitory assay	55
IV CORCHORUSIDES A AND B, TWO NEW α-GLUCOSIDASE	
INHIBITORS FROM THE LEAVES OF <i>Corchorus olitorius</i>.....	56
4.1 Introduction.....	56
4.1.1 Botanical aspect and distribution of <i>Corchorus olitorius</i>	56
4.1.2 Phytochemical and pharmacological investigation of <i>Corchorus olitorius</i>	57
4.2 Results and discussion.....	60
4.2.1 Isolation	60
4.2.2 Structure elucidation of Corchoruside A (1).....	63
4.2.3 Structure elucidation of Corchoruside B (2).....	66
4.2.4 α -Glucosidase inhibitory activity of the isolated compounds..	68
4.3 Experiment section.....	69

	Page
4.3.1 General experimental procedures	69
4.6.2 Plant material.....	69
4.6.3 Extraction and isolation	70
4.6.4 α -Glucosidase inhibitor assay	72
V CONCLUSION	83
REFERENCES	88
VITA	93



สถาบันวิทยบริการ
จุฬาลงกรณ์มหาวิทยาลัย

LIST OF TABLES

Table	Page
1.1 Criteria for the Diagnosis of Diabetes Mellitus and Impaired Glucose Homeostasis.....	5
2.1 Chemical constituents of <i>Aegle marmelos</i>	17
2.2 ¹ H, ¹³ C and HMBC NMR data of Anhydromarmeline (1) in CDCl ₃	23
2.3 ¹ H and ¹³ C NMR data for aegelinosides A (7 , CD ₃ OD) and B (8 , acetone- <i>d</i> ₆)...	25
2.4 α-Glucosidase inhibitory effect of isolated compounds from <i>Aegle marmelos</i> leaves.....	27
3.1 α-Glucosidase inhibitory effect of flavonoid glycosides (12-15).....	51
4.1 NMR data of corchoruside A (1 , CD ₃ OD) and corchoruside A nonacetate (1a , CDCl ₃).....	65
4.2 ¹ H, ¹³ C and HMBC NMR data of corchoruside B (2) in CDCl ₃	67
4.3 α-Glucosidase inhibitory effect of isolated compounds from <i>Corchorus olitorius</i> leaves.....	68

LIST OF FIGURES

Figure	Page
1.1 Estimated cases of diabetes (millions) in 13 countries in 2000 and projected to 2030.....	1
1.2 Estimated prevalence of diabetes (thousand) in different segment of Thailand in 2004.....	2
1.3 Metabolism of glucose regulation into bloodstream in type I and II diabetes....	2
1.4 Pathophysiology of hyperglycaemia and increased circulating fatty acids in type 2 diabetes.....	3
1.5 Insulin signal transduction pathways.....	6
1.6 Metabolic changes during the development of type 2 diabetes.....	8
1.7 In normal digestion, pancreatic α -amylase hydrolyzes complex starches into oligosaccharides, which are further hydrolyzed by α -glucosidase located in the intestinal brush border to glucose and other monosaccharides, which are then absorbed.....	10
1.8 Acarbose competitively inhibits the enzymatic hydrolysis of oligosaccharide by α -glucosidase in the small intestine.....	11
2.1 <i>Aegle marmelos</i>	15
2.2 Triterpenoids from <i>Aegle marmelos</i>	17
2.3 Coumarins from <i>Aegle marmelos</i>	18
2.4 Alkaloids from <i>Aegle marmelos</i>	18
2.5 The chemical structures of isolated compounds from <i>Aegle marmelos</i> leaves.	21
2.6 Selected HMBC correlations of 1	22
2.7 Selected HMBC correlations of 7	24
2.8 Partial ^1H NMR spectra of aglycones 5 (top) and 8a (bottom) obtained from hydrolysis of 7 and 8 , respectively.....	26
2.9 Hydrolysis of <i>p</i> -nitrophenyl- α -D-glucopyranoside by α -glucosidase.....	32
3.1 The chemical structures of flavonoid glycoside from <i>Aegle marmelos</i> leaves.	46
3.2 Key HMBC correlations of 12	47

Figure	Page
3.3 Key HMBC correlations of 13	48
3.4 Key HMBC correlations of 14	49
3.5 Key HMBC correlations of 15	50
4.1 <i>Corchorus olitorius</i>	56
4.2 Cardenolide glycosides from the seeds of <i>Corchorus olitorius</i>	57
4.3 Flavonoid glycosides and cinnamic acid derivatives from the leaves of <i>Corchorus olitorius</i>	58
4.4 Ursane triterpenes from the roots of <i>Corchorus olitorius</i>	58
4.5 The chemical structures of isolated compounds from <i>Corchorus olitorius</i> leaves.....	62
4.6 Selected HMBC correlations of 1	63
4.7 Selected HMBC correlations of 2	66
5.1 The chemical structures of compounds isolated from <i>Aegle marmelos</i> leaves.....	85
5.2 The chemical structures of compounds isolated from <i>Corchorus olitorius</i> leaves.....	86
S-2.1 The ¹ H NMR (CDCl ₃) spectrum of anhydromarmeline (1).....	35
S-2.2 The ¹³ C NMR (CDCl ₃) spectrum of anhydromarmeline (1).....	35
S-2.3 The COSY (CDCl ₃) spectrum of anhydromarmeline (1).....	36
S-2.4 The HSQC (CDCl ₃) spectrum of anhydromarmeline (1).....	36
S-2.5 The HMBC (CDCl ₃) spectrum of anhydromarmeline (1).....	37
S-2.6 Mass spectrum of anhydromarmeline (1).....	37
S-2.7 The ¹ H NMR (CD ₃ OD) spectrum of aegelinosides A (7).....	38
S-2.8 The ¹³ C NMR (CDCl ₃) spectrum of aegelinosides A (7).....	38
S-2.9 The COSY (CD ₃ OD) spectrum of aegelinosides A (7).....	39
S-2.10 The HSQC (CD ₃ OD) spectrum of aegelinosides A (7).....	39
S-2.11 The HMBC (CD ₃ OD) spectrum of aegelinosides A (7).....	40
S-2.12 Mass spectrum of aegelinosides A (7).....	40
S-2.13 The ¹ H NMR (acetone- <i>d</i> ₆) spectrum of aegelinosides B (8).....	41
S-2.14 The ¹³ C NMR (acetone- <i>d</i> ₆) spectrum of aegelinosides B (8).....	41

Figure	Page
S-2.15 The COSY (acetone- <i>d</i> ₆) spectrum of aegelinosides B (8).....	42
S-2.16 The HSQC (acetone- <i>d</i> ₆) spectrum of aegelinosides B (8).....	42
S-2.17 The HMBC (acetone- <i>d</i> ₆) spectrum of aegelinosides B (8).....	43
S-2.18 Mass spectrum of aegelinosides B (8).....	43
S-4.1 The ¹ H NMR (CD ₃ OD) spectrum of corchoruside A (1).....	74
S-4.2 The ¹³ C NMR (CDCl ₃) spectrum of corchoruside A (1).....	74
S-4.3 The COSY (CDCl ₃) spectrum of corchoruside A (1).....	75
S-4.4 The HSQC (CDCl ₃) spectrum of corchoruside A (1).....	75
S-4.5 The HMBC (CDCl ₃) spectrum of corchoruside A (1).....	76
S-4.6 Mass spectrum of corchoruside A (1).....	76
S-4.7 The ¹ H NMR (pyridine- <i>d</i> ₄) spectrum of corchoruside B (2).....	77
S-4.8 The ¹³ C NMR (pyridine- <i>d</i> ₄) spectrum of corchoruside B (2).....	77
S-4.9 The COSY (pyridine- <i>d</i> ₄) spectrum of corchoruside B (2).....	78
S-4.10 The HSQC (pyridine- <i>d</i> ₄) spectrum of corchoruside B (2).....	78
S-4.11 The HMBC (pyridine- <i>d</i> ₄) spectrum of corchoruside B (2).....	79
S-4.12 Mass spectrum of corchoruside B (2).....	79
S-4.13 The ¹ H NMR (CDCl ₃) spectrum of corchoruside A nonaacetate (1a).....	80
S-4.14 The ¹³ C NMR (CDCl ₃) spectrum of corchoruside A nonaacetate (1a).....	80
S-4.15 The COSY (CDCl ₃) spectrum of corchoruside A nonaacetate (1a).....	81
S-4.16 The HSQC (CDCl ₃) spectrum of corchoruside A nonaacetate (1a).....	81
S-4.17 The HMBC (CDCl ₃) spectrum of corchoruside A nonaacetate (1a).....	82
S-4.18 Mass spectrum of corchoruside A nonaacetate (1a).....	82

LIST OF SCHEMES

Schemes	Page
2.1 Isolation procedure of <i>Aegle marmalos</i> leaves.....	20
3.1 Isolation procedure of flavonoid glycosides from <i>Aegle marmalos</i> leaves.....	45
4.1 Isolation procedure of <i>Corchorus olitorius</i> leaves.....	61



สถาบันวิทยบริการ
จุฬาลงกรณ์มหาวิทยาลัย

LIST OF ABBREVIATIONS

Acetyl CoA	Acetyl coenzyme A
acetone- d_6	Deuterated acetone
brs	Broad singlet (NMR)
brd	Broad doublet (NMR)
^{13}C NMR	Carbon-13 nuclear magnetic resonance
DM	Diabetes mellitus
DMSO	Dimethyl sulfoxide
DMSO- d_6	Deuterated dimethyl sulfoxide
CDCl_3	Deuterated chloroform
CD_3OD	Deuterated methanol
COSY	Correlated spectroscopy
calcd	Calculated
2D NMR	Two dimensional nuclear magnetic resonance
d	Doublet (NMR)
dd	Doublet of doublet (NMR)
dL	Deciliter (s)
FPG	Fasting plasma glucose
GFP	Green fluorescent protein
Glut4	glucose transporter 4
^1H NMR	Proton nuclear magnetic resonance
HSQC	Heteronuclear single quantum correlation
HMBC	Heteronuclear multiple bond correlation experiment
HPLC	High performance liquid chromatography
Hz	Hertz
HRESIMS	High resolution electrospray ionization mass spectrum
h	Hour
2hrPPG	Two-hour postprandial glucose
IC_{50}	Concentration that required for 50% inhibition in <i>vitro</i>
IDDM	Insulin-dependent diabetes mellitus
IRS	Insulin-receptor substrates
J	Coupling constant

L	Liter (s)
M	Molar
MAP kinase	Mitogen-activated protein kinase
MeOH	Methanol
Mg	Milligram (s)
m	Multiplet (NMR)
mL	Milliliter (s)
m/z	Mass per charge
Na_2CO_3	Sodium carbonate
NIDDM	Non-insulin-dependent diabetes mellitus
NMR	Nuclear magnetic resonance
PEPCK	Phosphoenolpyruvate carboxykinase
PI (3) kinase	Phosphatidylinositol 3-kinase
PPAR	Peroxisome proliferator-activated receptor
pNPG	<i>p</i> -nitrophenyl α -D-glucoopyranoside
pyridine- d_5	Deuterated pyridine
STZ	streptozotocin
UV	Ultraviolet
U	Unit
VCC	Vacuum column chromatography
δ	Chemical shift
δ_{C}	Chemical shift of carbon
δ_{H}	Chemical shift of proton
λ_{max}	Maximum wavelength
μL	Microliter (s)
ε	Molar extinction coefficient
$[\alpha]_{\text{D}}$	Specific optical rotation

CHAPTER I

Introduction

Diabetes mellitus (DM) is a common metabolic disease characterized by elevated blood glucose levels, resulting from absent or inadequate pancreatic insulin secretion with or without concurrent impairment of insulin action. DM is currently out of the most costly and burdensome chronic diseases and is a condition that is increasing in epidemic proportions throughout the world. According to the World Health Organization (WHO, 2006), the prevalence of the disease will grow from 171 million in 2000 to 366 million people affected in 2030, which amount to an increase of 144% over the next 30 years (Figure 1.1). Deaths related to diabetes are estimated at about of global mortality. Overall direct health care cost of diabetes range from 2.5 to 15% of annual health care budgets, depending on local diabetes prevalence and treatments available (WHO, 2006). Thailand is inevitably moving towards the burden of such a public health problem. According to the cross country survey in the InterAsia study, the prevalence of diabetes in Thailand was 5% of 60 millions Thai people and the number of diabetic patient is expected to be double during in the next 10 years (Figure 1.2).

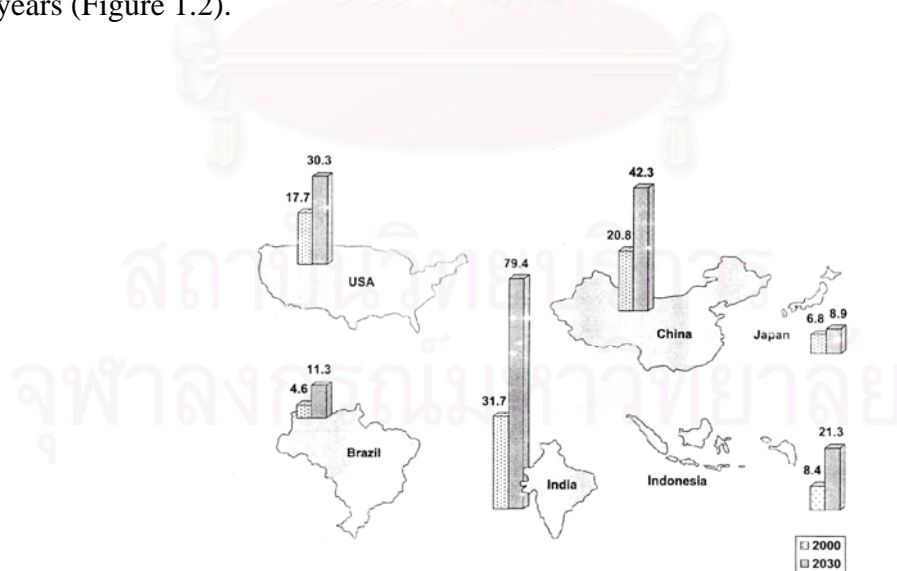


Figure 1.1 Estimated cases of diabetes (millions) in 13 countries in 2000 and projected to 2030 (Wild *et al.*, 2004).

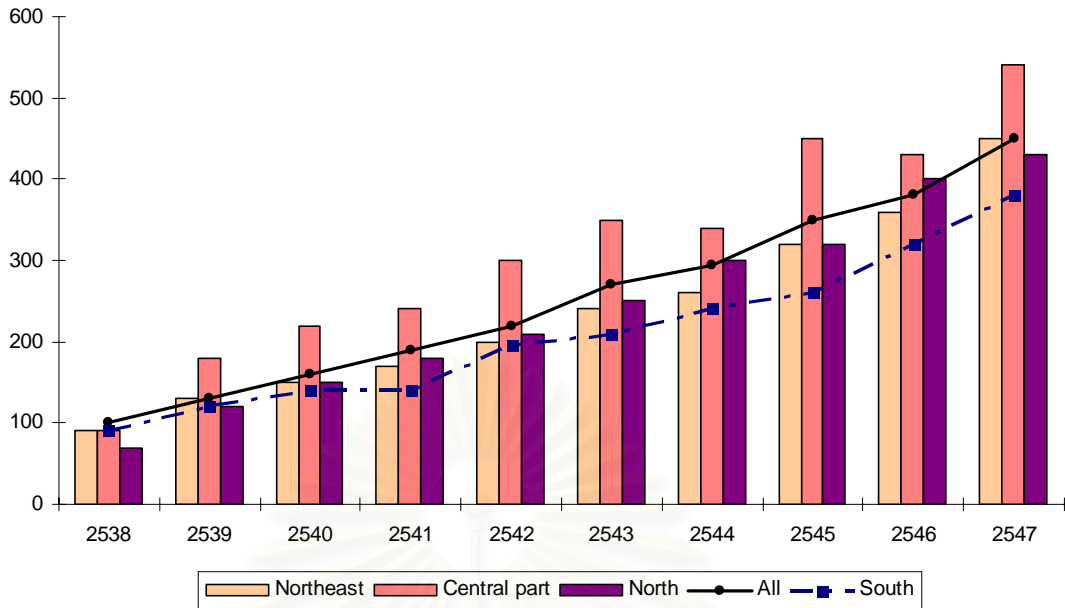


Figure 1.2 Estimated prevalence of diabetes (thousand) in different segment of Thailand in 2004.

1.1 Classifications, causes and complication of diabetes mellitus

Two types of diabetes mellitus (DM) are currently known; type 1 or insulin-dependent diabetes mellitus (IDDM) and type 2 or non-insulin-dependent diabetes mellitus (NIDDM) (Figure 1.3).

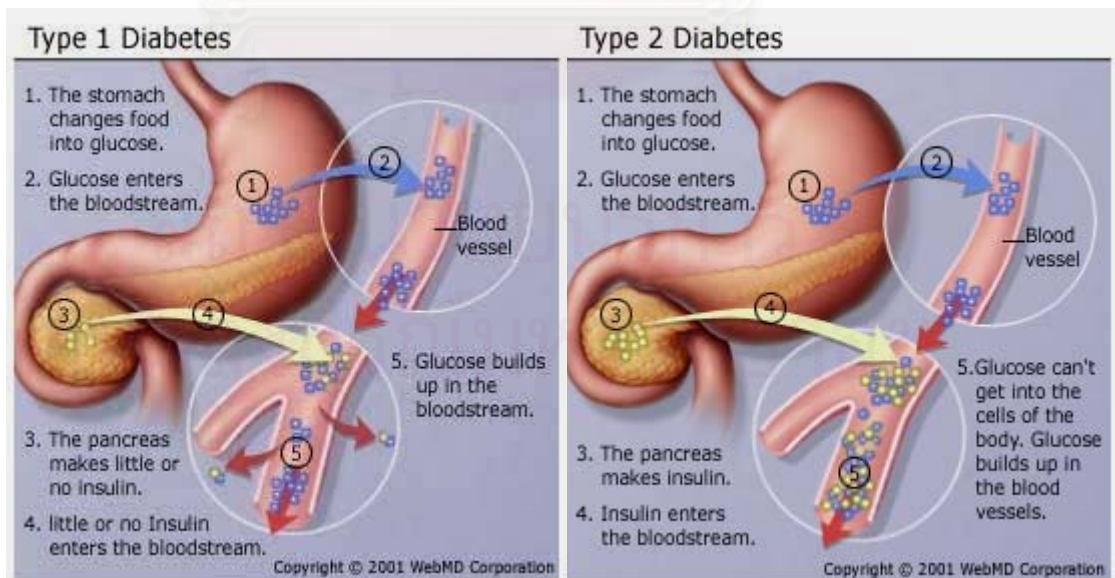


Figure 1.3 Regulation of glucose enters bloodstream in type 1 and 2 diabetes

Type 1 diabetes develops if the body is unable to produce any insulin. The metabolism of glucose regulation enters bloodstream in this type as show in Figure 1.3. Type 1 diabetes usually appears before the age of 40. This type of diabetes is the least common of the two main types and accounts for between 5 – 15% of all people with diabetes. Type 1 diabetes has been postulated that environmental factors such as certain viral infections and possibly chemical or nutritional agents may worsen these genetic factors.

Type 2 diabetes develops when the body can still secret some insulin, but not enough, or when the insulin that is produced does not work properly (known as insulin resistance) as show in Figure 1.3. Insulin secretion from the pancreas normally reduces glucose output by the liver, enhances glucose uptake by skeletal muscle, and suppresses fatty acid release from fat tissue. The various factors shown that contribute to the pathogenesis of type 2 diabetes affect both insulin secretion and insulin action. Decreased insulin secretion will reduce insulin signalling in its target tissues. Insulin resistance pathways affect the action of insulin in each of the major target tissues, leading to increased circulating fatty acids and the hyperglycaemia of diabetes. In turn, the raised concentrations of glucose and fatty acids in the bloodstream will feed back to worsen both insulin secretion and insulin resistance (Figure 1.4).

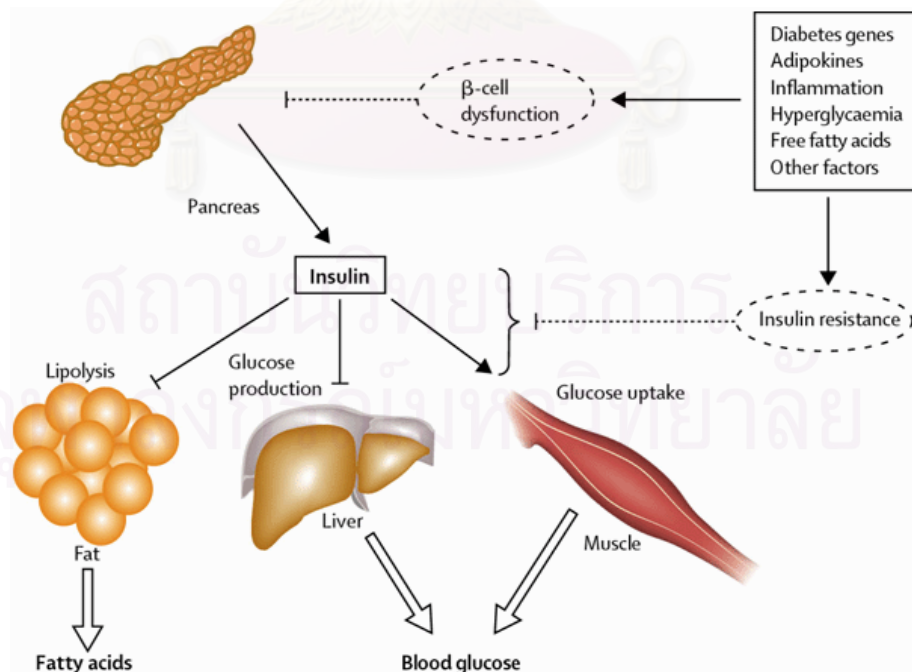


Figure 1.4 Pathophysiology of hyperglycaemia and increased circulating fatty acids in type 2 diabetes.

Type 2 diabetes is the most common type of diabetes, accounting for 90 to 95 percent of all diabetes. It usually develops after the age of 40. However, in the late 1990's, its incidence increased among young people. Experts are trying to determine why that is happening. It may be related to the increased incidence of obesity and sedentary lifestyles among young people. There are currently over 3 million people with diabetes in Thailand and there are more than half a million people with diabetes who have the condition and do not know it. About 80 percent of those with type 2 diabetes are overweight. It is more common among people who are older, sedentary or obese, or have a family history of the disease. It may reappear in women who had **gestational diabetes**. It is more common among people of Asian, Hispanic, African or Native American ancestry.

Type 2 diabetes is a progressive disease that can cause significant, severe complications such as heart disease, kidney disease, blindness and loss of limbs through amputation. Treatment differs at various stages of the condition. In its early stages, many people with type 2 diabetes can control their blood glucose levels by losing weight, eating properly and exercising. Many may subsequently need oral medication, and some people with type 2 diabetes may eventually need insulin shots to control their diabetes and avoid the disease's serious complications. Even though there is no cure for diabetes, proper treatment and glucose control enable people with type 2 diabetes to have normal and productive lives.

A major advance for people at risk of developing type 2 diabetes - such as family members of those with the condition - occurred recently when it was shown that diet and exercise can prevent or delay type 2 diabetes. People at high risk, who already had early signs of impaired glucose tolerance, significantly reduced their risk by losing only 5-7 percent of their body weight and performing moderate physical activity for 30 minutes/day.

1.2 Diagnostic criteria for diabetes mellitus

The diagnostic criteria for diabetes mellitus have been greatly simplified (Table 1.1). A normal fasting plasma glucose level is less than 110 mg/dL (6.1 mmol/L) and normal 2hrPPG levels are less than 140 mg/dL (7.75 mmol/L). Blood glucose levels above the normal level but below the criterion established for diabetes mellitus indicate impaired glucose homeostasis. Persons with fasting plasma glucose levels ranging from 110 to 126 mg/dL (6.1 to 7.0 mmol/L) are said to have impaired fasting glucose, while those with a 2hrPPG level between 140 mg/dL (7.75 mmol/L) and 200 mg/dL (11.1 mmol/L) are said to have impaired glucose tolerance. Both impaired fasting glucose and impaired glucose tolerance are associated with an increased risk of developing type 2 diabetes mellitus. Lifestyle changes, such as weight loss and exercise, are warranted in these patients.

Table 1.1 Criteria for the Diagnosis of Diabetes Mellitus and Impaired Glucose Homeostasis

Diabetes mellitus (DM) positive findings from any two of the following tests on different days:

DM with plasma glucose concentration ≥ 200 mg/dL (11.1 mmol/L)

or

FPG ≥ 126 mg/dL (7.0 mmol/L)

or

2hrPPG ≥ 200 mg/dL (11.1 mmol/L) after a 75 g glucose load

Impaired glucose homeostasis

Impaired fasting glucose: FPG from 110 to <126 mg/dL (6.1 to 7.0 mmol/L)

Impaired glucose tolerance: 2hrPPG from 140 to <200 mg/dL (7.75 to <11.1 mmol/L)

Normal

FPG <110 mg/dL (6.1 mmol/L)

2hrPPG <140 mg/dL (7.75 mmol/L)

FPG=fasting plasma glucose; 2hrPPG=two-hour postprandial glucose.

1.3 Metabolism of type 2 diabetes

Type 2 diabetes is largely a disease of misregulated glucose and lipid metabolism. Most cells in the body have insulin receptors in their plasma membrane. Normally an increase in blood insulin (which occurs within moments of consuming a carbohydrate-containing meal) results in an increased number of insulin receptors bound to insulin. This binding event activates the tyrosine kinase domain of the

receptor. The activated kinase domain phosphorylates itself and several other proteins called insulin-receptor substrates (IRS proteins). This creates a scaffold of bound proteins that results in the activation of other kinases (PI(3) kinase and Akt, and MAP kinase).

When the peptide hormone insulin binds to the insulin receptor, the intracellular tyrosine kinase domain of the receptor is activated. It phosphorylates tyrosines on itself and several other proteins that results in the activation of at least two separate signaling pathways. These signaling pathways change cellular metabolism and gene expression (Figure 1.5).

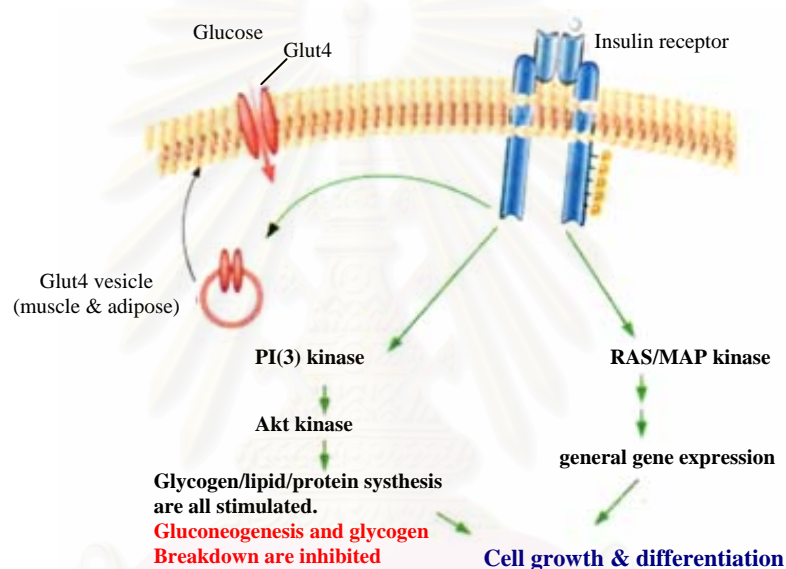


Figure 1.5 Insulin signal transduction pathways.

The results of these activated signaling pathways depend on the cell type:

1. In muscle and adipose cells, vesicles containing the insulin-regulated glucose transporter (Glut4) fuse with the plasma membrane, allowing these cells to take up more glucose from the blood.
2. In adipose, hormone-sensitive lipase is inhibited by insulin, preventing the release of fatty acids (making glucose the preferred energy source after a carbohydrate meal).
3. In both adipose and liver, enzymes involved in fatty acid synthesis (citrate lyase, acetyl CoA carboxylase and fatty acid synthase) are activated at the level of transcription and/or post-translational modification (phosphorylation).

4. Specifically in the liver, the key gluconeogenic enzymes (PEPCK, fructose 1,6 biphosphatase, and glucose 6-phosphatase) are down-regulated transcriptionally, and for some, allosterically. Glycogen synthesis and glycolysis are also stimulated in the liver by insulin.

Adipocytes were transfected with a vector expressing a fusion of Glut4 and green fluorescent protein (GFP). When insulin is added to the media containing the cells, the Glut4-GFP rapidly moves to the cell surface (single cells are shown). When insulin is removed from the media, the Glut4-GFP is endocytosed back into the cell. Before a person develops type 2 diabetes, their tissues become insulin resistant. This means that at a given level of blood insulin, there is a diminished effect on cellular metabolism (in muscles, fat, liver and probably other tissues). Since a “normal” level of blood insulin reduces blood glucose to <100 mg/dL when there is no insulin resistance, the β cells of the pancreas in people with insulin resistance secrete increased amounts of insulin to bring blood glucose down to normal levels. At these unusually high levels of blood insulin, the insulin-resistant cells can respond near normally to the insulin signal. This concept can be illustrated by a person who has suffered partial hearing loss; he will need to turn up his stereo or Ipod in order to hear as much of the music as someone with perfect hearing. What causes insulin resistance is not clear, although there is strong evidence that high concentrations of free fatty acids within cells may block portions of the signaling pathway. A common variant of the PPAR- γ gene may also contribute.

Insulin resistance becomes type 2 diabetes if and when the pancreatic β cells can no longer continue to produce the high concentrations of insulin necessary to overcome the insulin resistance. When this happens, glucose and fat metabolism are no longer properly regulated: (1) Insufficient amounts of the Glut4 glucose transporter are shuttled to the plasma membrane in muscles and adipose. (2) Liver gluconeogenesis is not appropriately inhibited; the liver synthesizes and secretes glucose even when blood glucose is already high. (3) The blood concentration of triacylglycerols, free fatty acids, and LDLs rises due to misregulation of lipoprotein and hormone-sensitive lipases.

Insulin resistance of target tissues is the first step (A→B) (Figure 1.6). Normal blood glucose (as indicated by the curved line) is maintained since insulin secretion is increased. As insulin resistance worsens and/or β cells secrete less insulin, the patient develops impaired glucose tolerance or pre-diabetes (defined as fasting blood glucose of 101-125 mg/dL) (B→C). As tissues become even more insulin resistant and β cells produce even smaller levels of insulin, the patient develops type 2 diabetes mellitus (C→D).

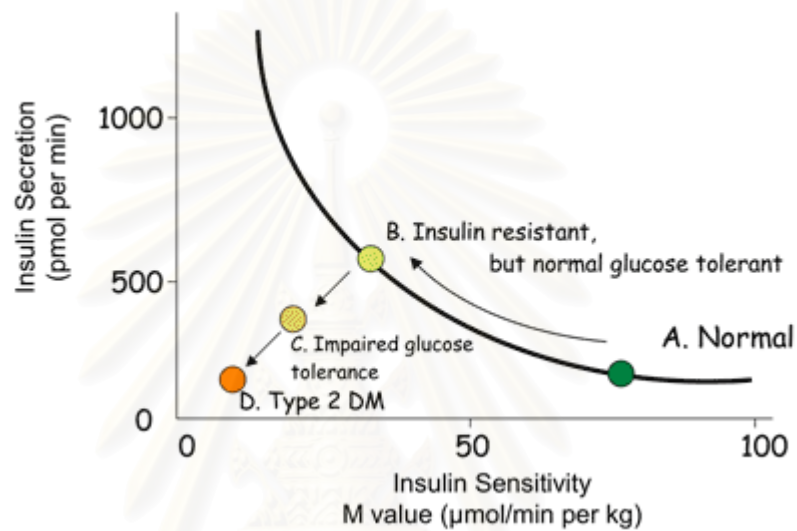


Figure 1.6 Metabolic changes during the development of type 2 diabetes.

1.4 Oral antidiabetic drugs

Oral diabetes medications help control blood glucose levels in people whose bodies still produce some insulin (the majority of people with type 2 diabetes). These diabetes medicines are usually prescribed to people with type 2 diabetes along with recommendations for making specific dietary changes and getting regular exercise. Several of these diabetes pills are often used in combination to achieve optimal blood glucose control. Remember that people with type 2 diabetes tend to have two problems that lead to increased glucose in the bloodstream: (1). They do not make enough insulin to move glucose into cells where it belongs. (2). The body's cells become "resistant" to insulin (insulin resistance), meaning they do not take in glucose as well as they should.

In time, people with type 2 diabetes develop called " β -cell failure." This means that the cells in the pancreas that make insulin no longer are able to release insulin in response to high blood glucose levels. Therefore, these people often require insulin injections, either in combination with their oral diabetes medications, or just insulin alone to manage their diabetes.

Oral diabetes medicines are grouped in categories based on type. There are several categories of oral diabetes medications, each works differently. The aim of oral therapy in type 2 diabetes is to reach normoglycemia to prevent later complications (retinopathy, nephropathy, neuropathy and microangiopathy). Near normal or improved glycemic control (ADA goals: preprandial plasma glucose of 90-130 mg/dL and peak postprandial plasma glucose <180 mg/dL; ADA, 2006) has been shown to significantly diminish the risk of long-term complications (Florence and Yeager, 1999).

One therapeutic approach for treating diabetes is to decrease the post-prandial hyperglycemia. This can be achieved by retarding the absorption of glucose through the inhibition of the carbohydrate-hydrolysing enzymes α -glucosidase (sucrase, maltase and isomaltase) in the digestive process of the small intestine (Figure 1.7). Inhibitors of these enzyme delay carbohydrate digestion and prolong overall carbohydrate digestion time, causing a reduction in the rate of glucose absorption and consequently blunting the post-prandial plasma glucose level (Rhabasa-Lhoret *et al.*, 2004). Furthermore, the α -glucosidase inhibitors decrease the postprandial increment

in plasma insulin levels, reducing triglyceride levels and anti-HIV activity (Bridges *et al.*, 1994; Fischer *et al.*, 1996). Currently, the α -glucosidase inhibitors are used orally as antidiabetes including acarbose (Precose[®] or Glucobay[®]), miglitol (Glyset[®]) and voglibose (Basen[®]) (Melo *et al.*, 2006).

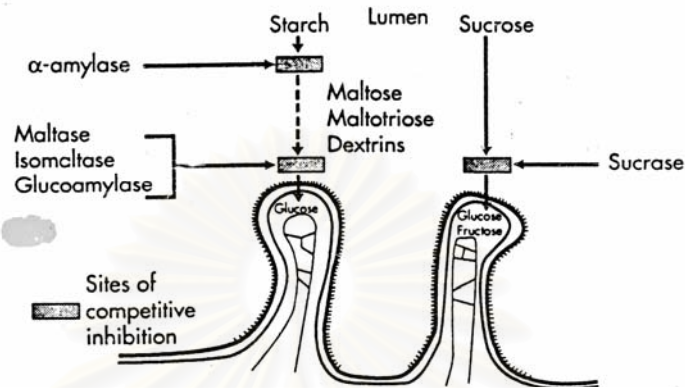
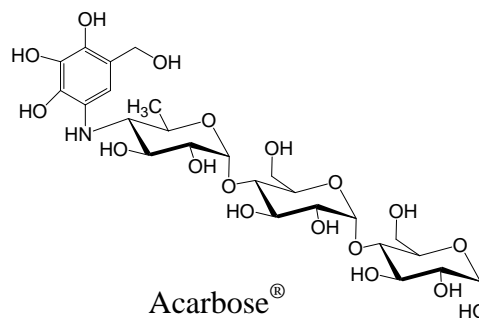


Figure 1.7 In normal digestion, pancreatic α -amylase hydrolyzes complex starches into oligosaccharides, which are further hydrolyzed by α -glucosidase located in the intestinal brush border to glucose and other monosaccharides, which are then absorbed.

Acarbose (Precose[®] or Glucobay[®]) has been produced as a secondary metabolite on a large scale from fermentation cultures of *Actinoplanes sp.* Catalytic hydrogenation of acarbose afforded fragments consisting of trisaccharide derivative, which have inhibitory activity on α -glucosidase and significantly decreases the postprandial increase in plasma glucose after the ingestion of mixed carbohydrate meal without changing the total amount of carbohydrate absorbed (Figure 1.8) (Bischoff, 1994). Importantly, therapeutic doses of acarbose[®] do not cause malabsorption, but long-term acarbose[®] administration have side effect such as flatulence, bloating, diarrhea and soft stools.



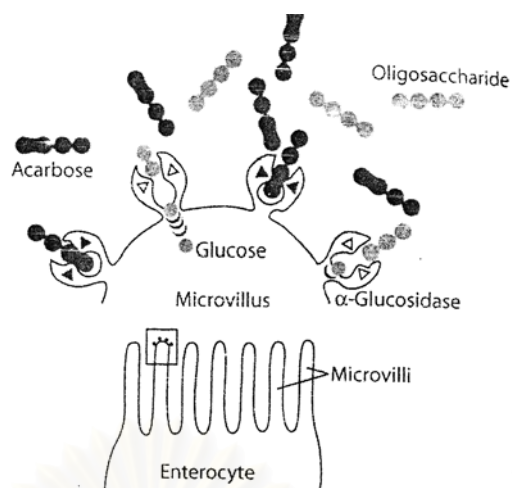
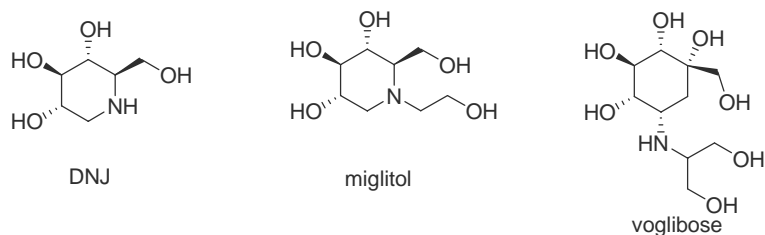


Figure 1.8 Acarbose[®] competitively inhibits the enzymatic hydrolysis of oligosaccharide by α -glucosidase in the small intestine.

1.5 Antidiabetes drugs from medicinal plants

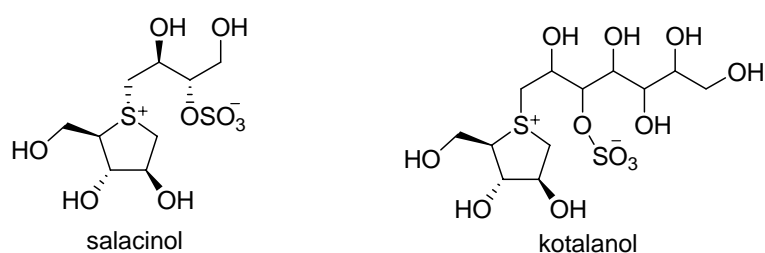
In many developing countries, the use of herbal medicine by the sufferers of chronic disease is encouraged because there is concern about the adverse effects of chemical drugs and treatment using medicines of natural origin appears to offer more gentle means of managing such disease (Bhattarai, 1993; Manandham, 1995; Shrestha and Joshi, 1993). Herbal drugs are prescribed widely because of their effectiveness, fewer side effect and relatively low cost. To this end, research has begun to embrace traditional medicines from various cultures, as scientists search for clues to discover new therapeutic drugs for diabetes (Li *et al.*, 2004). Traditional Indian and Chinese medicine have long used plant and herbal extracts as anti-diabetic agents (Chen *et al.*, 2001; Grover *et al.*, 2002). Therefore, investigation on such agents from traditional medicinal plants has become more important and researches are competing to find the new effective and safe therapeutic agent for the treatment of diabetes.

A recent review of hyperglycemia compounds mentioned the following plants with α -glucosidase activity such as 1-deoxynojirimycin (DNJ), which was isolated from *Morus alba* (Singab *et al.*, 2005). It was found to have inhibitory effect against α -glucosidase. However, the activity of DNJ *in vivo* against intestinal sucrase was lower than that seen *in vitro* and this initiated a synthetic to produce derivatives with enhanced activity. The *N*-alkyl derivatives were most effective and this led to the development of *N*-hydroxyethyl deoxynojirimycin (known as Miglitol or Glyset[®]) as an oral treatment of the type 2 diabetes (Melo *et al.*, 2006).



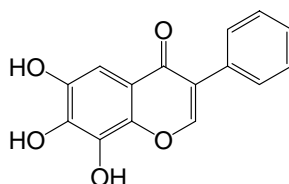
Voglibose (Basen[®]) can be regarded as derivative of 1-deoxynojirimycin (DNJ), which also has a high inhibitory activity against sucrase and maltase. It has been employed in Japan for the treatment of diabetes since 1994. In recent studies based on α -glucosidase inhibitory activity, it was shown to be 20 to 30 times more potent than acarbose, thus increasing glucose tolerance by inhibiting its digestion and absorption in the intestine, especially after meals (Yasuda *et al.*, 2003). Additionally, the use of voglibose led to less adverse effects including flatulency and abdominal distention, as shown in a random comparative study (Melo *et al.*, 2006).

Salacinol was isolated from an aqueous extract of the roots and stems of *Salacia reticulata* Wight (Yoshikawa *et al.*, 1997), which has been traditionally used in India and Sri Lanka for the treatment of diabetes. Salacinol displayed a strong inhibition for the increase of serum glucose levels in vivo screening along with competitive inhibition against intestinal α -glucosidase such as maltase, sucrase and isomaltase, in which the activity against isomaltase was higher than that of acarbose. Kotalanol, a derivative of 1,2,3-trihydroxy-propyl-salacinol showed more potent inhibitory activity against sucrase than salacinol and acarbose (Yoshikawa *et al.*, 1998), which was developed to diabetic drug that used generally in name Diabosol[®]. A recent study in healthy adults (Heacock, 2005) showed significant reduction of postprandial plasma glucose, serum insulin and increased breath hydrogen after ingestion of 1000 mg of *Salacia oblonga* extract. The increase in breath hydrogen is attributable to a mechanism involving inhibition of α -glucosidase.

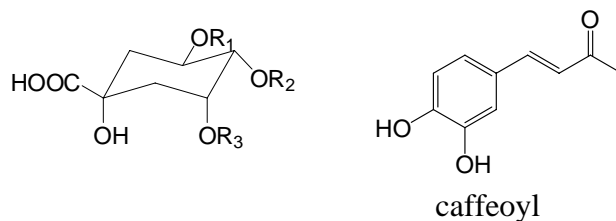


Pycnogenol[®], the standardized maritime pine bark extract derived from *Pinus pinaster* has been reported to display antidiabetes effect in patient (Liu *et al.*, 2004a and 2004b). Supplementation with 100 mg for 3 months significantly lowered blood glucose levels compared to Placebo and improved endothelial function was observed in type 2 diabetic patients. A recent study revealed that Pycnogenol[®], which mainly contained proxyanidin oligomers, potentially inhibited α -glucosidase with IC₅₀ value of 5 μ g/mL (Schäfer and Högger, 2007).

In addition, compounds possessing antidiabetes activity include flavonoids (flavonones, flavones, chalcones and their glycosides), xanthenes and polyphenols. They were exemplified by the reports of baicalein (5,6,7-trihydroxy flavone) from the root of *Scutellaria baicalensis* and its 6-hydroxy analogues from *Origanum majorana*. Baicalein strongly inhibited sucrase (IC₅₀ = 52 μ M) while its inhibitory effect against maltase was moderate (IC₅₀ = 500 μ M) (Nishioka *et al.*, 1998; Kawabata *et al.*, 2003). Investigation on structure-activity relationship among different flavones derivatives indicated that loss of hydroxyls from positions 5, 6, and 7 significantly reduced the activity. Some polyphenols, 3, 5-dicaffeoyl-quinic acid, 4,5-dicaffeoylquinic acid and 3,4-dicaffeoylquinic acid were found in the flower buds of *Tussilago farfara* L. These three compounds showed comparative maltase inhibitory activities (Gao *et al.*, 2007). A recent study reported that xanthenes were capable of inhibiting α -glucosidase with moderate to high activities. Prominent instances included isoprenyl tetrahydroxy xanthenes isolated from the root of *Cudrania tricuspidata*, which possessed highly potent α -glucosidase inhibition IC₅₀ 16.2-52.9 μ M (Seo *et al.*, 2007). In addition, mangiferin, a xantone from *Swertia chirayita*, reduced blood glucose levels in STZ-induced diabetic rats (Muruganandan, 2002).



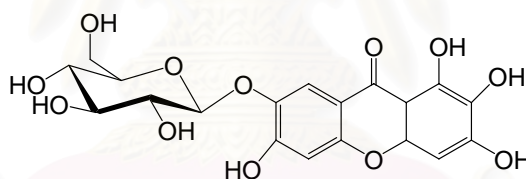
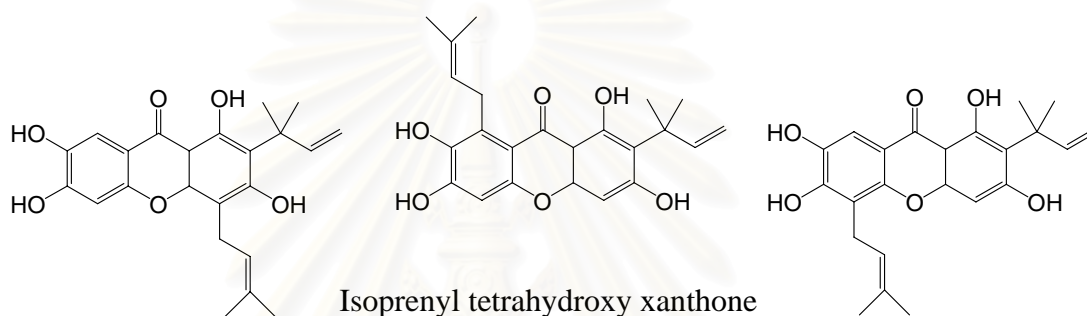
Baicalein



3,4-Dicaffeoylquinic acid : R¹ = H, R² = R³ = caffeoyl

3,5-Dicaffeoylquinic acid : R¹ = R² = caffeoyl, R³ = H

4,5-Dicaffeoylquinic acid : R¹ = R² = caffeoyl, R³ = H



Mangiferin

In Thailand, approximately 1,000 plants species have been registered for traditional medicine and about 200 of them are employed as antidiabetes agents. Although a large number of these plants which include *Aegle marmelos* (มะขาม) and *Corchorus olitorius* (ปลอกกระเจา), have been investigated for antidiabetes activity, the active principles have not been identified. In this research, the bioactive compounds from the leaves of *Aegle marmelos* and *Corchorus olitorius* will be determined as well as their inhibitory properties and mechanism of action.

CHAPTER II

PHENYLETHYL CINNAMIDES: A NEW SERIES OF α - GLUCOSIDASE INHIBITOR FROM THE LEAVES OF *Aegle marmelos*

2.1. Introduction

2.1.1 Botanical aspect and distribution of *Aegle marmelos*

Aegle Marmelos, commonly known as bael, is a spinous tree belonging to the plant family Rutaceae. It is known in Thai as madtoun “มะตูม”. There are different local names such as Bengal quince, golden apple, and stone apple. The tree is the only species in the genus *Aegle*. It grows wild in the Indian forests (up to 1000 meters of altitude), Ceylon, Burma, Thailand and Indo-China. It is also cultivated for commercial purposes. *A. Marmelos* is a small to medium-sized aromatic deciduous tree with light brown to green stem and strong axillary spines present on the branches. The average height of tree is 8.5 metres. It matures in about 60 years (Figure 2.1). Leaves are pale green, trifoliolate. Flowers are greenish white, sweetly scented. Fruits are yellowish green, with small dots on the outer surface, 5.3 cm to 72 cm in diameter and 77.2 g in weight. The pulp have an unusual texture and aroma with yellow color and mucilaginous. The pulp of dried fruits retains its yellow and also remains intact. Seeds are very numerous, embedded in the pulp, oblong, compressed, white, having cotton-like hairs on their outer surface.



Figure 2.1 *Aegle marmelos*.

2.1.2 Phytochemical and pharmacological investigation of *Aegle marmelos*

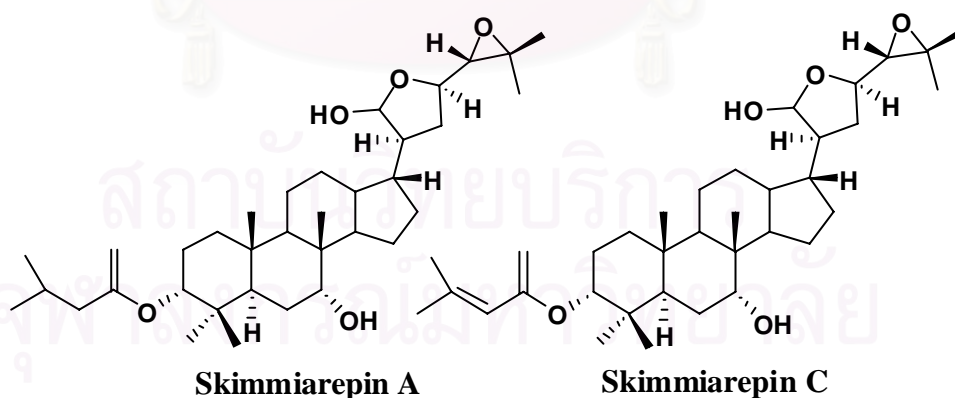
Aegle marmelos has been widely investigated for phytochemical constituents and those already identified include coumarins, alkaloids, terpenes, flavonoids, anthraquinones, lignan glucosides, tannins and volatile oil (Table 2.1), which are responsible for its medicinal properties. The various parts of this plant have been widely used in traditional medicine for the treatment of various disorders. The unripe fruits of *Aegle marmelos* are astringent, digestive and stomachic, used to cure diarrhea, dysentery and stomachalgia (Shoba and Thomas, 2001). The ripe fruit is a good and simple cure for dyspepsia (indigestion). The roots and the bark of the tree are used in the treatment of fever by making a decoction of them. The aqueous decoction of the leaf has been shown to have a significant hypoglycemic effect (Kamalakkannan and Prince, 2003). Bael leaf extract has also been found to help in the regeneration of damaged pancreas (β -cell) in diabetic rats and is found to be as effective as insulin in restoring blood glucose and body weight to normal levels (Jagetia *et al.*, 2004). Ponnachan *et al.* (1993a, 1993b) observed that the alkaloid extract prepared from leaves and crude aqueous leaf extract (1 g/kg for 30 days) exhibited hypoglycemic effect in alloxanized diabetic rats. In addition, aqueous leaf extract improved histopathological alterations in the pancreatic and kidney tissues of streptozotocin (STZ) induced diabetic rats (Das *et al.*, 1996).

Although the previous reports indicated blood glucose lowering activity of *Aegle marmelos* leaves, the active principle compounds have not been identified. Therefore this research is aim to identifying active compounds using α -glucosidase inhibition as guidance in order to study the structure and mechanism of action α -glucosidase inhibitors from its leaves with led to reduction of blood glucose levels. The objectives of this research can be summarized as follows:

1. To extract and isolate compounds from the leaves of *Aegle marmelos*.
2. To elucidate the structures of all isolated compounds.
3. To determine the α -glucosidase inhibitory activity of the isolated compounds.

Table 2.1 Chemical constituents of *Aegle marmelos*

Part of plant	Isolated compound	Type	Reference
Leaves	aegeline, marmeline, marmelineacetate, <i>N</i> -2-hydroxystyryl cinnamide, <i>O</i> -(3,3-dimethylallyl)-halfodinol, <i>N</i> -2-ethoxy-2-(4-methoxyphenyl)ethyl cinnamamide	alkaloid	Govindachari and Premila, 1993; Manandhar <i>et al.</i> , 1978
Fruits	aegeline, marmeline, marmeline acetate	alkaloid	Sharma <i>et al.</i> , 1980
Root	tembamide	alkaloid	Shoeb <i>et al.</i> , 1973
	decursinol, haplopine, xanthyletin	coumarin	Basu <i>et al.</i> , 1974
Bark	marmesin, anhydromarmesin	coumarin	Chatterjee <i>et al.</i> , 1977
	skimmiarepin A, skimmiarepin C	triterpenoid	Samarasekera <i>et al.</i> , 2003

**Figure 2.2** Triterpenoids from *Aegle marmelos*.

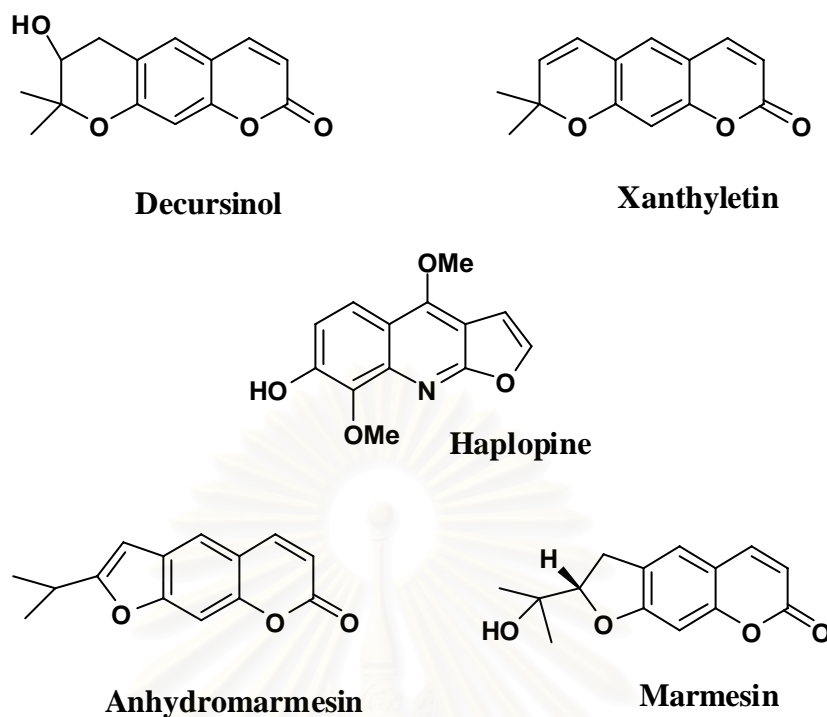
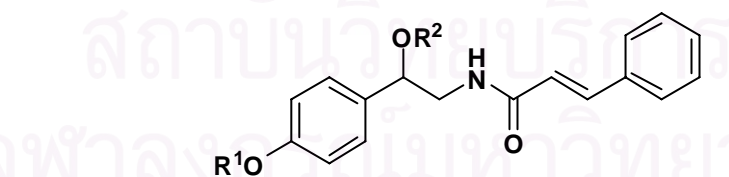
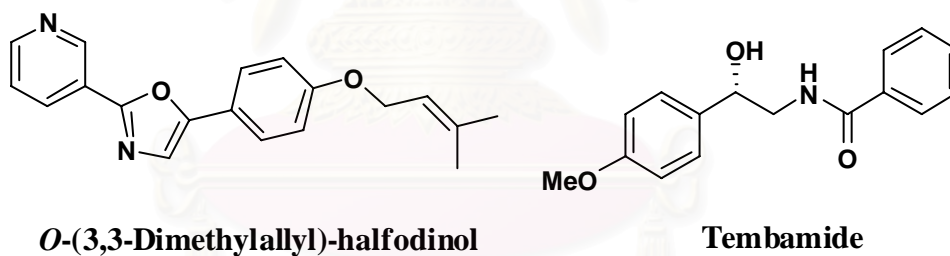


Figure 2.3 Coumarins from *Aegle marmelos*.



Aegeline : $R^1 = \text{Me}$, $R^2 = \text{H}$

Marmeline : $R^1 = \text{CH}_2\text{-CHCMe}_2$, $R^2 = \text{H}$

Marmeline acetate: $R^1 = \text{CH}_2\text{-CHCMe}_2$, $R^2 = \text{COMe}$

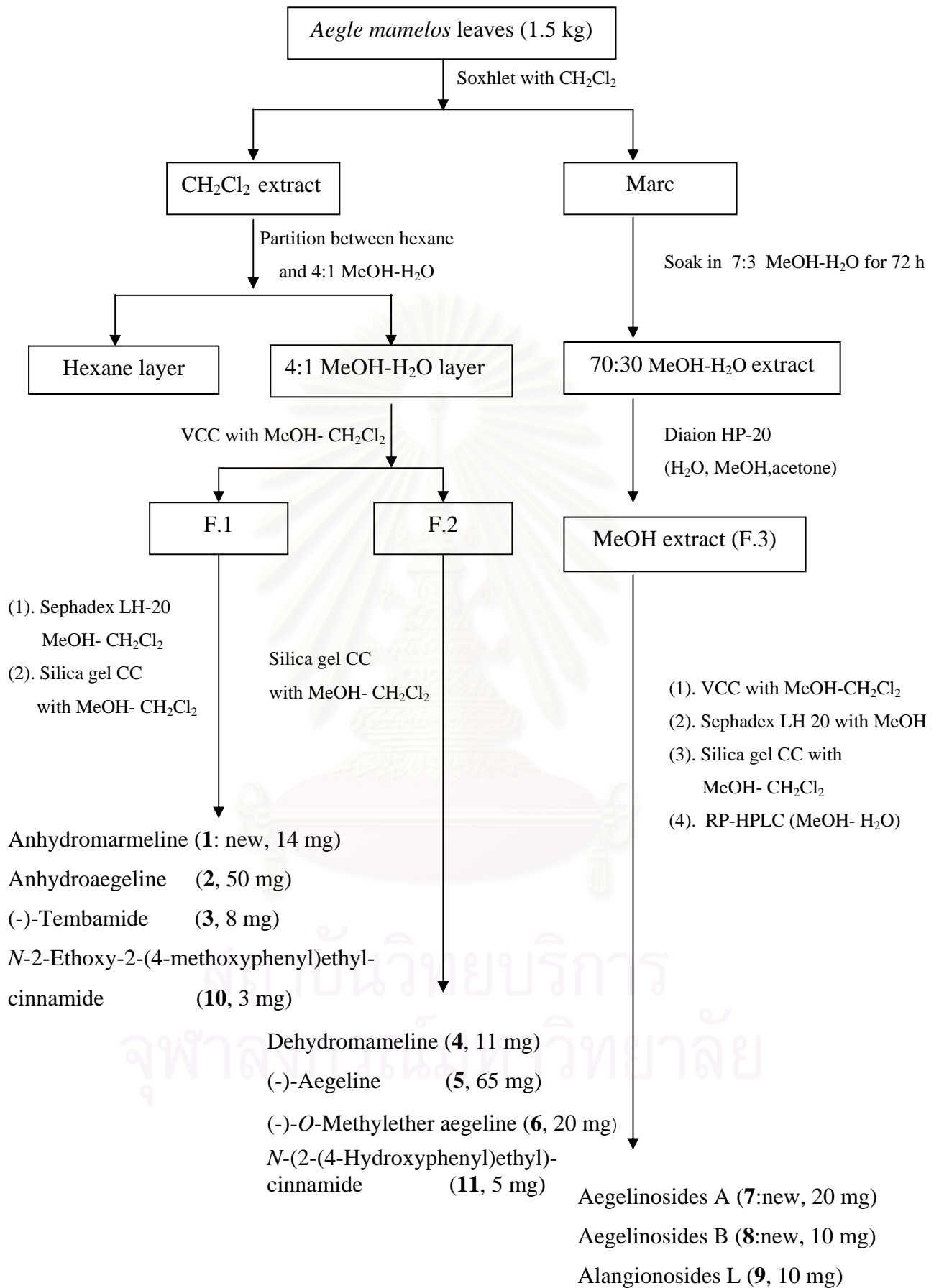
N-2-Methoxy-2-(4-methoxyphenyl)ethylcinnamamide : $R^1 = \text{Me}$, $R^2 = \text{Me}$

Figure 2.4 Alkaloids from *Aegle marmelos*.

2.2 Results and discussion

2.2.1 Isolation

The air dried leaves of *Aegle marmelos* were extracted with CH_2Cl_2 in a Soxhlet apparatus. The marc was extracted with 7:3 MeOH- H_2O at room temperature for 72 h. The CH_2Cl_2 extract was partitioned between 4:1 MeOH- H_2O and hexane. The methanolic layer was evaporated to dry and separated through vacuum column chromatography eluted with the gradient system to obtain three main fractions. Fraction 1 was purified by sephadex LH-20 and silica gel column chromatography to afford a new phenylethyl cinnamides named anhydromarmeline (**1**) together with three known phenylethyl cinnamides, anhydroaegeline (**2**), (-)-tembamide (**3**) and *N*-2-ethoxy-2-(4-methoxyphenyl)ethyl-cinnamide (**10**). Fraction 2 was purified by silica gel CC to afford dehydroaegeline (**4**), (-)-aegeline (**5**), (-)-*O*-methylether aegeline (**6**) and *N*-(2-(4-Hydroxyphenyl) ethyl)-cinnamide (**11**). The 70:30 MeOH- H_2O extract was separated via Diaion HP-20, yielding H_2O , MeOH and acetone fractions. The MeOH fraction was purified by VCC technique. Repeated column chromatography onto sephadex LH-20 followed by silica gel and RP-HPLC afforded two new phenylethyl cinnamide glycosides named aegelinosides A (**7**) and B (**8**) together with a known megastigmane glycosides named alangionosides L (**9**) (Scheme 2.1, Figure 2.5) .



Scheme 2.1 Isolation procedure of *Aegle marmelos* leaves.

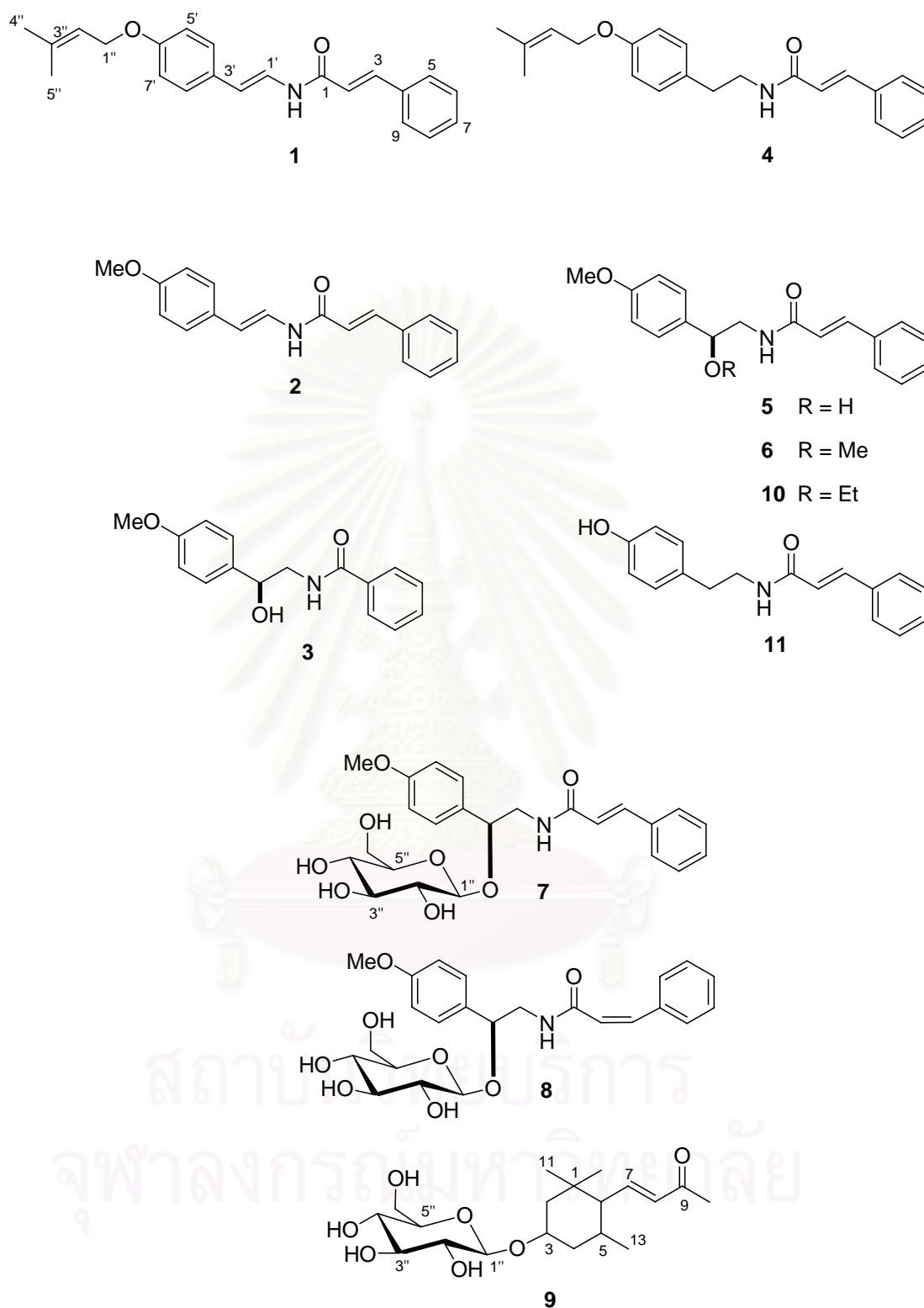


Figure 2.5 The chemical structures of isolated compounds from *Aegle marmelos* leaves.

2.2.2 Structure elucidation of anhydromarmeline (1)

Anhydromarmeline (**1**) was obtained as yellow needle. The molecular formula was established as $C_{22}H_{23}NO_2$ by HRESIMS. The UV spectrum exhibited absorption ($\log \epsilon$) at 277 (4.81) and 333 (4.46). The 1H NMR spectrum displayed most signals in aromatic region (6.1-7.7), in addition to upfield resonances that ascribable to oxygenated prenyl moiety [δ_H 5.49 (m, 1H), 4.50 (d, $J = 6.8$ Hz), 1.80 and 1.74 (s, each 3H)]. The ^{13}C NMR showed 22 signals, five of which were quaternary carbons which included resonance of amide (δ_C 162.7). Interpretation of 2D NMR resulted in the construction of two separated aromatic systems, which were connected through amide linkage. A monosubstituted benzene [δ_H 7.53 (2H) and 7.38 (3H)] was connected to *trans*-olefinic protons [δ_H 7.75 (d, $J = 15.2$ Hz) and 6.44 (d, $J = 15.2$ Hz)], which were in turn linked to amide carbon based on HMBC correlations from H-2 and H-3 to C-1. The other aromatic motif were assigned to a *para*-substituted benzene [δ_H 7.28 (d, $J = 8.4$ Hz, 2H) and 6.86 (d, $J = 8.4$ Hz, 2H)], which was accommodated by the oxygenated prenyl ($Me_2C=CHCH_2O-$) and ethyleneamine ($-CH=CH-NH-$) moieties. A large coupling constant (14.4 Hz) of olefinic protons (H-1' and H-2') pointed out that they were *E*-oriented. Therefore the gross structure of anhydromarmeline (**1**) was depicted. (Table 2.2, Figure 2.6.)

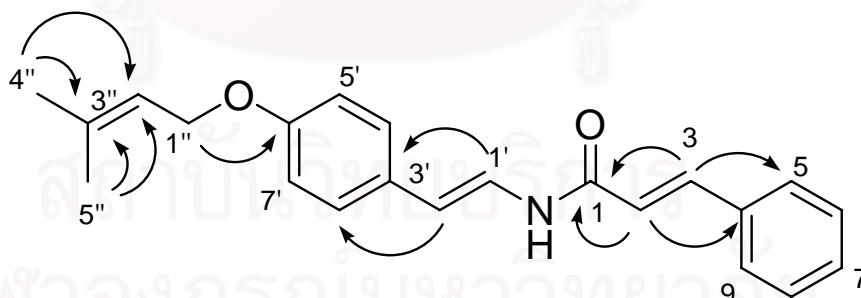


Figure 2.6 Selected HMBC correlations of **1**.

Table 2.2. ^1H , ^{13}C and HMBC NMR data of Anhydromarmeline (**1**) in CDCl_3

position	δ_{C}	δ_{H} (mult, J in Hz)	HMBC correlations
1	162.7		
2	119.7	6.44, d, 15.2	C-1, C-4
3	143.8	7.75, d, 15.2	C-1, C-5
4	132.4		
5,9	128.0	7.53, m	
6,8	129.1	7.38, m	
7	130.1	7.38, m	
1'	137.5	7.53, m	C-3'
2'	119.9	6.14, d, 14.4	C-8'
3'	112.2		
4',8'	126.7	7.28, d, 8.4	
5',7'	115.0	6.86, d, 8.4	
6'	158.1		
1''	65.4	4.50, d, 6.8	C-6'
2''	119.9	5.49, m	
3''	138.3		
4''	25.8	1.80, s	C-2'', C-3''
5''	18.2	1.74, s	C-2'', C-3''

2.2.3 Structure elucidation of aegelinoside A and B (7-8)

Aegelinoside A (**7**) was isolated from 7:3 MeOH- H_2O extract and displayed $[\text{M}+\text{Na}]^+$ ion in HRESIMS at m/z 482.1781 that corresponding with molecular formula of $\text{C}_{24}\text{H}_{29}\text{NO}_8$. The ^1H NMR spectrum of **7** in CD_3OD showed signals of aromatic and olefinic protons in the range of 6.6-7.6 (11H) and oxygenated methylene proton and methine protons (δ_{H} 3.0-5.2, 10H). The ^{13}C NMR spectrum displayed 24 signals, which included resonance of amide (δ_{C} 166.5). The resonances of δ_{H} 7.57 (m, 2H), 7.50 (d, $J = 15.6$ Hz, 1H), 7.35 (m, 3H) and 6.65 (d, $J = 15.6$ Hz, 1H) were

ascribable to *trans*-cinnamide based on COSY and HMBC data. The signals at δ_{H} 7.35 (d, $J = 8.8$ Hz, 2H) and 6.92 (d, $J = 8.8$ Hz, 2H) were assigned to *p*-disubstituted benzene which was accommodated by methoxy group (δ_{H} 3.78 and δ_{C} 54.1) at C-6' and oxygenated ethyl amine moiety (-OCH-CH₂-NH-) at C-3'. The HMBC cross peaks observed for H-2, H-3 and H-1' to C-1 indicated that these two separated aromatic systems were linked through amide bond. The remaining oxygenated methylenes and methines were assigned to β -D-glucose residue, which was attached to C-2' based on HMBC correlation from H-1'' (4.12, d, $J = 7.2$ Hz) to C-2'. Therefore overall structure of **7** was accomplished. The absolute configuration of C-2' was determined by chemical degradation. Hydrolysis of **7** in 1M HCl under reflux yielded D-glucose and (-)-aegeline; the latter of which was identical in all respects, particularly optical rotation ($[\alpha]_{\text{D}}^{26} -27.6$), to *R*-aegeline (lit. $[\alpha]_{\text{D}}^{25} -35.9$) (Table 2.3., Figure 2.7).

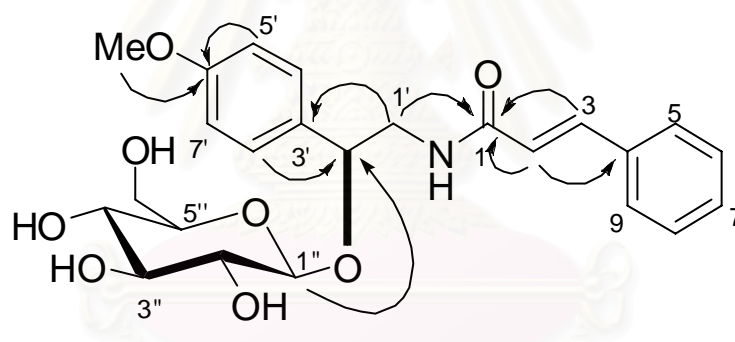


Figure 2.7 Selected HMBC correlations of **7**.

สถาบันวิทยบริการ
จุฬาลงกรณ์มหาวิทยาลัย

Table 2.3 ^1H and ^{13}C NMR data for aegelinosides A (**7**, CD_3OD) and B (**8**, acetone- d_6)

position	Aegelinoside A (7)		Aegelinoside B (8)	
	^{13}C	^1H	^{13}C	^1H
1	166.5		166.4	
2	120.5	6.65, d, 15.6	124.1	6.05, d, 12.8
3	140.5	7.50, d, 15.6	136.4	6.68, d, 12.8
4	135.4		135.9	
5, 9	127.5	7.57, m	129.8	7.68, m
6, 8	128.1	7.35, m	128.0	7.31, m
7	129.3	7.35, m	129.4	7.31, m
1'	46.0	3.57, d, 6.4	45.4	3.56, m 3.38, m
2'	77.0	5.00, t, 6.4	77.9	4.89, dd, 7.6, 4.4
3'	130.0		131.3	
4', 8'	128.0	7.35, d, 8.8	128.2	7.37, d, 8.6
5', 7'	113.7	6.92, d, 8.8	113.5	6.89, d, 8.6
6'	159.6		159.4	
1''	99.5	4.12, d, 7.2	100.5	4.18, d, 7.2
2''	73.7	3.28, m	73.7	3.24, m
3''	76.3	3.23, m	76.8	3.27, m
4''	70.4	3.26, m	70.5	3.32, m
5''	76.6	3.09, m	76.3	3.18, m
6''	61.5	3.87, dd, 11.6, 2.0 3.67, dd, 11.6. 5.6	62.0	3.65, m 3.84, m
OMe	54.1	3.78, s	54.4	3.78, s

Aegelinoside B (**8**) was isomeric of **7** as evidenced by a molecular formula of $C_{24}H_{29}NO_8$. Although direct comparison of their 1H and ^{13}C NMR spectra could not be made since they were recorded in different solvents, **8** revealed signals essentially identical to those of **7**. Significant difference we have observed was slightly upfield olefinic protons H-2 (6.05, d, $J = 12.8$ Hz) and H-3 (6.68, d, $J = 12.8$ Hz). A relative small coupling constant ($J_{23} = 12.8$ Hz) indicated that Δ^2 in **8** was *cis*-oriented instead of *trans*-oriented in **7**. The gross structure of **8** was subsequently confirmed by 2D NMR data. The absolute configuration of C-2' was also deduced by chemical degradation. Acid hydrolysis of **8** afforded D-glucose and the corresponding hydrolysate named aegeline B (**8a**, Figure 2.8), whose minus sign of specific rotation ($[\alpha]_D^{26} -20.6$) was reminiscent to that of a 2'*R*-phenylethyl cinnamide.

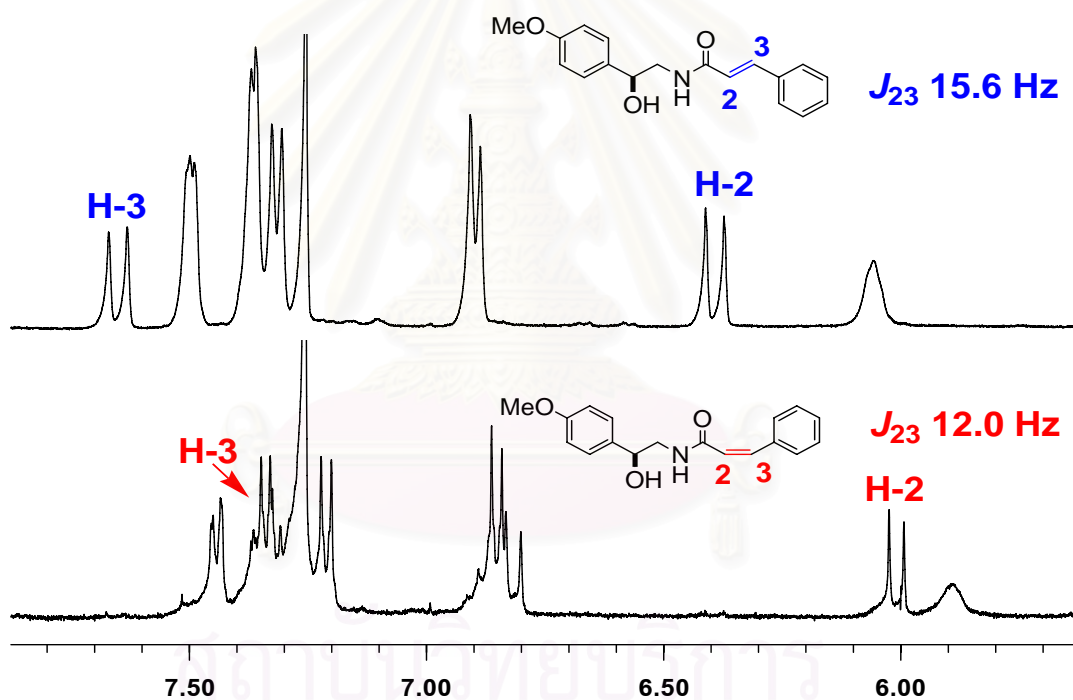


Figure 2.8 Partial 1H NMR spectra of aglycones **5** (top) and **8a** (bottom) obtained from hydrolysis of **7** and **8**, respectively.

2.2.4 α -Glucosidase inhibitory activity of the isolated compounds

The α -glucosidase inhibitory activity of compound **1-11** isolated from *Aegle marmelos* leaves was evaluated by colorimetric method and the results are shown in Table 2.4.

Table 2.4 α -Glucosidase inhibitory effect of isolated compounds from *Aegle marmelos* leaves

Compounds	IC ₅₀ (mM)
Anhydromarmeline (1)	4.93 ± 0.12
Andydroaegeline (2)	3.21 ± 0.02
(-)-Tembamide (3)	> 10
Dehydromarmeline (4)	> 10
(-)-Aegeline (5)	4.66 ± 0.04
(-)- <i>o</i> -Methylether aegeline (6)	> 10
Aegelinosides A (7)	> 10
Aegelinosides B (8)	> 10
Alangionosides L (9)	> 10
<i>N</i> -2-Ethoxy-2-(4-methoxyphenyl)ethyl-cinnamide (10)	> 10
<i>N</i> -(2-(4-Hydroxyphenyl)ethyl)-cinnamide (11)	2.41 ± 0.05
Acarbose ^{® a}	0.62 ± 0.03
1-Deoxynojirimycin(DNJ) ^a	0.17 ± 0.02

^aStandard control

From Table 2.4 *N*-(2-(4-Hydroxyphenyl)ethyl)-cinnamide (**11**) has the most potent α -glucosidase inhibitory activity with the IC₅₀ value of 2.41 mM, while andydraoegeline (**2**), (-)-aegeline (**5**) and anhydromarmeline (**1**) showed moderate inhibition with IC₅₀ values of 3.21, 4.66 and 4.93 mM, respectively. In addition, *N*-2-ethoxy-2-(4-methoxyphenyl)ethyl-cinnamide (**10**), alangionosides L (**9**), dehydromarmeline (**4**), aegelinosides A (**7**), (-)-tembamide (**3**), (-)-*O*-methylether aegeline (**6**), and aegelinosides B (**8**) showed weak inhibitory effect (< 30% inhibition) at concentration of 1 mg/mL.

These results suggested that the presences of hydroxyl group at C-6' position on phenylethyl cinnamide moiety are necessary to enhance α -glucosidase inhibitory activity. When the α -glucosidase inhibitory activities of compounds **1**, **2** and **11** were compared, it was found that the potency increased in the order of **11** > **2** > **1**. This indicates that 6'-OH in compound **11** was crucial, primarily as H-bonding donor to interact with α -glucosidase since hydroxyl group is an H-bonding donor/acceptor, while methoxy group can only act as H-bonding acceptor. The observation revealed that replacement of methoxy group at C-6' by the prenyl residue decreased α -glucosidase inhibitory activity. These results suggested that the prenyl group can not act as H-bonding dornor/acceptor to interact with α -glucosidase.

As for α -glucosidase inhibitory activities of compounds **2**, **5**, **6**, **7** and **10**, it was found to have the potency increased in the order of **2** > **5** > **6**, **7** and **10**. It is likely that replacement of unsaturation at C-1' and C-2' by any hydroxylated moiety (-OH, -OMe, -OGlc and -OEt) caused no enhancement in inhibitory effect. Thus unsaturation at C-1' and C-2' is required for exerting inhibition. When the α -glucosidase inhibitory activities of compounds **3**, **5** and **8**. were compared, it was found that the potency increased in the order of **5** > **3** and **8**. It could be implied that of *trans*-cinnamate residue in **5** by benzoate in **3** and *cis*-cinnamate in **8** resulted in decreased inhibition.

In conclusion, the enhanced activity found in phenylethyl cinnamide containing hydroxyl group or methoxy group at C-6' position and unsaturation at C-1'/C-2' indicated that these structural feathers were associated with antagonizing active sites of α -glucosidase enzyme. Relatively weak inhibition of phenylethyl cinnamides, compared with positive controls Acarbose[®] and DNJ, suggests that these active principles possibly reduce blood glucose levels in other pathways such as stimulation of insulin secretion, reduction of hepatic gluconeogenesis and increase in insulin receptor sensitivity, respectively. It is expected that these preliminary observations will provide the basis for further examination of the suitability of *Aegle marmelos* as a medicinal supplement that contributes toward the treatment and prevention of diabetes.

2.3 Experiment section

2.3.1 General experimental procedures

The ^1H and ^{13}C -NMR spectra (in CDCl_3 , CD_3OD and acetone- d_6) were determined with a nuclear magnetic resonance spectrometer of Varian model Mercury+ 400. The chemical shift in δ (ppm) was assigned with reference to the signal from the residual protons in deuterated solvents and using TMS as an internal standard in some cases. EIMS and HRESIMS were obtained from Mass Spectrometer Model VG TRIO 2000 and a Micromass LCT mass spectrometer, respectively. Optical rotations were measured on a Jasco P-1010 polarimeter. UV spectra were recorded on Shimadzu UV-160A photodiode array spectrophotometer. HPLC was conducted on Water[®] 600 controller equipped with a Water[®] 2996 photodiode array detector (USA). Cosmosil 5C18-ARII column (10 \times 250 mm) was used for separation purpose. Sephadex LH-20 and silica gel 60 Merck cat. No. 7734 and 7729 were used for open column chromatography. Thin layer chromatography (TLC) was performed on precoated Merck silica gel 60 F₂₅₄ plates (0.25 mm thick layer).

2.3.2 Plant material

The leaves of *Aegle marmelos* were collected in Nakhon Phathom, Thailand in April 2007.

2.3.3 Extraction and isolation

The air-dried leaves of *Aegle marmelos* (1.5 kg) were extracted with CH_2Cl_2 using Soxhlet extractor. The marc was extracted with 7:3 MeOH- H_2O at room temperature for 72 h. The CH_2Cl_2 extract was dissolved in 4:1 MeOH- H_2O and partitioned with hexane. The 4:1 MeOH- H_2O extract was further purified by chromatographic techniques. The aqueous methanolic extract (40 g) was separated through vacuum column using stepwise MeOH- CH_2Cl_2 (0:1, 5:95, 10:90, 20:80 and 50:50), yielding three major fractions. Fractions 1 were further purified on Sephadex LH-20 (1:9 MeOH- CH_2Cl_2). Repeat column chromatography over silica gel CC

using MeOH-CH₂Cl₂ (5:95) afforded a new phenylethyl cinnamide named anhydromarmeline (**1**, 14 mg, 9.3x10⁻⁴ % w/w) together with three known phenylethyl cinnamides, anhydroaegeline (**2**, 50 mg, 3.3x10⁻³ % w/w), (-)-tembamide (**3**, 8 mg, 5.3x10⁻⁴ % w/w) and *N*-2-ethoxy-2-(4-methoxyphenyl)ethyl-cinnamide (**10**, 3 mg, 2.0x10⁻⁴ % w/w). In addition, dehydromarmeline (**4**, 11 mg, 7.3x10⁻⁴ % w/w), (-)-aegeline (**5**, 65 mg, 4.3x10⁻³ % w/w), (-)-*O*-methylether aegeline (**6**, 20 mg, 1.3x10⁻³ % w/w) and *N*-(2-(4-Hydroxyphenyl)ethyl)-cinnamide (**11**, 5 mg, 3.3x10⁻⁴ % w/w) were also obtained from fraction 2, on purification using silica gel (10:90 MeOH-CH₂Cl₂). The 7:3 MeOH-H₂O extract was loaded onto Diaion HP-20 and excessively eluted with H₂O, MeOH and acetone. The combined MeOH fractions (60 g) was separated by VCC (stepwise 5:95, 10:90, 15:85, 50:50, 70:30 and 100:0 MeOH-CH₂Cl₂) The combined fractions eluted with 15:85 and 50:50 MeOH-CH₂Cl₂ were subsequently purified by Sephadex LH-20 (3:7 MeOH-CH₂Cl₂) followed by RPHPLC (ODS, 65:35 MeOH-H₂O, UV 254 nm), yielding two new phenylethyl cinnamide glycoside named aegelinosides A (**7**, 20 mg, 1.3x10⁻³ % w/w, *t*_R 32.4 min) and B (**8**, 10 mg, 6.7x10⁻⁴ % w/w, *t*_R 27.1 min) together with a known megastigmane glycosides named alangionosides L (**9**, 10 mg, 6.7x10⁻⁴ % w/w).

Anhydromarmeline (**1**): yellow needle, UV (MeOH) λ_{max} (log ε) 277 (4.81), 333 (4.46); HRESIMS *m/z* [M+H]⁺ 334.2260 (calcd for C₂₄H₂₉NO₈Na, 334.1807); ¹H NMR (CDCl₃, 400 MHz) and ¹³C NMR (100 MHz) see table 2.2.

Anhydroaegeline (**2**): yellow needle, ¹H NMR (CDCl₃, 400 MHz) δ_H 3.81 (3H, s, 6'-OCH₃), 6.85 (2H, d, *J* = 8.4 Hz, H-5' and H-7'), 7.29 (2H, d, *J* = 8.4 Hz, H-4' and H-8'), 6.14 (1H, d, *J* = 15.6 Hz, H-2'), 7.75 (1H, d, *J* = 15.6 Hz, H-1'), 6.84 (1H, d, *J* = 14.8 Hz, H-2), 7.38 (3H, m, H-6, H-7 and H-8), 7.53 (3H, m, H-3, H-5 and H-9).

(-)-Tembamide (**3**): white crystals; ¹H NMR (CDCl₃, 400 MHz) δ_H 3.77 (3H, s, 6'-OCH₃), 6.89 (2H, d, *J* = 8.8 Hz, H-5' and H-7'), 7.26 (2H, d, *J* = 8.8 Hz, H-4' and H-8'), 5.50 (1H, t, H-2'), 3.96 (1H, dd, H-1'), 4.26 (1H, dd, H-1'), 7.34 (3H, m, H-6, H-7 and H-8), 7.57 (2H, m, H-5 and H-9).

Dehydromarmeline (**4**): colourless crystals; ^1H NMR (CDCl_3 , 400 MHz) δ_{H} 1.74 (3H, s, H-5''), 1.79 (3H, s, H-4''), 5.49 (H, m, H-3''), 4.49 (2H, d, H-1''), 6.88 (2H, d, $J = 8.4$ Hz, H-5' and H-7'), 7.12 (2H, d, $J = 8.8$ Hz, H-4' and H-8'), 2.82 (2H, dd, H-2'), 3.62 (2H, dd, H-2'), 6.31 (1H, d, $J = 15.6$ Hz, H-2), 7.61 (1H, d, $J = 15.6$ Hz, H-3), 7.35 (3H, m, H-6, H-7 and H-8), 7.49 (2H, m, H-5 and H-9).

(-)-Aegelin (**5**): colourless needles; ^1H NMR (acetone- d_6 , 400 MHz) δ_{H} 3.78 (3H, s, 6'-OCH₃), 6.89 (2H, d, $J = 8.8$ Hz, H-5' and H-7'), 7.33 (2H, d, $J = 8.8$ Hz, H-4' and H-8'), 3.39 (1H, m, H-1'), 3.62 (1H, m, H-1'), 7.55 (1H, d, $J = 15.6$ Hz, H-2), 7.76 (1H, d, $J = 15.6$ Hz, H-3), 7.39 (3H, m, H-6, H-7 and H-8), 7.58 (2H, m, H-5 and H-9).

(-)-*O*-Methyletheraegeline (**6**): colourless crystals ; ^1H NMR (CDCl_3 , 400 MHz) δ_{H} 3.81 (3H, s, 6'-OCH₃), 6.90 (2H, d, $J = 8.4$ Hz, H-5' and H-7'), 7.25 (2H, d, $J = 8.4$ Hz, H-4' and H-8'), 3.28 (3H, s, 2'-OCH₃), 4.28 (1H, dd, H-2'), 3.30 (1H, m, H-1'), 3.85 (1H, m, H-1'), 6.41 (1H, d, $J = 15.6$ Hz, H-2), 7.63 (1H, d, $J = 15.6$ Hz, H-3), 7.36 (3H, m, H-6, H-7 and H-8), 7.50 (2H, m, H-5 and H-9).

Aegelinoside A (**7**): colourless liquid , $[\alpha]_{\text{D}}^{25} -26.3^\circ$ (c 0.05, MeOH); UV (MeOH) λ_{max} (log ϵ) 274 (4.73); HRESIMS m/z $[\text{M}+\text{Na}]^+$ 482.1787 (calcd for $\text{C}_{24}\text{H}_{29}\text{NO}_8\text{Na}$, 482.1797); ^1H NMR (CDCl_3 , 400 MHz) and ^{13}C NMR (100 MHz) see table 2.3.

Aegelinoside B (**8**): colourless liquid , $[\alpha]_{\text{D}}^{25} -33.3^\circ$ (c 0.05, MeOH); UV (MeOH) λ_{max} (log ϵ) 260 (4.43); HRESIMS m/z $[\text{M}+\text{Na}]^+$ 482.1786 (calcd for $\text{C}_{24}\text{H}_{29}\text{NO}_8\text{Na}$, 482.1791); ^1H NMR (CDCl_3 , 400 MHz) and ^{13}C NMR (100 MHz) see table 2.3.

Alangionoside L (**9**): colourless liquid ; ^1H NMR (CD_3OD , 400 MHz) δ_{H} 0.81 (3H, s, H-11), 1.07 (3H, s, H-12), 0.77 (3H, s, H-13), 2.22 (3H, s, H-10), 1.40 (1H, t, H-2), 1.81 (1H, t, H-2), 1.06 (1H, t, H-4), 2.15 (1H, t, H-4), 6.65 (1H, d, $J = 16$ Hz), 6.01 (1H, d, H-8), 3.18 (H, dd, H-2'), 3.31 (H, t, H-3'), 3.38 (H, t, H-4'), 4.06 (H, d, H-5'), 4.35 (H, d, H-1'), 3.65 (H, dd, H-6'), 3.82 (H, dd, H-6').

N-2-Ethoxy-2-(4-methoxyphenyl)ethyl-cinnamide (**10**) : white crystals ; ^1H NMR (CDCl_3 , 400 MHz) δ_{H} 3.73 (3H, s, 6'- OCH_3), 6.83 (2H, d, $J = 8.8$ Hz, H-5' and H-7'), 7.32 (2H, d, $J = 8.8$ Hz, H-4' and H-8'), 5.94 (1H, dd, H-2'), 3.65 (1H, dd, H-1'), 3.98 (1H, dd, H-1'), 6.32 (1H, d, $J = 16$ Hz, H-2), 7.58 (1H, d, $J = 16$ Hz, H-3), 7.29 (3H, m, H-6, H-7 and H-8), 7.45 (2H, m, H-5 and H-9).

N-(2-(4-Hydroxyphenyl)ethyl)-cinnamide (**11**) ; ^1H NMR (CD_3OD , 400 MHz) δ_{H} 6.62 (2H, d, $J = 8.0$ Hz, H-5' and H-7'), 6.94 (2H, d, $J = 8.0$ Hz, H-4' and H-8'), 2.62 (2H, t, H-2'), 3.34 (1H, t, H-1'), 6.52 (1H, d, $J = 15.6$ Hz, H-2), 7.38 (1H, d, $J = 15.6$ Hz, H-3), 7.29 (3H, m, H-6, H-7 and H-8), 7.45 (2H, m, H-5 and H-9).

2.3.4 α -Glucosidase inhibitory assay

The α -glucosidase inhibitory activity was performed using colorimetric method (Adisakwattana *et al.*, 2004) with a slight modification. The α -glucosidase activity was determined by measuring the product *p*-nitrophenol released from *p*-nitrophenyl α -D-glucopyranoside at UV 405 nm using microplate reader (Figure 1.9).

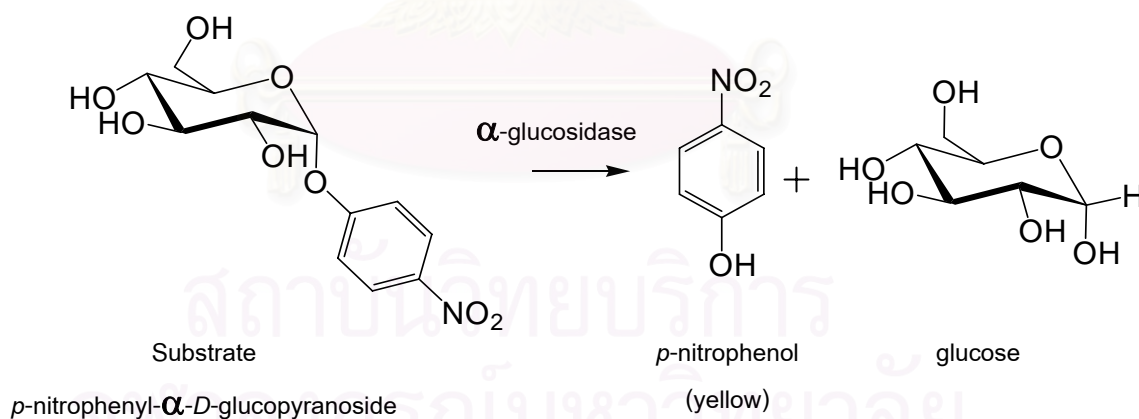


Figure 2.9 Hydrolysis of *p*-nitrophenyl- α -D-glducopyranoside by α -glucosidase

Chemical and equipment

The α -glucosidase (EC 3.2.1.20) from Baker's yeast and *p*-nitrophenyl α -D-glucopyranoside (pNPG) as a synthetic substrate were purchased from Sigma-Aldrich (St. Louis, MO, USA). The substrate solution *p*-nitrophenyl α -D-glucopyranoside was prepared in 0.1 M phosphate buffer, adjusted to pH 6.9, to simulate a model of intestinal fluid. Briefly, yeast glucosidase was dissolved in 0.1 M phosphate buffer, pH 6.9, to yield 57 U/mL stock-solution, and further diluted with 0.1 M phosphate buffer to get 1 U/mL. Acarbose (Glucobay[®] 50 N 1; Bayer Vital, Leverkusen, Germany) as a synthetic inhibitor of α -glucosidase was obtained from a local pharmacy. Bio-Rad microplate reader model 3550 UV was used to measure the absorbance at 405 nm of enzyme reaction.

Procedures

In the 96-well plate, 10 μ L of test compounds dissolved in DMSO were incubated for 10 min with 50 μ L of yeast α -glucosidase enzyme (1 U/mL). After 10 min of incubation, 50 μ L of substrate (pNPG) was added into a microplate. The reaction was terminated by addition of a 1 M Na₂CO₃ solution. The increment in absorption at 405 nm due to the hydrolysis of pNPG by α -glucosidase enzyme. Percent inhibition was calculated according to the equation shown below.

$$\% \text{ inhibition} = \left(\frac{A_{\text{blank}} - A_{\text{sample}}}{A_{\text{blank}}} \right) \times 100$$

A_{blank} is the absorbance of control without test solution

A_{sample} is the absorbance of sample with test solution

The IC₅₀ value was determined from a plot of percentage inhibition on the y axis against concentration of sample on the x axis. Acarbose[®] and 1-deoxynojirimycin (DNJ) were used as positive control. The experiment was performed in triplicate.



Supporting information

สถาบันวิทยบริการ
จุฬาลงกรณ์มหาวิทยาลัย

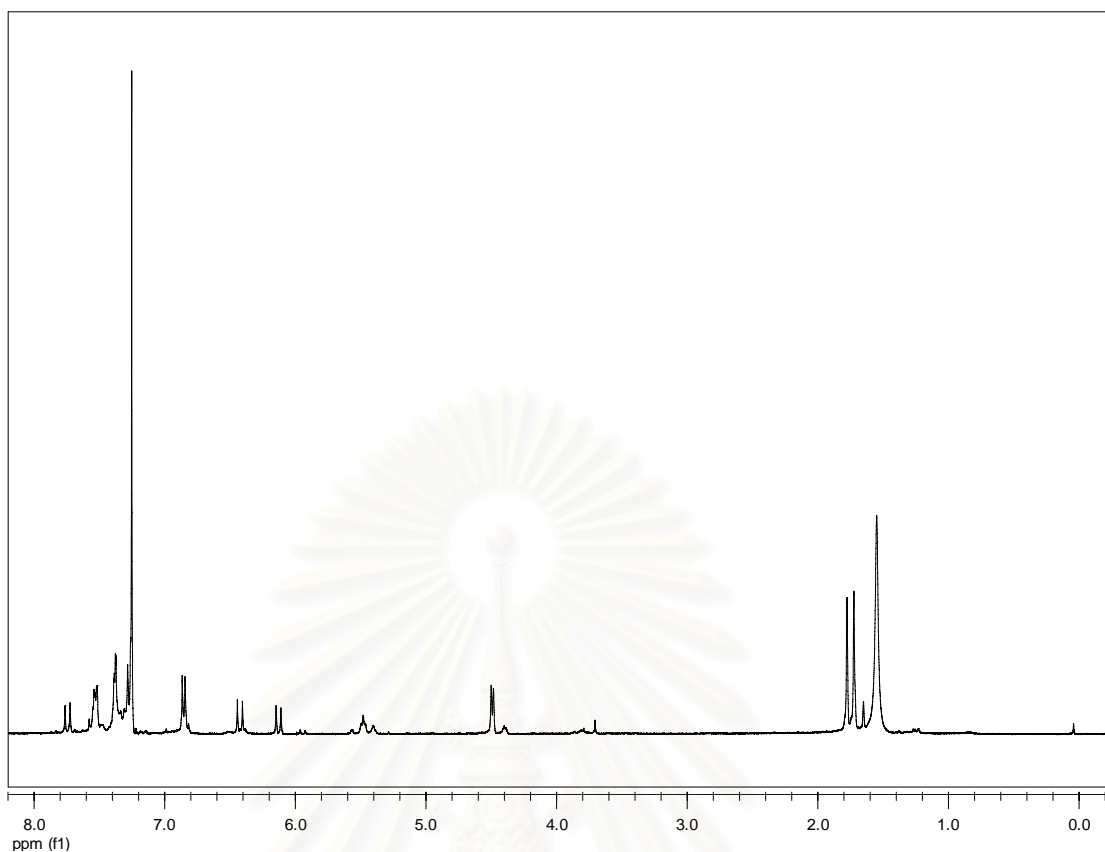


Figure S-2.1 The ^1H NMR (CDCl_3) spectrum of anhydromarmeline (**1**).

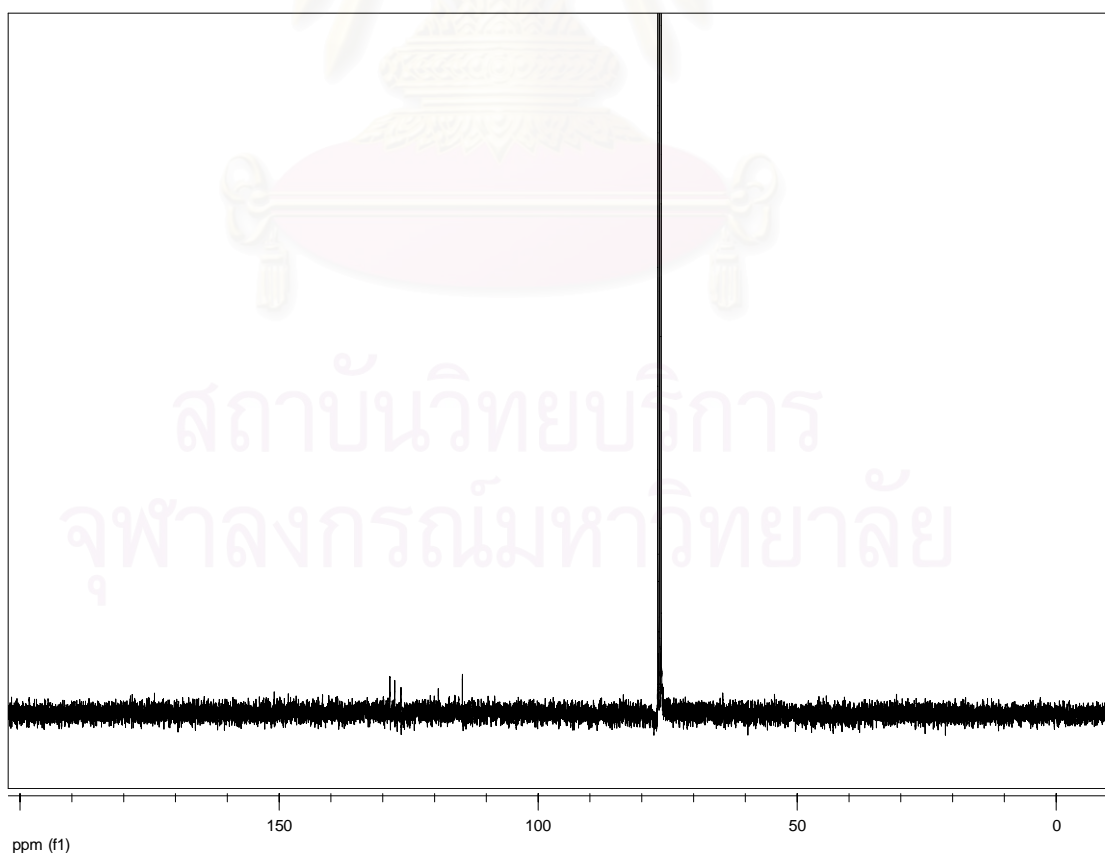


Figure S-2.2 The ^{13}C NMR (CDCl_3) spectrum of anhydromarmeline (**1**).

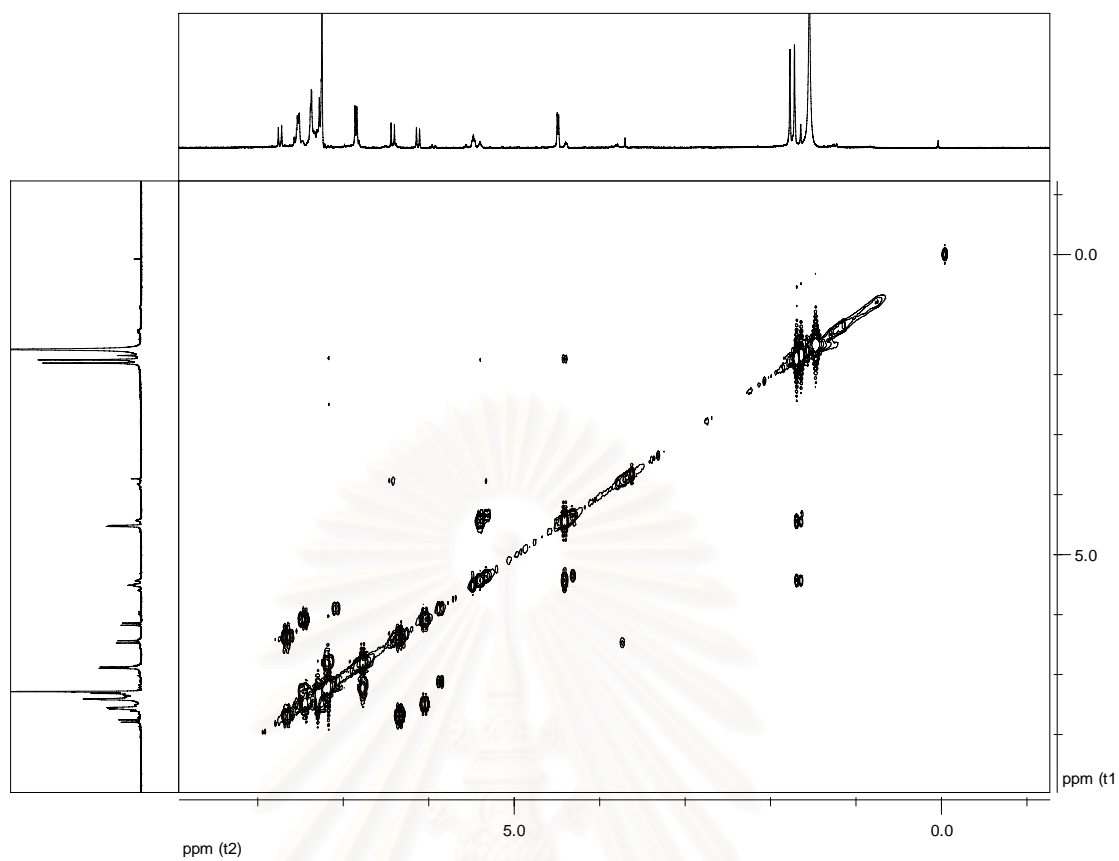


Figure S-2.3 The COSY (CDCl₃) spectrum of anhydromarmeline (**1**).

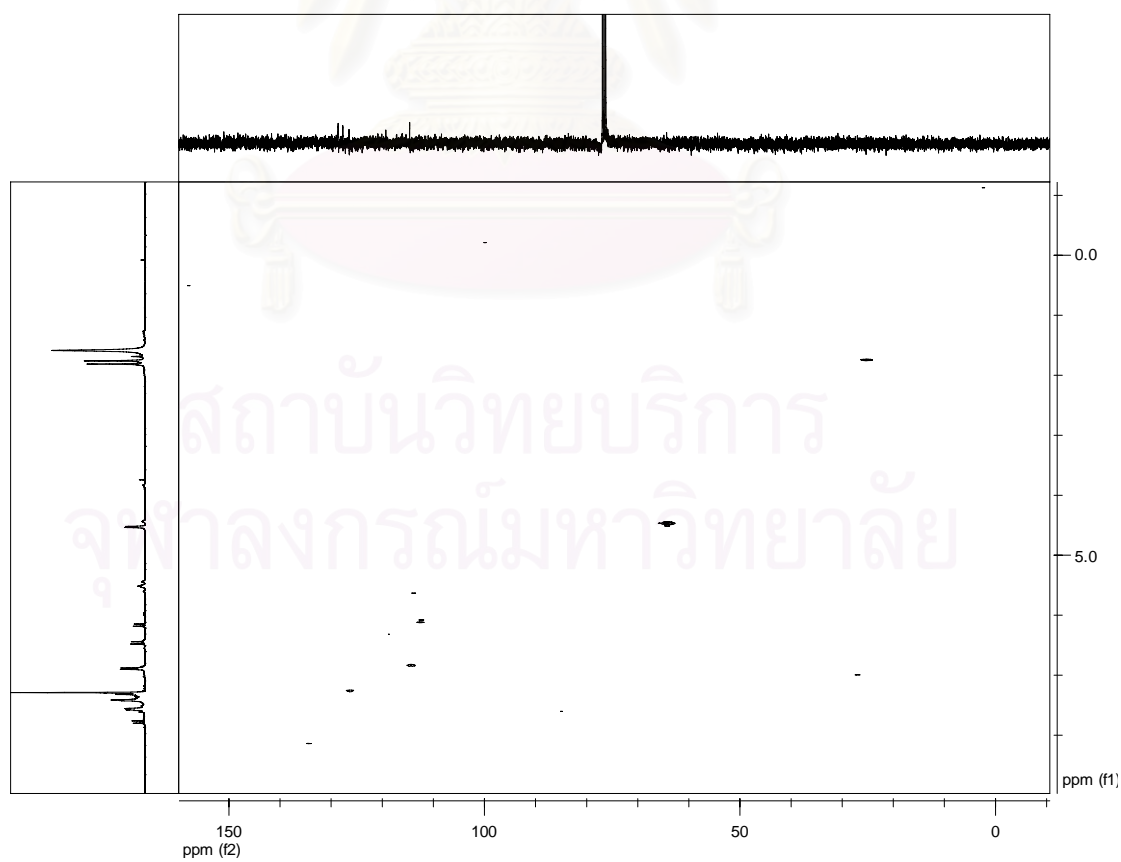


Figure S-2.4 The HSQC (CDCl₃) spectrum of anhydromarmeline (**1**).

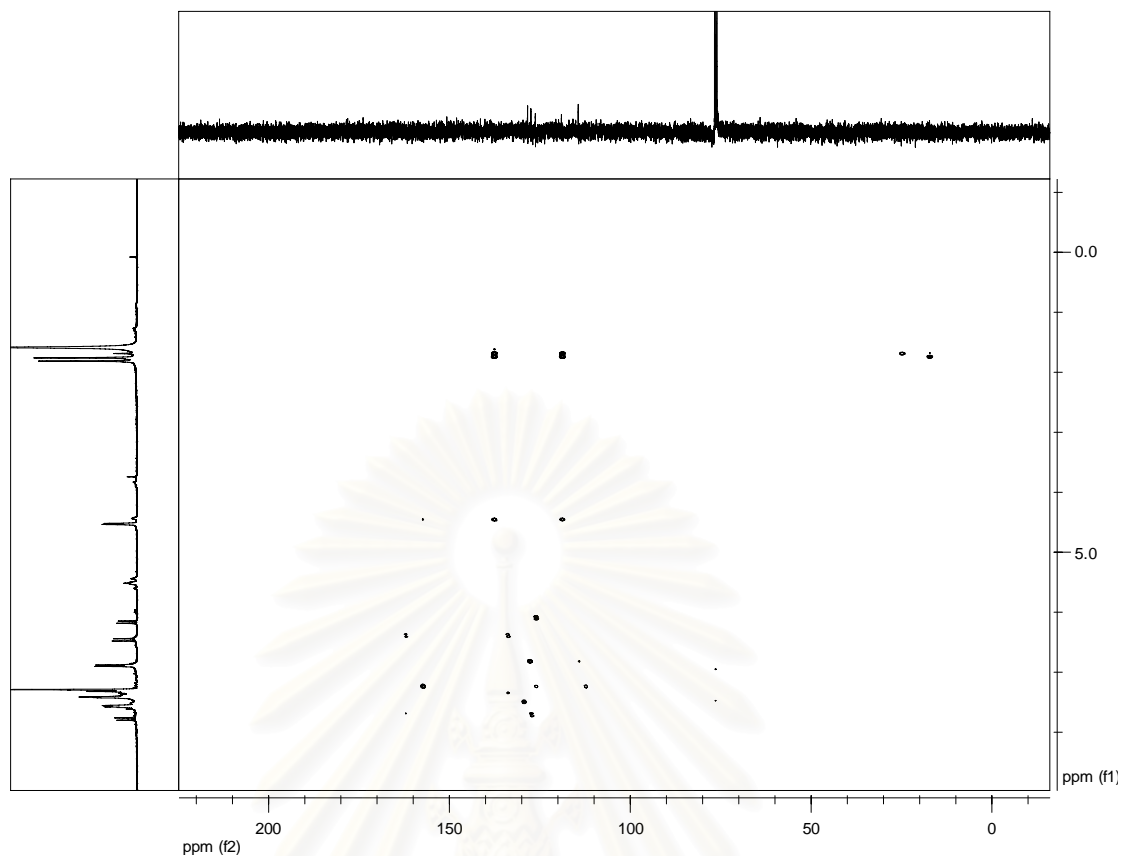


Figure S-2.5 The HMBC (CDCl₃) spectrum of anhydromarmeline (1).

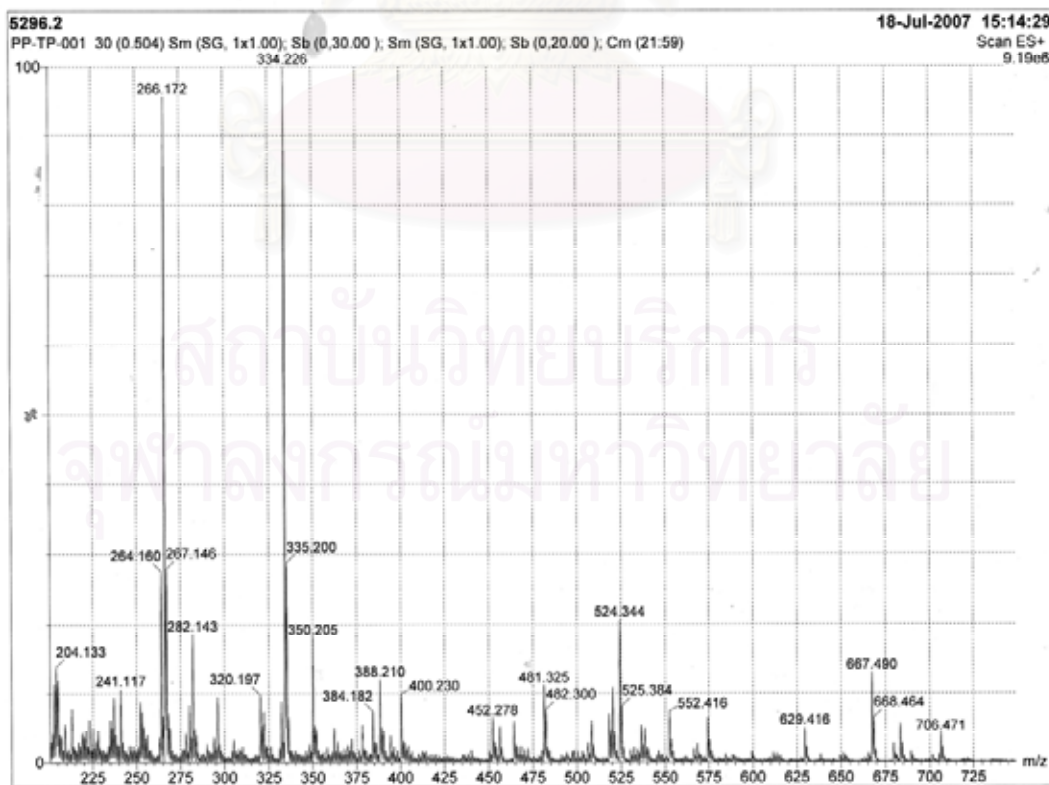


Figure S-2.6 Mass spectrum of anhydromarmeline (1).

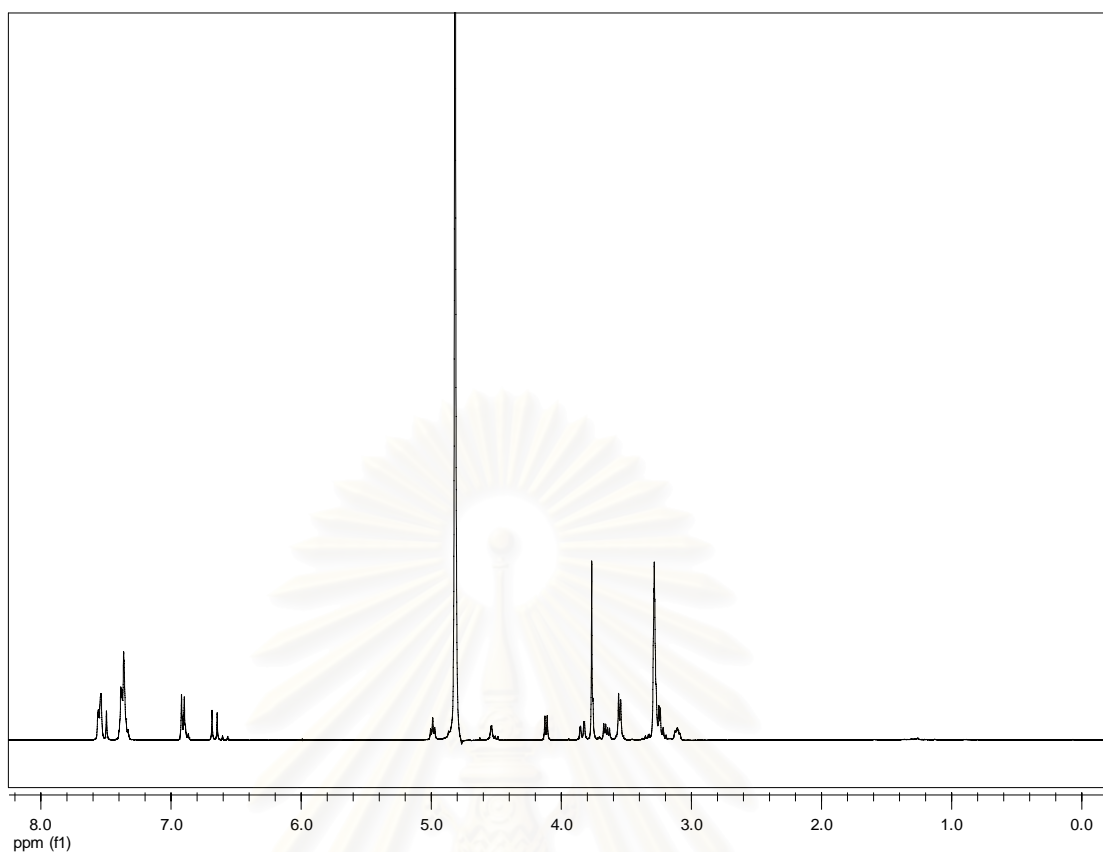


Figure S-2.7 The ^1H NMR (CD_3OD) spectrum of aegelinoside A (**7**).

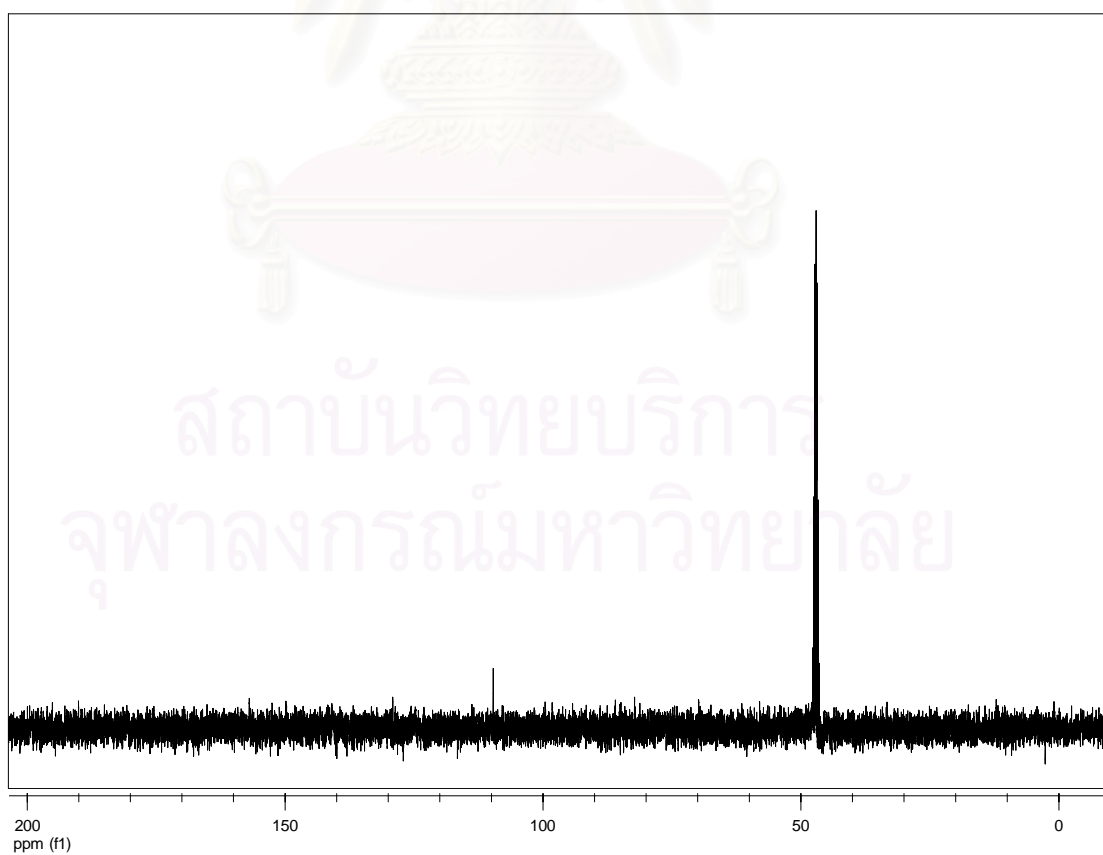


Figure S-2.8 The ^{13}C NMR (CDCl_3) spectrum of aegelinoside A (**7**).

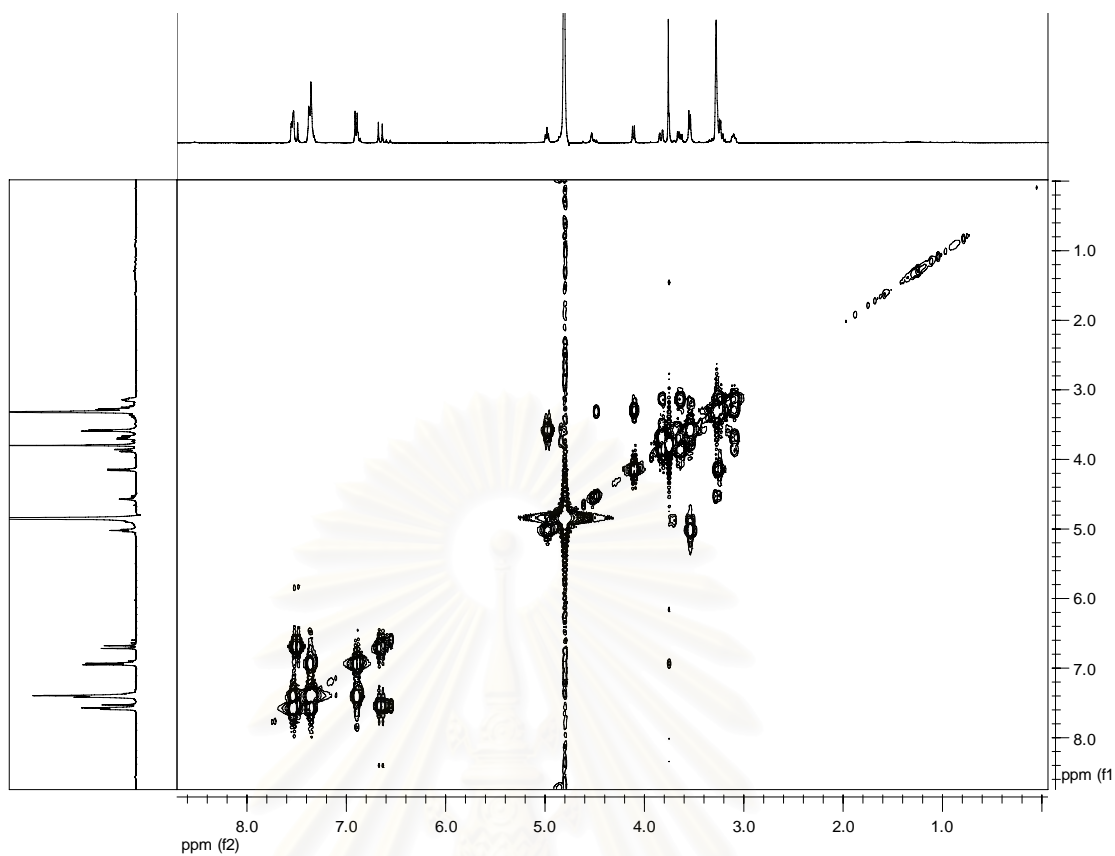


Figure S-2.9 The COSY (CD₃OD) spectrum of aegelinoside A (7).

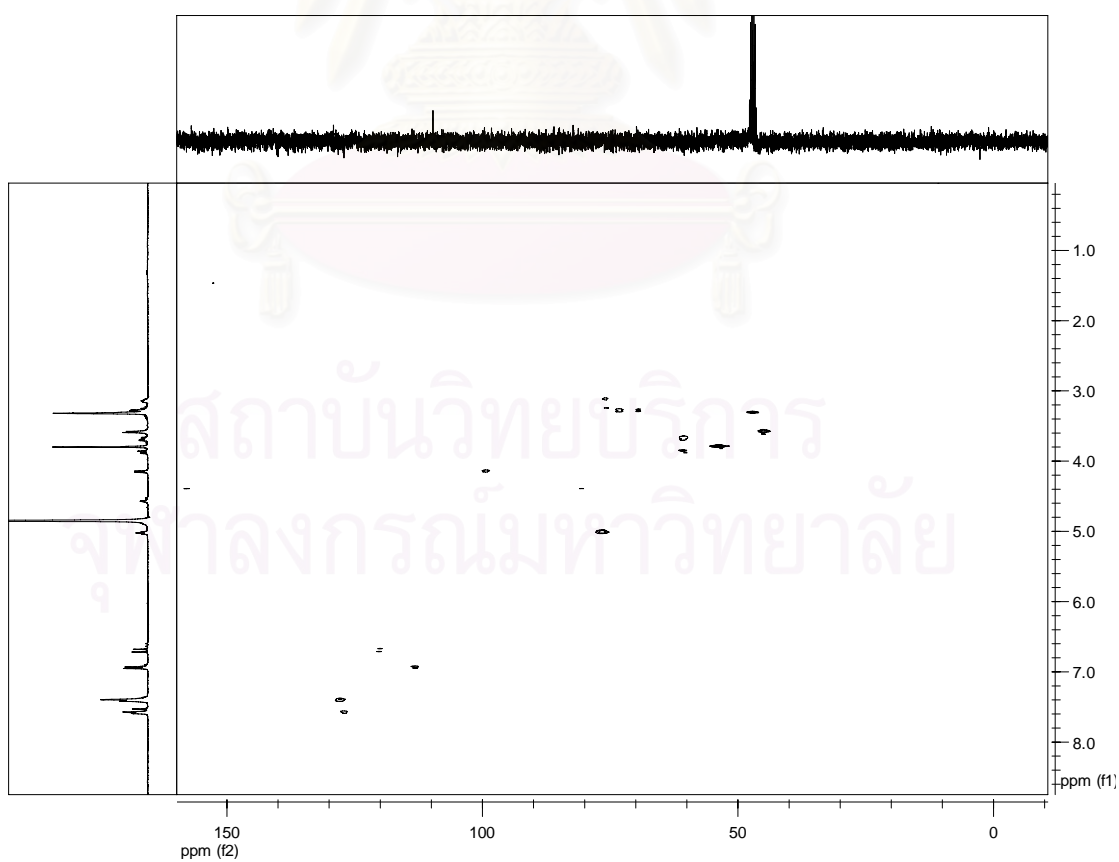


Figure S-2.10 The HSQC (CD₃OD) spectrum of aegelinoside A (7).

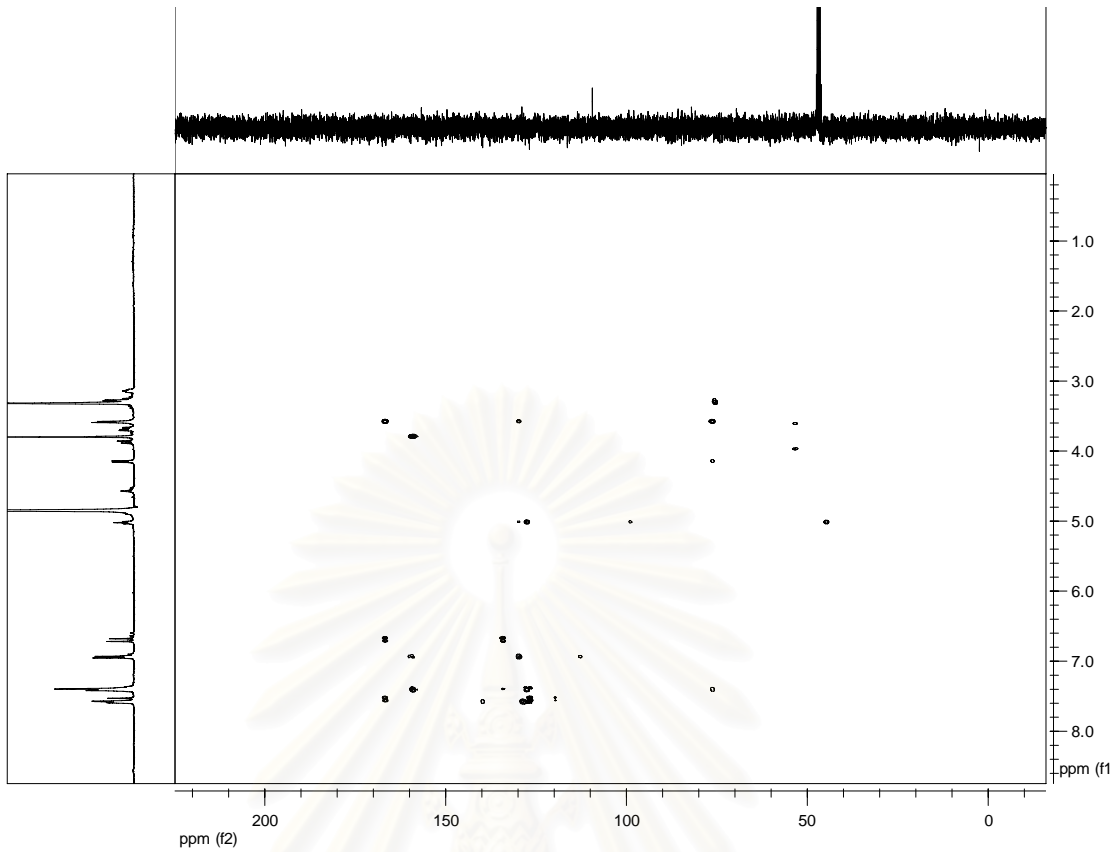


Figure S-2.11 The HMBC (CD_3OD) spectrum of aegelinoside A (7).

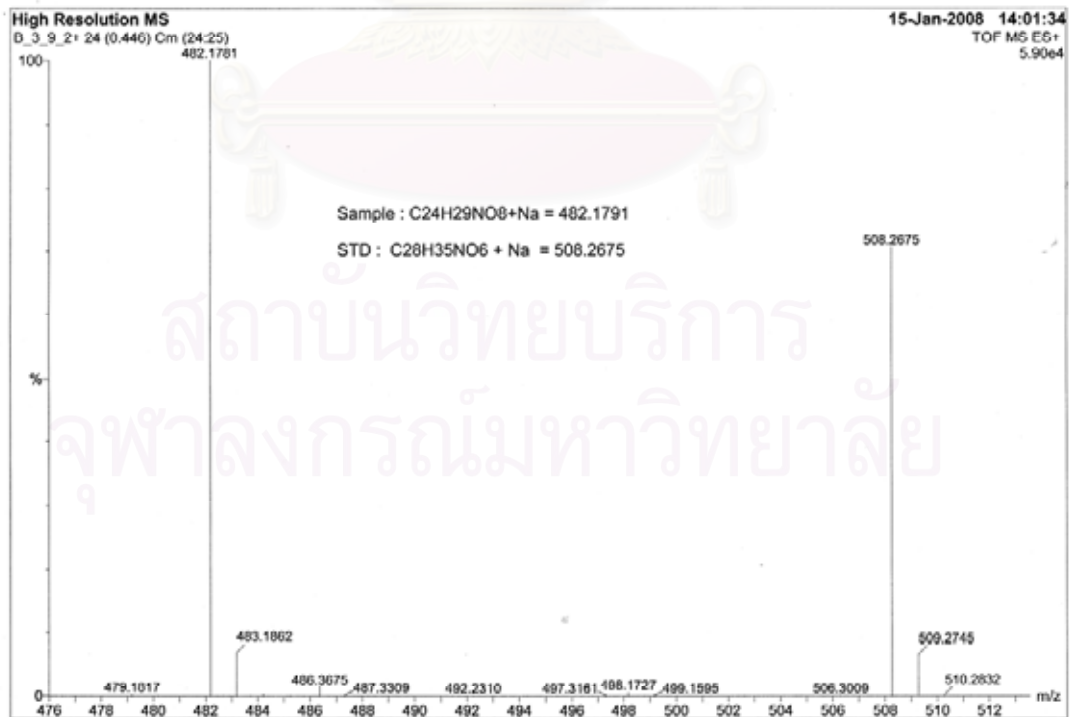


Figure S-2.12 Mass spectrum of aegelinoside A (7).

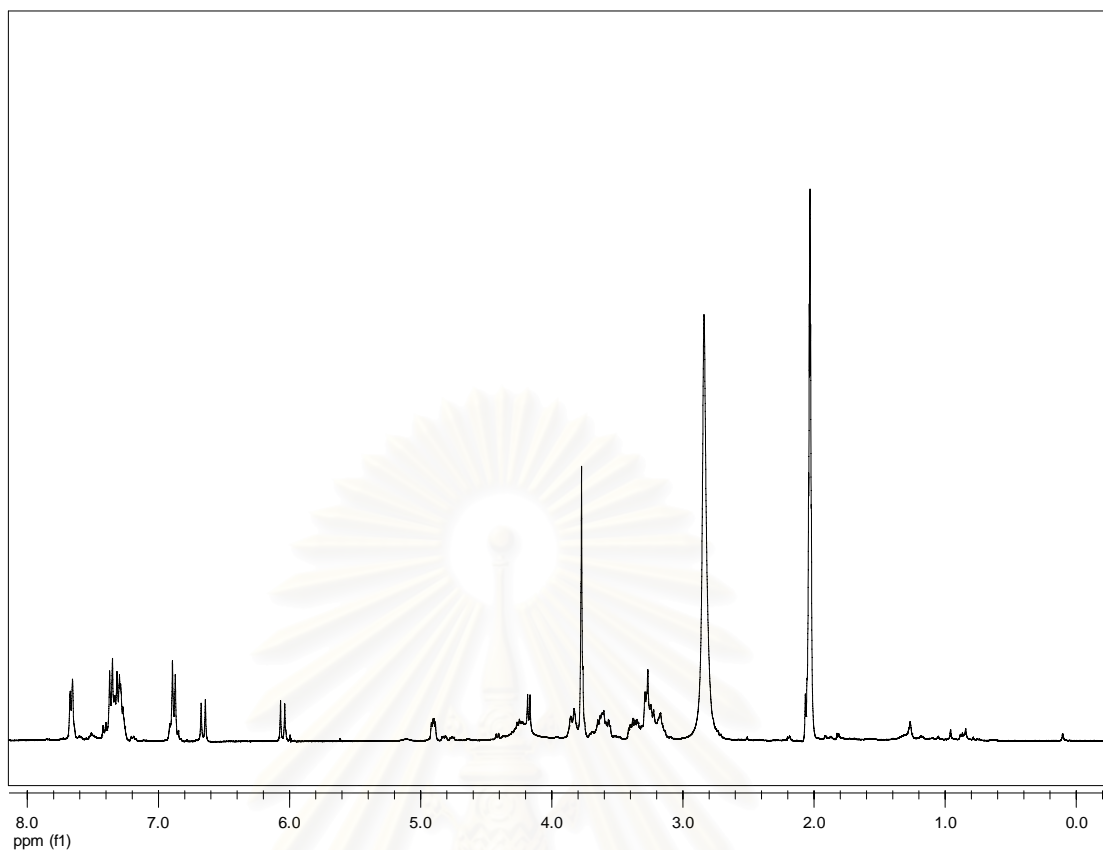


Figure S-2.13 The ^1H NMR (acetone- d_6) spectrum of aegelinoside B (**8**).

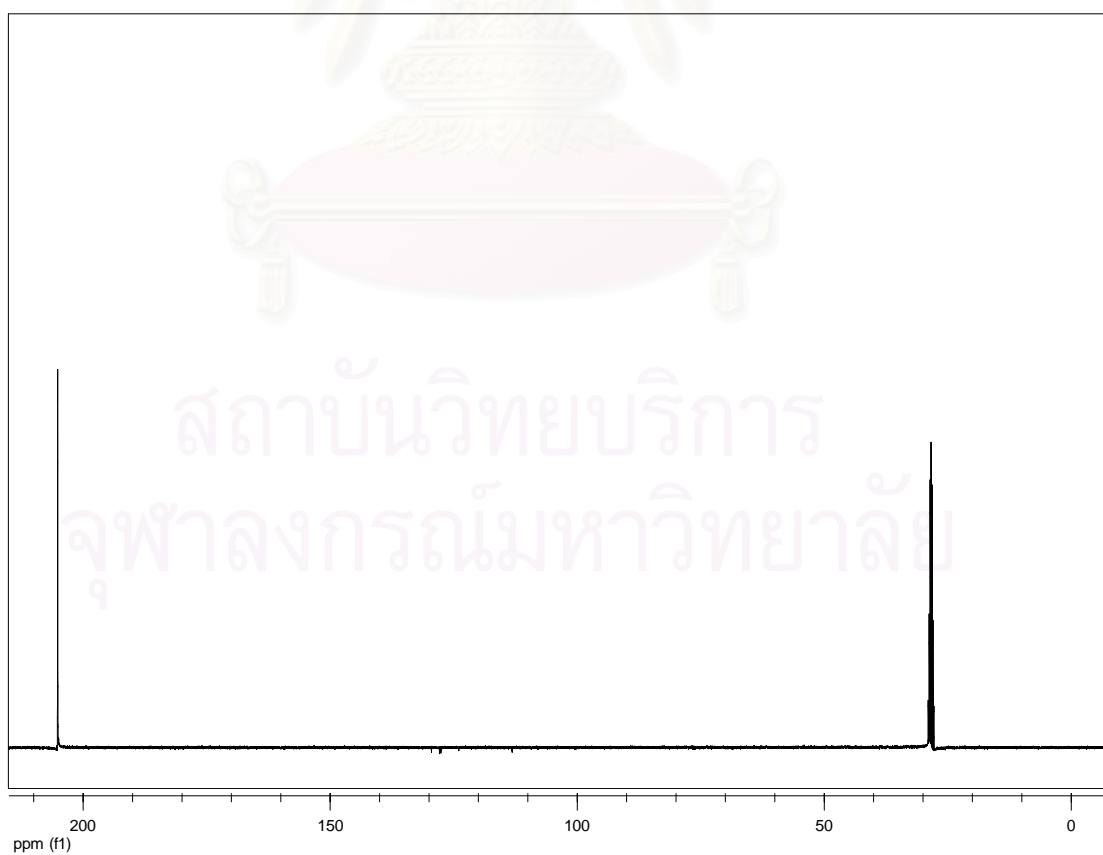


Figure S-2.14 The ^{13}C NMR (acetone- d_6) spectrum of aegelinoside B (**8**).

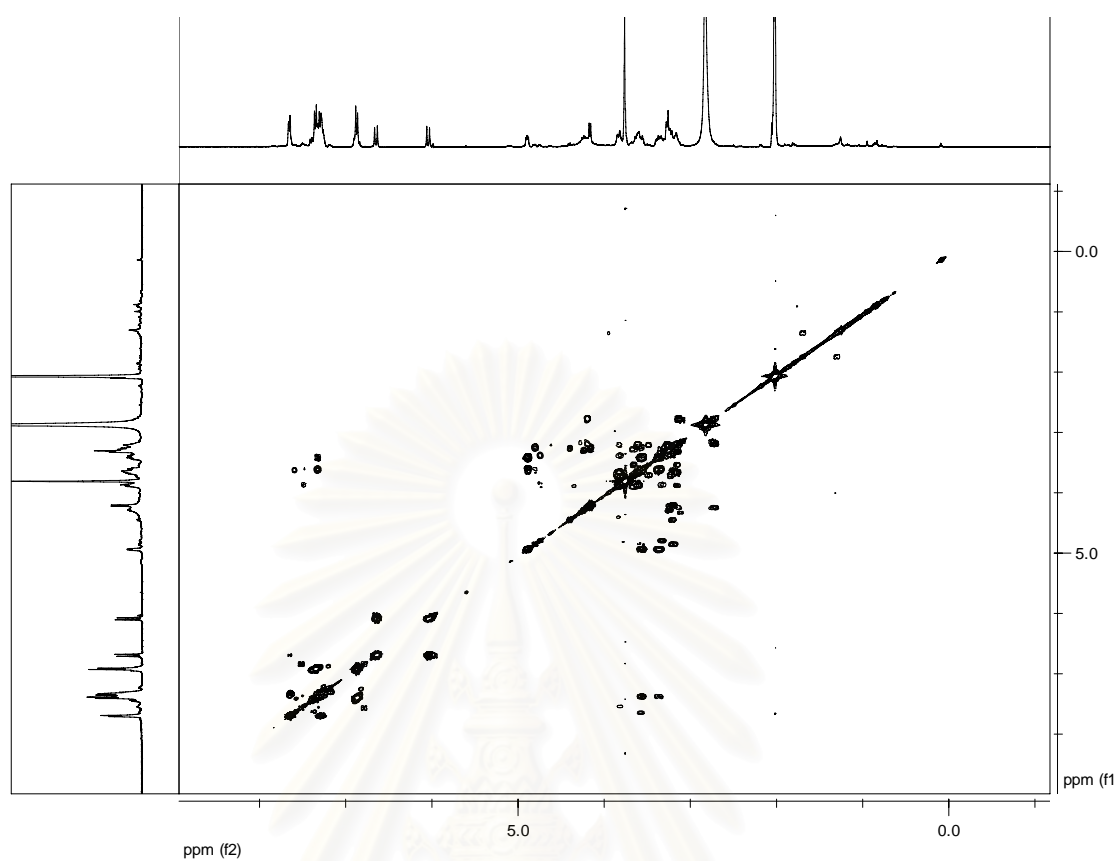


Figure S-2.15 The COSY (acetone- d_6) spectrum of aegelinoside B (**8**).

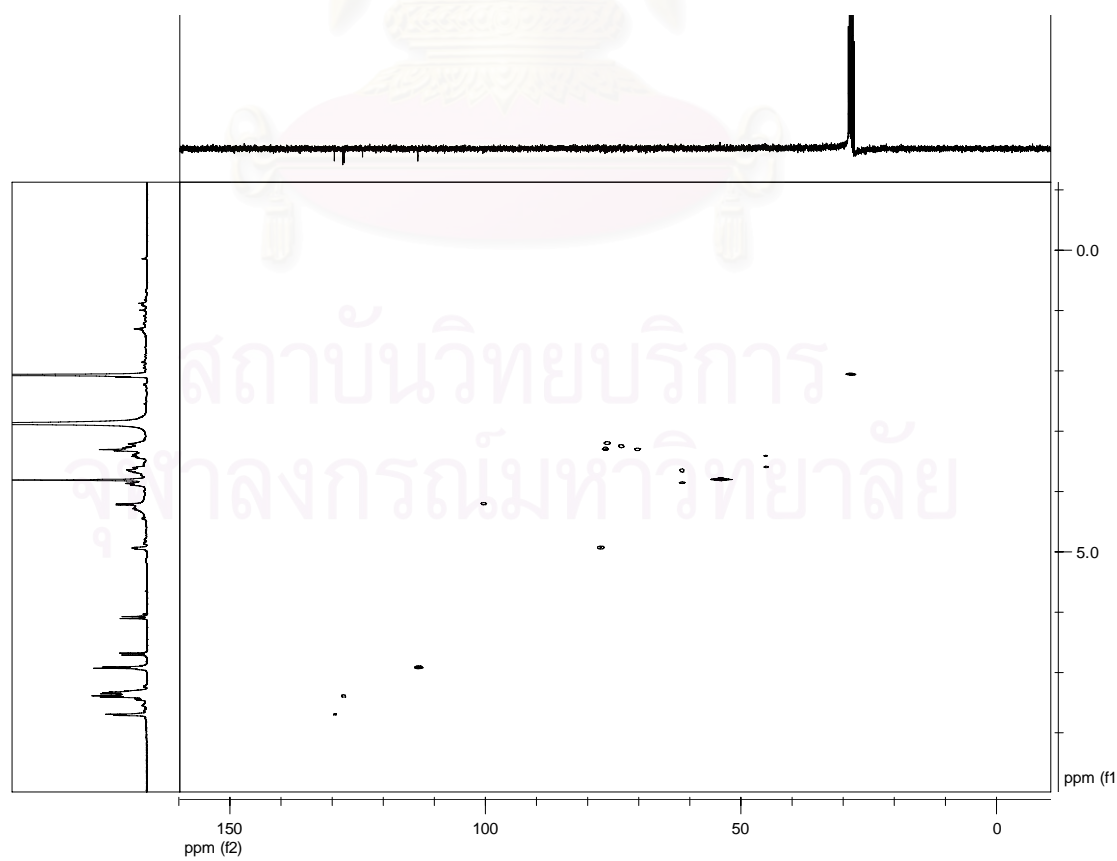


Figure S-2.16 The HSQC (acetone- d_6) spectrum of aegelinoside B (**8**).

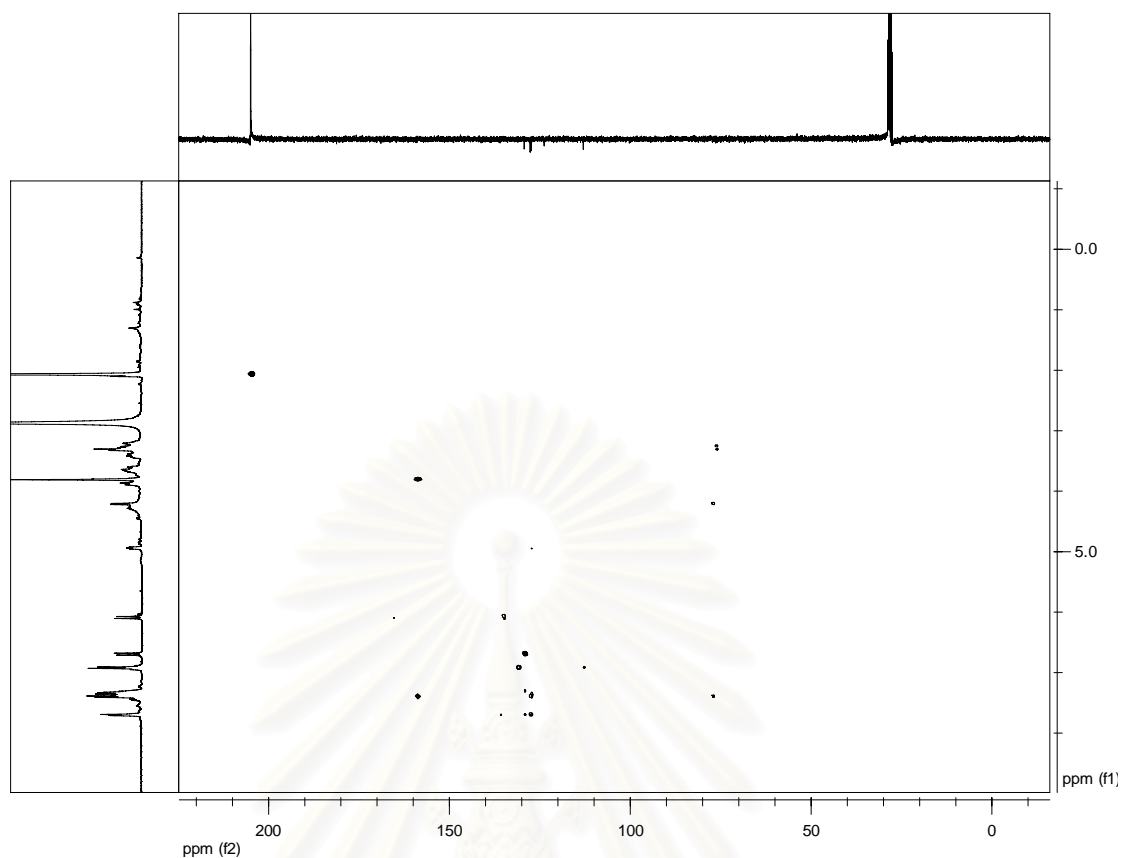


Figure S-2.17 The HMBC (acetone- d_6) spectrum of aegelinoside B (**8**).

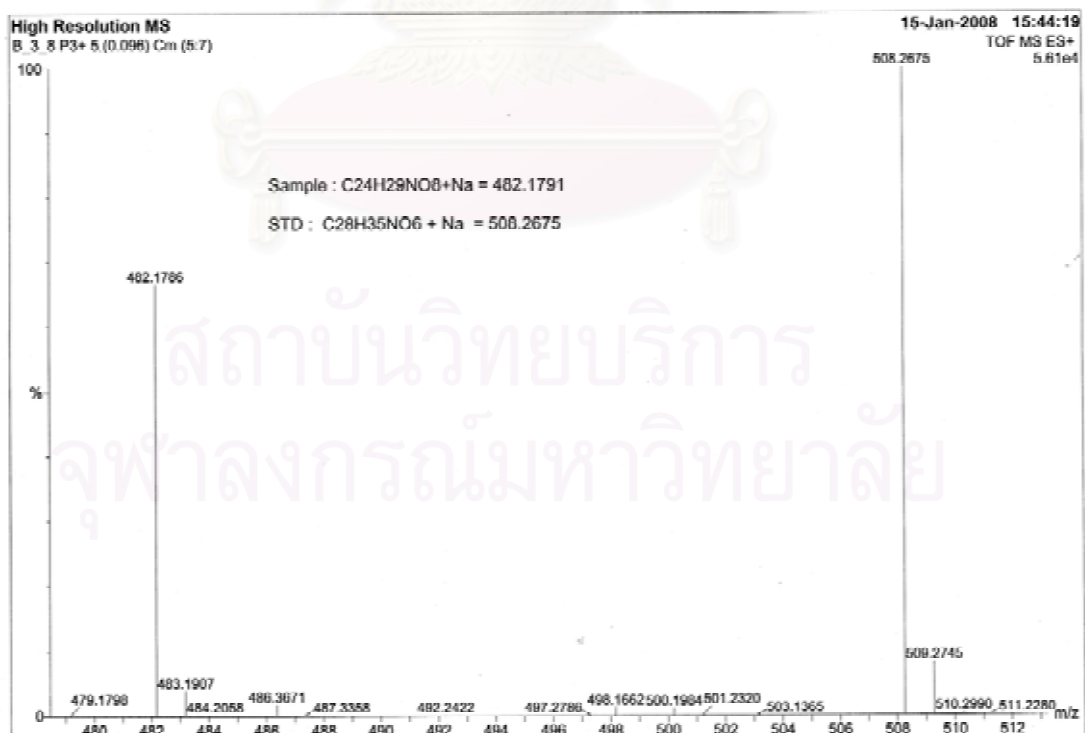


Figure S-2.18 Mass spectrum of aegelinoside B

CHAPTER III

FLAVONOID GLYCOSIDES: α -GLUCOSIDASE INHIBITORS FROM THE LEAVES OF *Aegle marmelos*

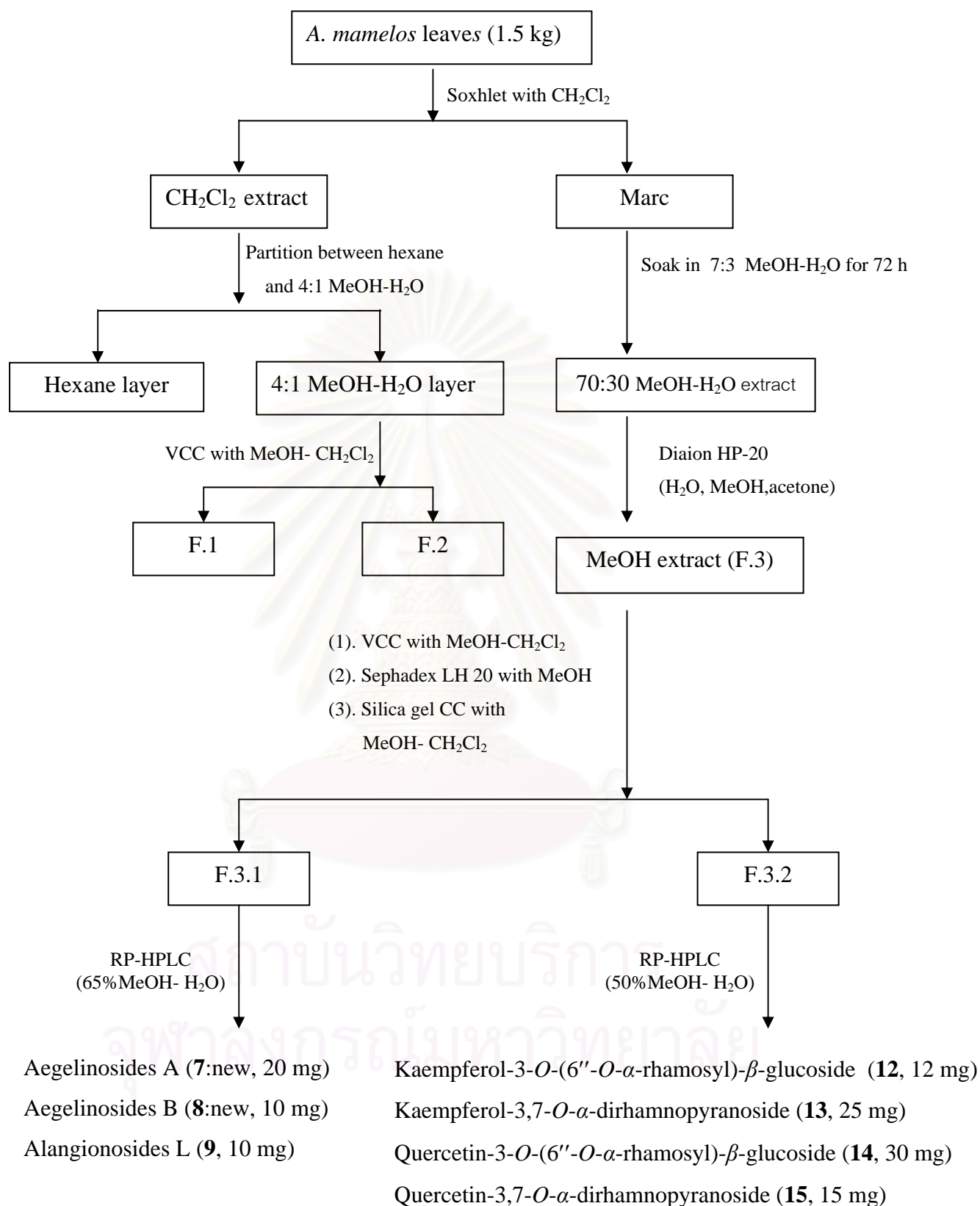
3.1 Introduction

During bioassay-guided isolation of α -glucosidase inhibitors from fraction F.3 (Chapter II), certain fraction (F.3.2) was found to have higher inhibitory effect than the phenylethyl cinnamide fractions. After fraction F.3.2 was preliminarily examined by ^1H NMR technique, the spectrum showed characteristic signals of flavonoid glycosides. To identify the active principles, isolation and purification of fraction F.3.2 were carried out.

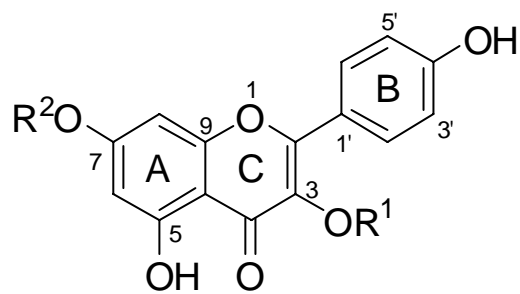
3.2 Results and discussion

3.2.1 Isolation

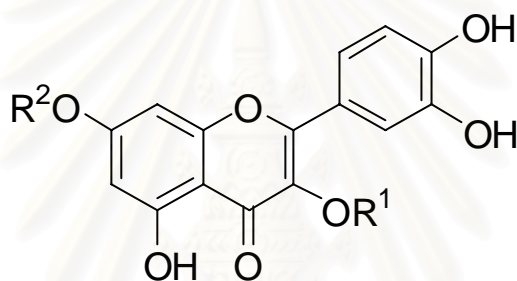
The air dried leaves (1.5 kg) of *Aegle marmelos* were extracted with CH_2Cl_2 in a Soxhlet apparatus (scheme 3.1). The marc was extracted with 7:3 MeOH- H_2O at room temperature for 72 h. The methanolic extract was chromatographed on a Diaion HP-20 column and eluted with H_2O , MeOH and acetone. The MeOH extract was purified by VCC technique. Repeated column chromatography using Sephadex LH-20 followed by silica gel afforded two major fractions (F.3.1 and F.3.2). Fraction 3.1 was separated by reversed-phase preparative HPLC using MeOH- H_2O to afford **7**, **8**, and **9** (chapter II). Fraction 3.2 was purified by reversed-phase preparative HPLC using MeOH- H_2O (1:1) to obtain four known flavonoid glycosides: kaempferol-3-*O*-(6''-*O*- α -rhamosyl)- β -glucoside (**12**), kaempferol-3,7-*O*- α -rhamnopyranoside (**13**), quercetin-3-*O*-(6''-*O*- α -rhamosyl)- β -glucoside (**14**), and quercetin-3,7-*O*- α -rhamnopyranoside (**15**) (Figure 3.1). The structures of known compounds were identified by comparison of their ^1H and ^{13}C NMR data with previous reports.



Scheme 3.1 Isolation procedure of flavonoid glycosides from *Aegle marmelos* leaves.



- 12 $R^1 = \text{Glc}(6-1)\text{Rha}$ $R^2 = \text{H}$
 13 $R^1 = \text{Rha}$ $R^2 = \text{Rha}$



- 14 $R^1 = \text{Glc}(6-1)\text{Rha}$ $R^2 = \text{H}$
 15 $R^1 = \text{Rha}$ $R^2 = \text{Rha}$

Figure 3.1 The chemical structures of flavonoid glycoside from *Aegle marmelos* leaves.

สถาบันวิทยบริการ
 จุฬาลงกรณ์มหาวิทยาลัย

3.2.2 Structure elucidation of kaempferol-3-*O*-(6''-*O*- α -rhamosyl)- β -glucoside (**12**)

Kaempferol-3-*O*-(6''-*O*- α -rhamosyl)- β -glucoside (nicotiflorin) (**12**) was obtained as yellow liquid. The positive ion ESIMS spectrum of **12** exhibited $[M+Na]^+$ ion at m/z 617.269 which was consistent with the molecular formula of $C_{28}H_{34}O_{14}$. The 1H and ^{13}C NMR spectrum of **12** showed characteristic signals of kaempferol and sugar moieties. The identity of kaempferol was verified from the two doublets for aromatic ring B at δ_H 8.08 (2H, $J = 8.8$ Hz) and 6.92 (2H, $J = 8.8$ Hz) which were assigned to H-2'/H-6' and H-3'/H-5', respectively. The two meta coupled protons resonated at δ_H 6.24 and 6.44 ($J = 1.6$ Hz), were assigned for H-6 and H-8, respectively in aromatic ring A. In addition, the presence of two anomeric protons at δ_H 5.21 (d, $J = 6.8$ Hz) and δ_H 4.53 (s), as well as one methyl groups at δ_H 1.12 indicated that compound **12** comprised rhamnose and glucose units. The HMBC correlation observed between the anomeric proton at δ_H 4.53 (H-1''') and C-6'' (δ_C 67.2) indicate that rhamnose was connected to the C-6'' position of glucose. The large coupling constant ($J = 6.8$ Hz) of H-1'' indicated that β -configuration of glucose while HMBC correlation between H-1'' and C-3 confirmed glucosidic linkage to kaempferol. The complete structure and key HMBC correlation for **12** were shown in Figure 3.2.

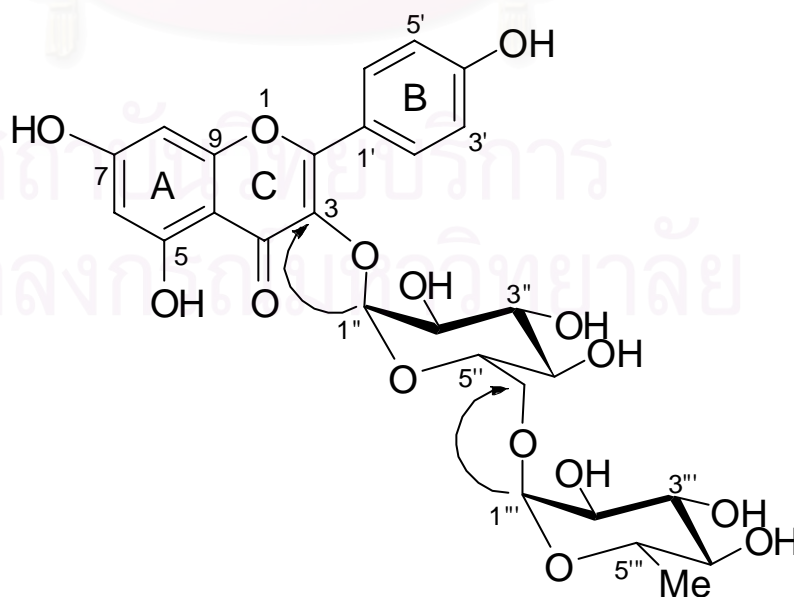


Figure 3.2 Key HMBC correlations of **12**.

3.2.3 Structure elucidation of kaempferol-3,7-*O*- α -dirhamnopyranoside (13)

Kaempferol-3,7-*O*- α -dirhamnopyranoside (**13**) was obtained as yellow liquid. The positive ESIMS spectrum of **13** exhibited $[M+Na]^+$ ion at m/z 602.172, which was consistent with the molecular formula of $C_{27}H_{30}O_{14}$. The 1H and ^{13}C NMR spectra of **13** were similar to those of **12** except for the presence of two doublet methyl groups at δ_H 0.94 and 1.26, which were ascribable to two rhamnose units. The glycosidic linkages between rhamnosyl units and aglycone were determined by HMBC correlations of H-1''/C-3 and H-1'''/C-7. The configuration of the anomeric protons were defined as α -orientation by their small coupling constants of H-1'' and H-1'''. The NMR data of **13** were coincided well with those previously published (Mulinacci *et al.*, 1995; Fico *et al.*, 2003).

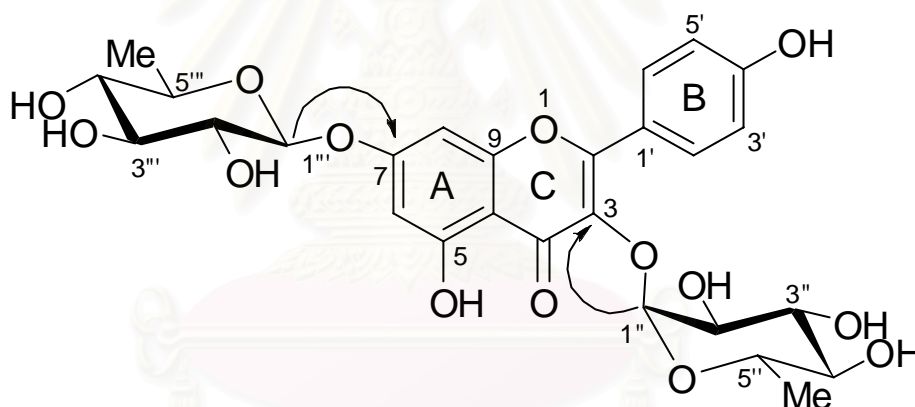


Figure 3.3 Key HMBC correlations of **13**.

สถาบันวิทยบริการ
จุฬาลงกรณ์มหาวิทยาลัย

3.2.4 Structure elucidation of quercetin-3-O-(6''-O- α -rhamosyl)- β -glucoside (**14**)

Quercetin-3-O-(6''-O- α -rhamosyl)- β -glucoside or rutin (**14**) was obtained as yellow liquid. The positive ESIMS spectrum of **14** exhibited $[M+Na]^+$ ion at m/z 617.269, which was consistent with the molecular formula of $C_{28}H_{34}O_{14}$. The 1H and ^{13}C NMR spectrum of **14** showed a typical pattern of a flavonol glycoside. The aglycone moiety was identified as quercetin from two methine signals at δ_H 6.15 and 6.34, which were assigned to H-6 and H-8 for aromatic ring A, and three resonances at δ_H 7.48 (s), 6.80 (d, $J = 8.8$ Hz) and 7.50 (d, $J = 8.8$ Hz) for the ring B. The presence two anomeric protons appeared at δ_H 5.30 (d, $J = 7.2$ Hz) and 4.34 (s), as well as one methyl groups at δ_H 0.95 indicated that the sugar moieties contained rhamnose and glucose unit. The signal at δ_H 5.30 (H-1'') of the anomeric proton correlated with the resonance at δ_C 136.5 (C-3), indicating that glucose was connected through C-3 with a coupling constant characteristic of β -configuration. The HMBC correlation observed between the anomeric proton at δ_H 4.34 (H-1''') and C-6'' (δ_C 67.5) indicated that rhamnose was connected to the C-6'' position of glucose (Figure 3.4). The NMR data of **14** were consistent with those previously reported in *Morinda cifrifolia* (Wang *et al.*, 1999).

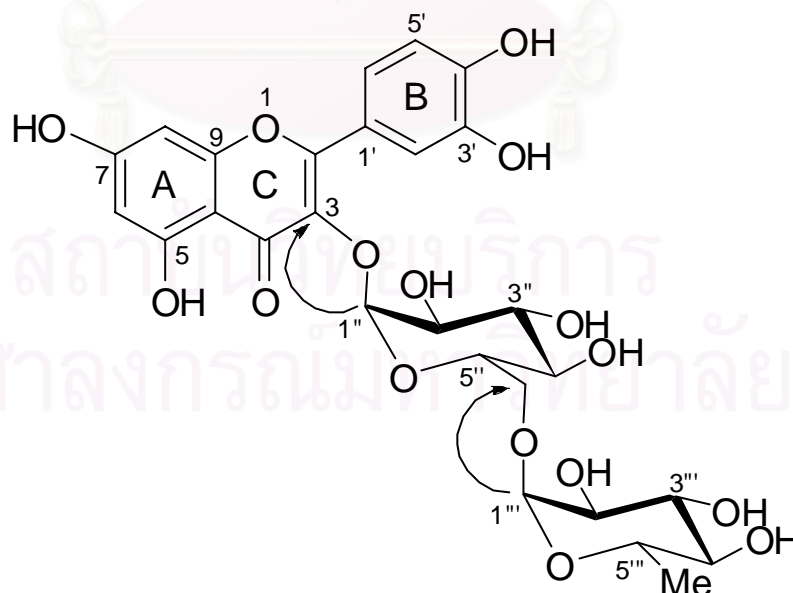


Figure 3.4 Key HMBC correlations of **14**.

3.2.5 Structure elucidation of quercetin 3,7-*O*- α -dirhamnopyranoside (**15**)

Quercetin-3,7-*O*- α -dirhamnopyranoside (**15**) was obtained as yellow liquid. The positive ESIMS spectrum of **15** exhibited $[M+Na]^+$ ion at m/z 617.372, which was consistent with the molecular formula of $C_{27}H_{30}O_{15}$. The NMR spectra of **15** showed signals similar to those of **14**, except the presence of two methyl groups at δ_H 0.95 and 1.08, indicating that **15** comprised the two rhamnose units. The HMBC correlations between the anomeric proton at δ_H 5.21 (H-1'') and C-3 (δ_C 135.0) as well as between H-1''' (δ_H 5.51) and C-7 (δ_C 162.2) indicated the *O*-linkage of α -rhamnosides to the aglycone (Figure 3.5). The NMR data of **15** were coincided well with those previously published (Fico *et al.*, 2003).

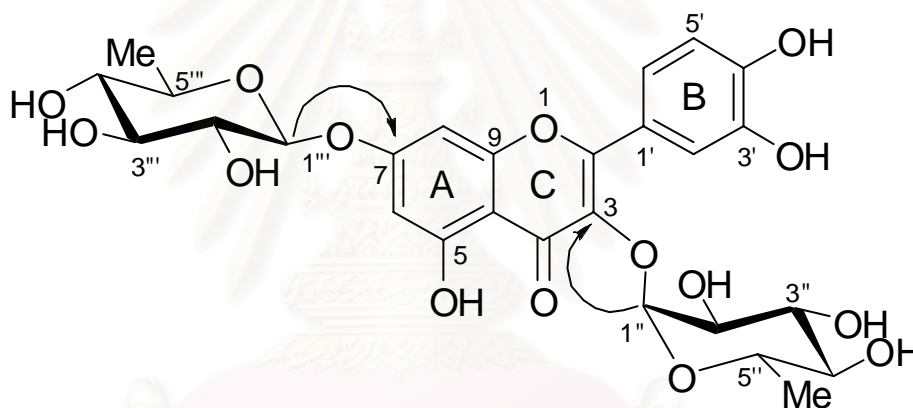


Figure 3.5 Key HMBC correlations of **15**.

สถาบันวิทยบริการ
จุฬาลงกรณ์มหาวิทยาลัย

3.2.6 α -Glucosidase inhibitory activity of the isolated compounds

The α -glucosidase inhibitory activities of flavonoid glycosides (**12-15**) were evaluated by colorimetric method and the results are shown in Table 3.1.

Table 3.1 α -Glucosidase inhibitory effect of flavonoid glycosides (**12-15**)

Compound	IC ₅₀ (mM)
Kaempferol 3- <i>O</i> -(6''- <i>O</i> - α -rhamosyl)- β -glucoside (12)	0.62 \pm 0.04
Kaempferol 3,7- <i>O</i> - α -dirhamnopyranoside (13)	0.77 \pm 0.01
Quercetin-3- <i>O</i> -(6''- <i>O</i> - α -rhamosyl)- β -glucoside (14)	0.34 \pm 0.03
Quercetin 3,7- <i>O</i> - α -dirhamnopyranoside (15)	0.46 \pm 0.02
Acarbose ^{® a}	0.62 \pm 0.03
1-Deoxynojirimycin(DNJ) ^a	0.17 \pm 0.02

^aStandard control

According to table 3.1, quercetin-3-*O*-(6''-*O*- α -rhamosyl)- β -glucoside (**14**) showed the strongest inhibitory effect among the flavonol glycosides with the IC₅₀ value of 0.34 mM, while quercetin-3,7-*O*- α -dirhamnopyranoside (**15**) was also found to be active against α -glucosidase with slightly less extent (IC₅₀ 0.46 mM). Both **14** and **15** were found to have higher inhibitory activity than the positive control acarbose[®] (IC₅₀ 0.62 mM). On the other hand, kaempferol-3-*O*-(6''-*O*- α -rhamosyl)- β -glucoside (**12**) showed comparable α -glucosidase inhibitory activity to acarbose[®], while kaempferol 3,7-*O*- α -dirhamnopyranoside (**13**) showed moderate inhibition with IC₅₀ value of 0.77 mM.

Apparently phenolic hydroxyl groups at C-3' and C-4' of ring B played a key role in inhibitory activity. The highest activity was observed for compounds **14** and **15**, compared to compounds **12** and **13**. The structure activity relationships of these flavonoid glycosides were in agreement with data reported in the literature (Shibano *et al.*, 2008; Lee *et al.*, 2008). These results suggested that the inhibitory activity was dependent upon the number of hydroxyl groups on the flavonoid B ring. Hence, the 3'-OH and 4'-OH substitution found in compounds **14** and **15** were crucial, primarily

as H-bonding donor to interact directly with a specific part of the enzyme by constructing an H-bond, while 4'-OH in compounds **12** and **13** attributed less extent.

A comparison of flavonol glycosides having glycosylation on ring A (**13** and **15**) with the corresponding hydroxylated compounds (**12** and **14**) revealed that replacement of hydroxyl group on ring A obviously enhanced the inhibitory activity (**14** > **15** and **12** > **13**). Therefore 7-OH was critical in exerting inhibitory activity, which was consistent with those previously published (Matsumoto *et al.*, 2004; Matsui *et al.*, 2004; Kawaguchi *et al.*, 2007)

It should be noted that flavonol glycosides containing one sugar unit attached to C-3 of ring C revealed weaker inhibitory activity than those having two sugar units. This observation was consistent with those reported by Matsumoto *et al.*

In summary, the enhanced activity should be found in flavonol glycoside containing hydroxyl groups at C-3' and C-4' of ring B and C-7 of ring A, as well as two sugar units at C-3 of ring C. Of particular interest, compound **14**, a major effective constituent of *A. marmelos* leaves, was approximately 2 times higher active than acarbose®. Therefore **14** would be expected to delay absorption of dietary carbohydrates in small intestine, leading to suppression of plasma glucose.

3.3 Experiment section

3.3.1 General experimental procedures

The ^1H and ^{13}C -NMR spectra (in CD_3OD and $\text{DMSO-}d_6$) were recorded with a Varian Mercury+ 400 NMR spectrometer. The chemical shift in δ (ppm) was assigned with reference to the signals of residual protons in deuterated solvents, and TMS was used as an internal standard in some cases. ESIMS were obtained from Model VG TRIO 2000 MS Spectrometer. Adsorbents used for separation were silica gel 60 Merck, No. 7734 and 7729 for column chromatography (TLC) was performed on aluminium sheets precoated with silica gel (Merck Kieselgel 60 PF254). Gel filtration chromatography was performed on sephadex LH-20. Column chromatography was performed with Diaion HP-20. UV spectra were recorded on Shimadzu UV-160A photodiode array spectrophotometer. HPLC was conducted on Water[®] 600 controller equipped with a Water[®] 2996 photodiode array detector (USAd). Cosmosil 5C18-ARII column (10 × 250 mm) was used for separation purpose.

3.3.2 Plant material

The leaves of *Aegle marmelos* were collected in Nakhon Phathom, Thailand in April 2007.

3.3.3 Extraction and isolation

The air-dried leaves of *Aegle marmelos* (1.5 kg) were extracted with CH_2Cl_2 using Soxhlet extractor. The marc was extracted with 7:3 MeOH- H_2O at room temperature for 72 h. The 7:3 MeOH- H_2O extract was loaded onto Diaion HP-20 and excessively eluted with H_2O , MeOH and acetone. The combined MeOH fractions (60 g) was separated by VCC (stepwise 5:95, 10:90, 15:85, 50:50, 70:30 and 100:0 MeOH- CH_2Cl_2). The combined fractions eluted with 15:85 and 50:50 MeOH- CH_2Cl_2 were subsequently purified by Sephadex LH-20 (3:7 MeOH- CH_2Cl_2) followed by silica gel (20:80 MeOH- CH_2Cl_2) to obtain two major fractions (3.1 and 3.2). Fraction

3.1 was separated by reversed-phase preparative HPLC (ODS, 65:35 MeOH-H₂O, UV 254 nm) to afford **7**, **8**, and **9**. Fraction 3.2 was purified by HPLC using (ODS, 50:50 MeOH-H₂O, UV 254 nm), yielding four known flavonoid glycosides, kaempferol-3-*O*-(6''-*O*- α -rhamosyl)- β -glucoside (**12**, 12 mg, 8.0×10^{-4} % w/w, t_R 51.5 min), kaempferol-3,7-*O*- α -dirhamnopyranoside (**13**, 25 mg, 1.7×10^{-3} % w/w, t_R 35.4 min), quercetin-3-*O*-(6''-*O*- α -rhamosyl)- β -glucoside (**14**, 30 mg, 2.0×10^{-3} % w/w, t_R 28.9 min), and quercetin-3,7-*O*- α -dirhamnopyranoside (**15**, 15 mg, 1.0×10^{-3} % w/w, t_R 22.6 min). The structure of known compounds were identified by comparison of their ¹H and ¹³C NMR data with those in the previous reports.

Kaempferol-3-*O*-(6''-*O*- α -rhamosyl)- β -glucoside (**12**): yellow liquid, ¹H NMR (CD₃OD, 400 MHz) δ_H 8.08 (2H, d, $J = 8.8$ Hz, H-2' and H-6'), 6.92 (2H, d, $J = 8.8$ Hz, H-3' and H-5'), 6.24 (1H, d, $J = 1.6$ Hz, H-6), 6.44 (1H, d, $J = 1.6$ Hz, H-8), 5.21 (1H, d, $J = 6.8$ Hz, H-1''), 3.45 (1H, m, H-2''), 3.41 (1H, m, H-3''), 3.50 (1H, m, H-4''), 3.28 (1H, m, H-5''), 3.81 and 3.38 (2H, m, H-6''), 4.53 (1H, br s, H-1'''), 3.62 (1H, m, H-2'''), 3.52 (1H, m, H-3'''), 3.35 (1H, m, H-4'''), 1.03 (3H, d, $J = 6.0$ Hz, H-6''') ¹³C NMR (CD₃OD, 100 MHz) δ_C 157.8 (C-2), 133.6 (C-3), 157.4 (C-5), 99.0 (C-6), 165.1 (C-7), 93.8 (C-8), 161.6 (C-9), 104.4 (C-10), 121.4 (C-1'), 131.2 (C-2' and C-6'), 115.0 (C-3' and C-5'), 103.0 (C-1''), 76.0 (C-2''), 76.8 (C-3''), 74.4 (C-4''), 70.2 (C-5''), 67.2 (C-6''), 101.5 (C-1'''), 70.8 (C-2'''), 71.2 (C-3'''), 72.4 (C-4'''), 68.5 (C-5'''), 20.2 (C-6''').

Kaempferol 3,7-*O*- α -dirhamnopyranoside (**13**) yellow liquid, ¹H NMR (CD₃OD, 400 MHz) δ_H 7.82 (2H, d, $J = 8.4$ Hz, H-2' and H-6'), 6.92 (2H, d, $J = 8.4$ Hz, H-3' and H-5'), 6.50 (1H, br s, H-6), 6.76 (1H, br s, H-8), 5.41 (1H, br s, H-1''), 4.20 (1H, br s, H-2''), 3.70 (1H, m, H-3''), 3.59 (1H, m, H-4''), 3.35 (1H, m, H-5''), 0.95 (3H, d, $J = 6.0$ Hz, H-6''), 5.57 (1H, br s, H-1'''), 4.02 (1H, br s, H-2'''), 3.82 (1H, m, H-3'''), 3.65 (1H, m, H-4'''), 3.51 (1H, m, H-5'''), 1.26 (3H, d, $J = 6.0$ Hz, H-6''') ¹³C NMR (CD₃OD, 100 MHz) δ_C 158.4 (C-2), 134.5 (C-3), 156.8 (C-5), 99.5 (C-6), 161.7 (C-7), 94.5 (C-8), 106.5 (C-10), 121.0 (C-1'), 130.8 (C-2' and C-6'), 115.5 (C-3' and C-5'), 102.8 (C-1''), 70.5 (C-2''), 70.7 (C-3''), 70.0 (C-4''), 71.7 (C-5''), 16.5 (C-6''), 98.5 (C-1'''), 70.3 (C-2'''), 70.4 (C-3'''), 69.9 (C-4'''), 72.2 (C-5'''), 16.8 (C-6''').

Quercetin-3-*O*-(6''-*O*- α -rhamosyl)- β -glucoside (rutin) (**14**) yellow liquid, ^1H NMR (DMSO- d_6 , 400 MHz) δ_{H} 12.52 (1H, s, 5-OH), 7.49 (2H, br d, $J = 8.8$ Hz, H-2' and H-6'), 6.80 (1H, d, $J = 8.8$ Hz, H-5'), 6.15 (1H, br s, H-6), 6.34 (1H, br s, H-8), 5.30 (1H, d, $J = 6.8$ Hz, H-1''), 4.34 (1H, br s, H-1'''), 4.34 (1H, m, H-2'''), 0.95 (3H, d, $J = 6.0$ Hz, H-6''') and 3.00-3.84 (sugar protons) ^{13}C NMR (DMSO- d_6 , 100 MHz) δ_{C} 157.1 (C-2), 136.5 (C-3), 156.5 (C-5), 99.6 (C-6), 164.8 (C-7), 94.2 (C-8), 161.7 (C-9), 104.9 (C-10), 121.5 (C-1'), 116.6 (C-2'), 145.2 (C-3'), 148.9 (C-4'), 115.6 (C-5'), 122.1 (C-6'), 102.6 (C-1''), 67.5 (C-6''), 101.5 (C-1'''), 71.0 (C-2'''), 72.2 (C-4'''), 68.6 (C-5'''), 18.2 (C-6''').

Quercetin 3,7-*O*- α -dirhamnopyranoside (**15**) yellow liquid, ^1H NMR (DMSO- d_6 , 400 MHz) δ_{H} 12.55 (1H, s, 5-OH), 7.25 (1H, d, $J = 8.4$ Hz, H-6'), 6.83 (1H, d, $J = 8.4$ Hz, H-5'), 7.30 (1H, br s, H-2'), 6.41 (1H, br s, H-6), 6.72 (1H, br s, H-8), 5.21 (1H, d, $J = 6.8$ Hz, H-1''), 0.95 (3H, d, $J = 6.0$ Hz, H-6'''), 5.51 (1H, br s, H-1'''), 3.35 (1H, m, H-5'''), 1.08 (3H, d, $J = 6.0$ Hz, H-6''') and 3.00-3.84 (sugar protons) ^{13}C NMR (DMSO- d_6 , 100 MHz) δ_{C} 158.2 (C-2), 135.0 (C-3), 156.2 (C-5), 99.8 (C-6), 162.2 (C-7), 94.8 (C-8), 159.0 (C-9), 105.8 (C-10), 120.6 (C-1'), 116.2 (C-2'), 145.6 (C-3'), 149.8 (C-4'), 121.7 (C-6'), 102.2 (C-1''), 71.3 (C-2''), 17.9 (C-6''), 98.8 (C-1'''), 70.5 (C-2'''), 18.7 (C-6''').

3.3.4 α -Glucosidase inhibitory assay

The α -glucosidase inhibitory effect of isolated flavonoid glycosides was evaluated using the same procedure described in Chapter II.

CHAPTER IV

CORCHORUSIDES A AND B, TWO NEW α -GLUCOSIDASE INHIBITORS FROM THE LEAVES OF *Corchorus olitorius*

4.1 Introduction

4.1.1 Botanical aspect and distribution of *Corchorus olitorius*

Corchorus olitorius, commonly known as Jew's Mallow, is an annual herb that belongs to the family Tiliaceae. It is known in Thai as Pokrajow “ปอกระเจา”. There are many different local names such as Nalta Jute (English), Tossa Jute (English), Jute Roax/Rouge (French), Langkapsel-Jute (German), Juta Rosa (Italian), Taiwan-Tsunaso (Japanese) and Zhong-shuo (Chinese). *C. olitorius* is usually known as a fiber plant and cultivated in North Africa, Southeast Asia, The Middle and Near East. *C. olitorius* is an erect woody herb. These are tall, slender, shrubby annuals, 8-12 ft (2.5-3.5 m). Leaves are to 15 cm long short stalked, ovate to elliptic, margin serrated. Leaf blade usually with basal protrusions. Flowers are yellow and the fruits are short-stalked, cylindrical capsule that splits into 5 parts. Seed grayish black, angled.



Figure 4.1 *Corchorus olitorius*.

4.1.2 Phytochemical and pharmacological investigation of *Corchorus olitorius*

Corchorus olitorius has been widely investigated for phytochemical constituents. Previous investigations of this plant have led to the isolation of flavonoids, triterpenoids and cardiac glycosides. The seeds of this plant were found to contain various cardenolide glycosides such as erysimoside, olitoriside, corchoroside A, coroloside, helveticoside, glucoevatromonoside, deglucoacoroloside and evatromonoside (Figure 4.2) (Nakamura *et al.*, 1998). The leaves of *C. olitorius* have revealed the presence of flavonoid glycosides such as quercetin 3-galactoside, quercetin 3-glucoside, quercetin 3-(6-malonylglucoside) and quercetin 3-(6-malonylgalactoside) as well as cinnamic acids named 5-caffeoylquinic acid and 3,5-dicaffeoylquinic acid (Azuma *et al.*, 1999) (Figure 4.3). The ursane triterpenes such as corosin, ursolic acid and corosolic acid, have been isolated from the root of this plant (Hasan *et al.*, 1984) (Figure 4.4).

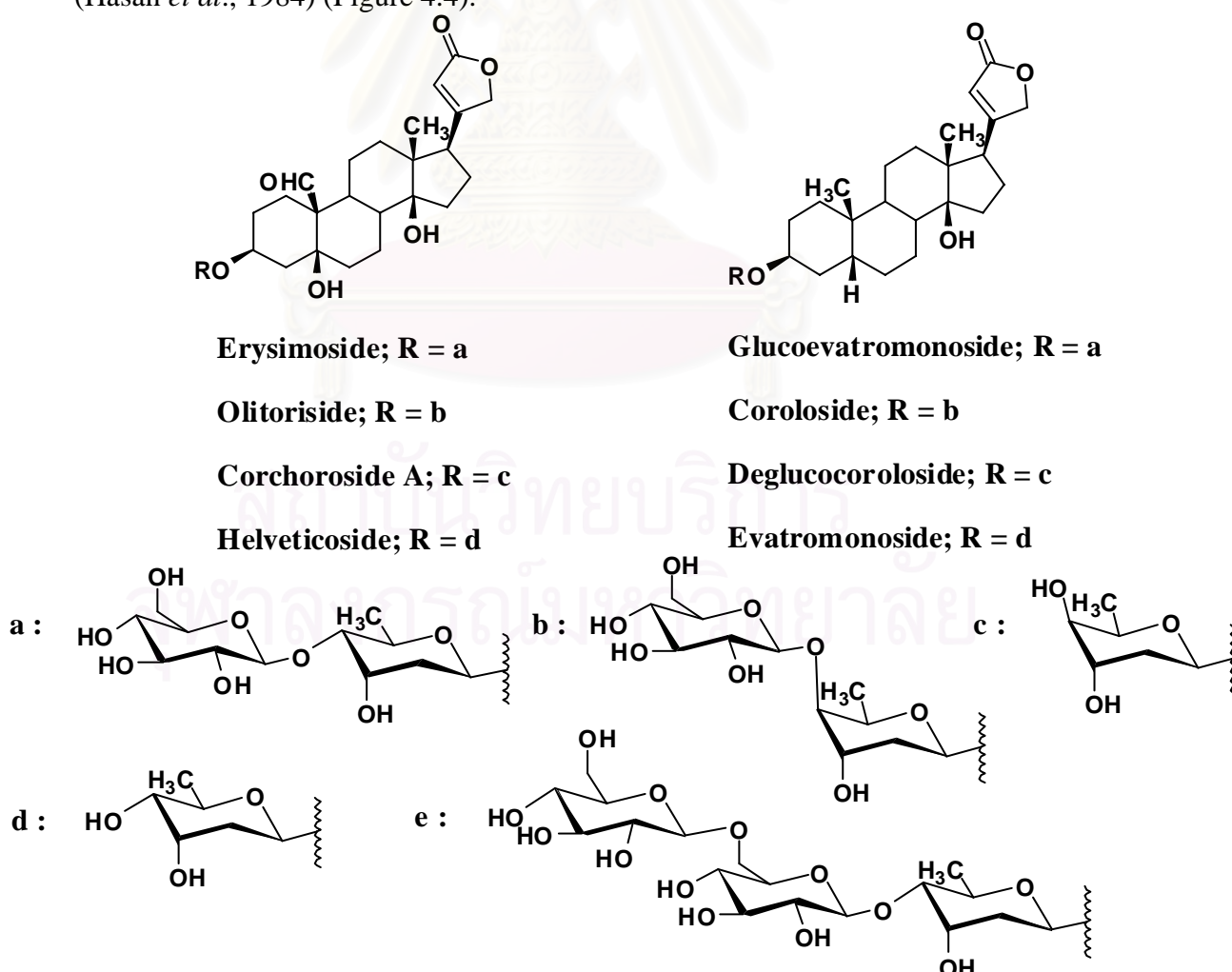
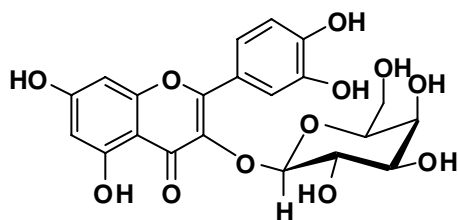
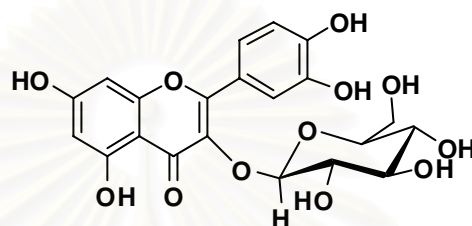


Figure 4.2 Cardenolide glycosides from the seeds of *Corchorus olitorius*



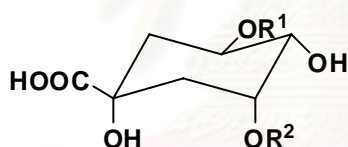
Quercetin 3-galactoside: R = H

Quercetin 3-(6-malonylgalactoside): R = COCH₂CO₂H

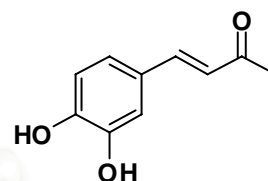


Quercetin 3-glucoside: R = H

Quercetin 3-(6-malonylglucoside): R = COCH₂CO₂H



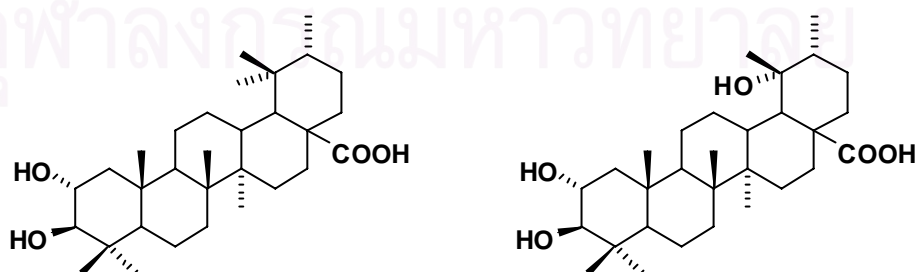
5-Caffeoylquinic acid: R¹ = caffeoyl, R² = H



Caffeoyl

3,5-Dicaffeoylquinic acid: R¹ = caffeoyl, R² = caffeoyl

Figure 4.3 Flavonoid glycosides and cinnamic acid derivatives from the leaves of *Corchorus olitorius*.



Corosin

Corosolic acid

Figure 4.4 Ursane triterpenes from the roots of *Corchorus olitorius*.

Corchorus olitorius has been used in cooking, commonly known in Middle Eastern and Mediteranean regions as “Molokhiya” or “Melokhiya”. It has also been popular in Japan as nutritious noodle known as “Moroheiya”. *C. olitorius* possesses intriguing pharmacological activities such as peripheral and central antinociceptive, antibacterial, in addition to Indian ethnopharmacological treatment of chronic cystitis, gonorrhoea, dyuria, pain, fever and tumors (Zakaria *et al.*, 2006).

Of interest, the aqueous extract of *C. olitorius* leaves reduced the diffusion rate of glucose and the permeation rate of glucose in the cultured caco-2-cells. This result indicated that *C. olitorius* was effective in suppressing blood glucose elevation in rats and humans (Innami *et al.*, 2005).

However, to date the active principles have not been identified. Therefore, the purpose of the present study was to investigate the active components responsible for suppressing blood glucose level of the plant using α -glucosidase inhibition as guidance. The objectives of this research can be summarized as follows :

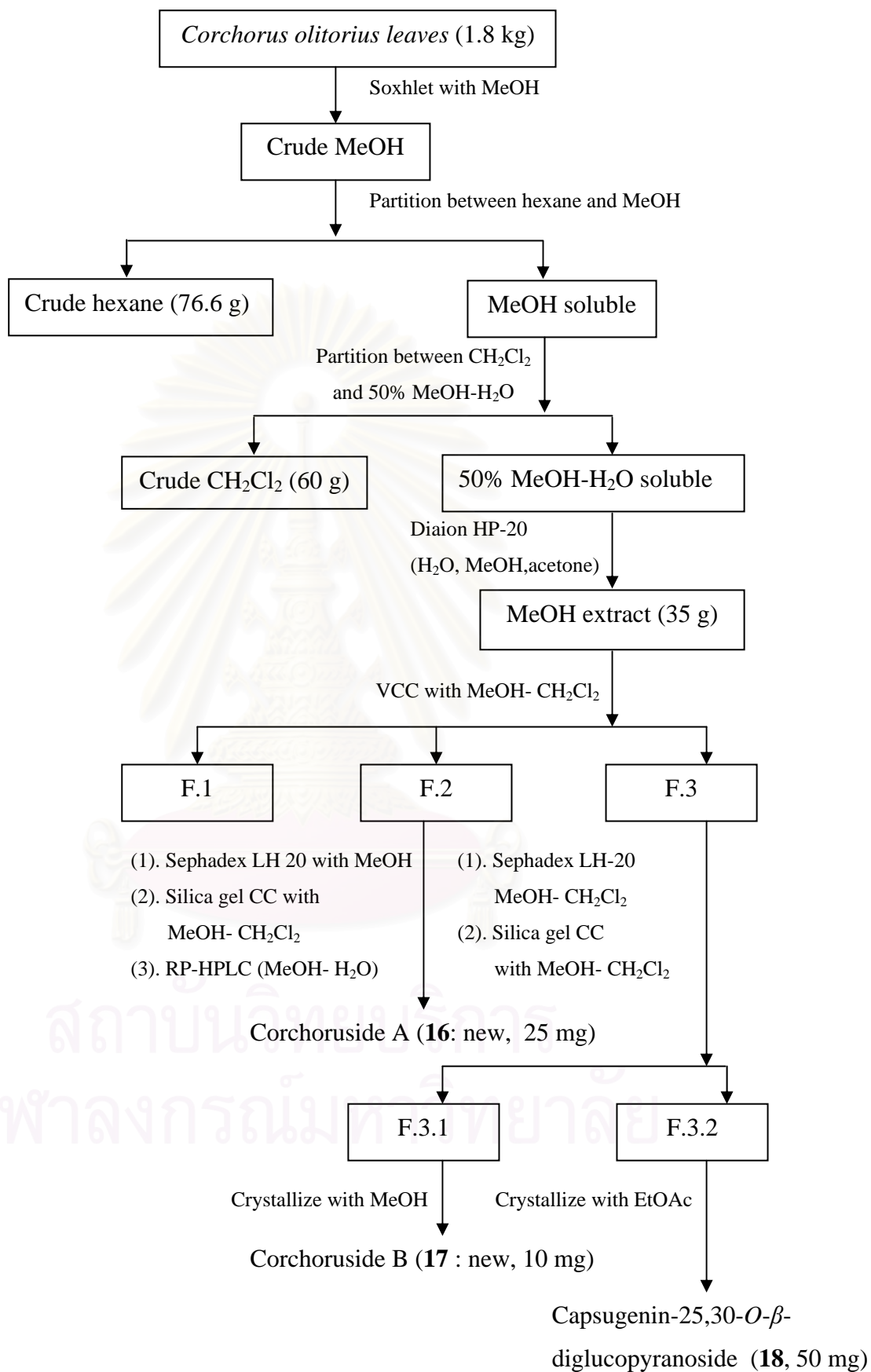
1. To extract and isolate compounds from the leaves of *C. olitorius*.
2. To elucidate the structures of all isolated compounds.
3. To determine the α -glucosidase inhibitory activity of the isolated compounds.

4.2 Results and discussion

4.2.1 Isolation

The air dried leaves of *Corchorus olitorius* were extracted with MeOH in a Soxhlet apparatus. The combined extracts were partitioned between MeOH and hexane. This MeOH layer was adjusted to 50% MeOH-H₂O and partitioned. The methanolic layer was evaporated under reduced pressure and applied on a Diaion HP-20 column chromatography, which was eluted with H₂O, MeOH and acetone. The MeOH fraction was separated through vacuum column chromatography eluted with a gradient system to obtain three main fractions. Fraction 2 (F.2) was purified by Sephadex LH-20 column, silica gel column chromatography followed by preparative HPLC, affording a new flavonol glycoside named corchoruside A (**16**). Fraction 3 (F.3) was purified by Sephadex LH-20 column, silica gel column chromatography to obtain two fractions. Fraction 3.1 (F.3.1) was crystallized with MeOH to yield a new flavonol glycoside named corchoruside B (**17**) and fraction 3.2 (F.3.2) was crystallized with EtOAc to afford capsugenin-25,30-*O*- β -diglucoopyranoside (**18**). (Scheme 4.1, Figure 4.5). The identity of known compound **18** was confirmed by spectroscopic data and preparation of acetylated products **18a** and **18b**.





Scheme 4.1 Isolation procedure of *Corchorus olitorius* leaves.

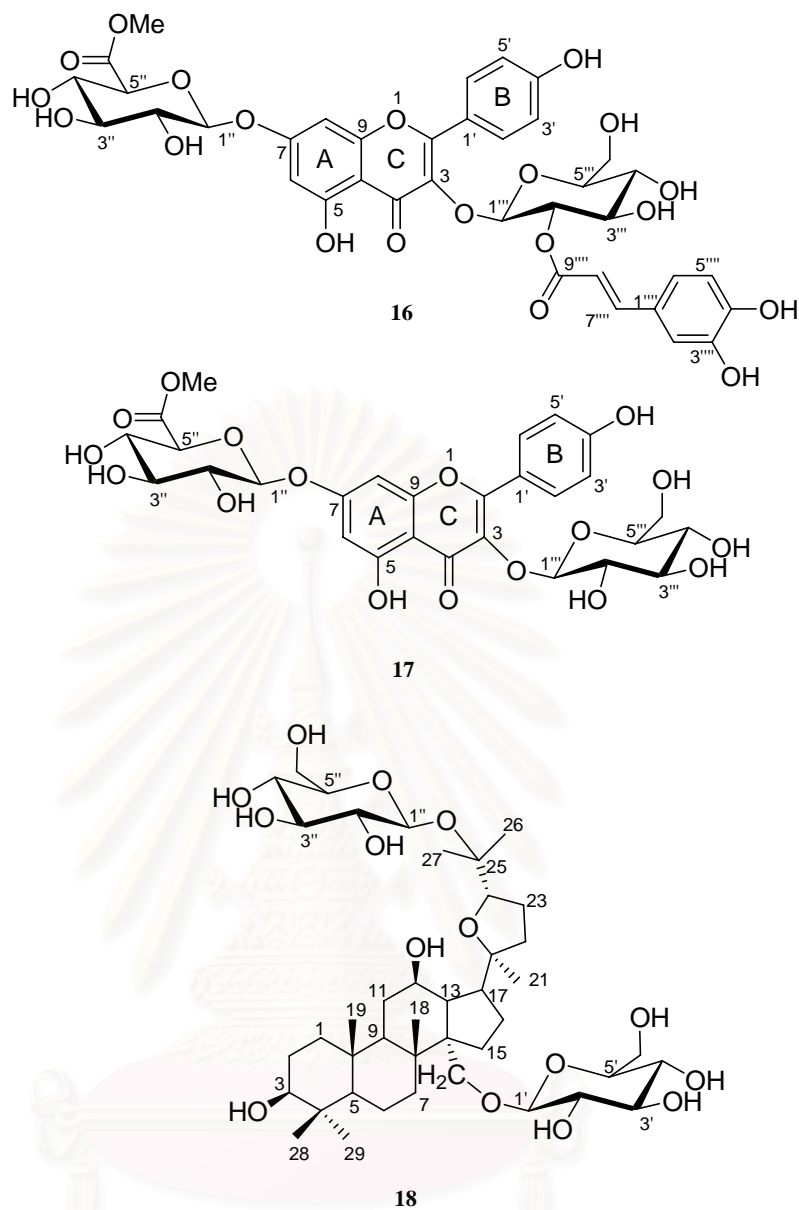


Figure 4.5 The chemical structures of isolated compounds from *Corchorus olitorius* leaves.

4.2.2 Structure elucidation of corchoruside A (16)

Corchoruside A (**16**) was isolated as yellow liquid. Its molecular formula was established as $C_{37}H_{36}O_{20}$ from analysis of the HRESIMS pseudomolecular ion $[M+Na]^+$ peak at m/z 823.1692 $[M+Na]^+$. The UV absorption maxima at 245, 267 and 333 in methanol were indicative of flavonoid moiety. The 1H NMR spectrum of **16** indicated a flavonol glycoside moiety, as it displayed two methine signals at δ_H 6.65(s) and 6.35(s) for aromatic ring A as well as two *ortho*-coupled doublet signals at δ_H 6.91 (2H, d, $J = 6.8$ Hz) and 8.02 (2H, d, $J = 6.8$ Hz) assignable to H-2', 6' and H-3', 5', respectively for aromatic ring B. Analysis of ^{13}C and 2D NMR data confirmed the flavonoid moiety as kaempferol. In addition, the 1H NMR signals of a *trans*-olefinic double bond (δ_H 6.29 and 7.56, $J = 16.0$ Hz) in conjunction with an aromatic ring system (two coupled doublets at δ_H 6.78 and 6.90 and one singlet at δ_H 7.04) as well as the relevant ^{13}C NMR signals in Table 4.1 indicated a 3,4-hydroxy-*trans*-cinnamoyl (caffeoyl) moiety.

In particular, the 1H NMR spectrum showed two anomeric proton signals at δ_H 5.13 (d, $J = 5.2$ Hz) and 5.68 (d, $J = 8.0$ Hz), which were indicative of two sugar units. The COSY, HSQC and HMBC data supported the presence of glucose (Glc) and methyl glucuronate moieties (Me-GlcU). The large coupling constants of anomeric protons indicated a β -configuration for both mono saccharides. Starting from proton [δ_H 5.68 (H-1'')] of glucose, HMBC correlation between δ_H 5.68 and δ_C 133.8 indicated the *O*-linked of β -glucose to the flavonol moiety at C-3. In addition, the HMBC cross peaks of H-2'''/C-9'''' and H-8'''/C-9'''' unambiguously confirmed that the caffeoyl moiety is linked to the C-2''' of the β -glucose.

The structure of methyl glucuronate was established from the 1H , ^{13}C NMR spectra and HMBC analysis. The ^{13}C NMR spectrum showed seven carbon including characteristic signal of anomeric carbon (δ_C 99.6), one carboxyl carbon (δ_C 169.4) and one methoxyl carbon (δ_C 49.5) (Table 4.1). The HMBC correlation (Figure 4.6) between the anomeric proton (H-1'') and δ_C 162.6 indicated that β -linked methyl glucuronate was connected to C-7 of kaempferol.

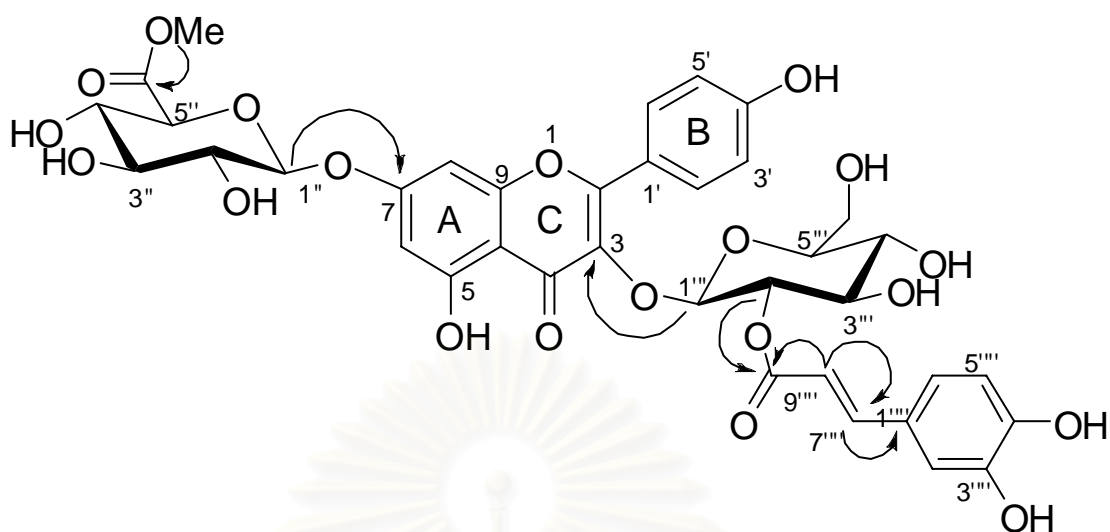


Figure 4.6 Selected HMBC correlations of **16**.

However, certain data of **16** such as C-1' of ring B and C-4 of ring C remained unclear because of weak correlations in HMBC spectrum. This problem was circumvented by formation of acetylated product. Treatment of **16** with Ac₂O in dry pyridine at ambient temperature afforded corresponding nonaacetate derivative (**16a**). The HMBC spectrum showed cross peak between H-3' and C-1' (δ_C 121.4) while signal of C-4 (δ_C 172.0) was observed in ¹³C NMR spectrum. These results confirmed the new structure of compound **16** as corchoruside A.

สถาบันวิทยบริการ
จุฬาลงกรณ์มหาวิทยาลัย

Table 4.1 NMR data of corchoruside A (**16**, CD₃OD) and corchoruside A nonaactate (**16a**, CDCl₃).

position	16		16a^a	
	δ_C	δ_H (mult, <i>J</i> in Hz)	δ_C	δ_H (mult, <i>J</i> in Hz)
2	157.7		152.2	
3	133.8		136.0	
4	<i>b</i>		172.0	
5	156.4		157.3	
6	94.2	6.65, s	102.1	6.86, d, 2.0
7	162.6		159.6	
8	99.1	6.38, s	109.6	6.59, d, 2.0
9	160.4		150.4	
10	106.4		113.5	
1'	<i>b</i>		121.4	
2',6'	131.1	8.02, d, 6.8	130.0	7.97, d, 8.4
3',5'	115.0	6.91, d, 6.8	<i>b</i>	7.17, d, 8.8
4'	160.4		155.0	
Me-GlcU				
1''	99.6	5.13, d, 5.2	98.1	5.29, d, 8.0
2''	70.2	3.40, m	68.2	5.06, m
3''	77.4	3.34, m	72.0	3.62, m
4''	71.6	3.62, m	68.8	5.30, m
5''	75.3	4.16, d, 9.2	72.8	4.23, d, 4.4
6''	169.4		166.0	
7''	49.5	3.34, s	53.0	3.68, s
Glc				
1'''	99.2	5.68, d, 8.0	99.2	5.68, d, 7.6
2'''	74.3	5.03, d, 8.4	74.3	5.21, m
3'''	74.8	3.64, m	74.8	5.28, m
4'''	73.1	3.52, m	73.1	5.27, m
5'''	75.6	3.55, m	75.6	5.17, m
6'''	61.2	3.57, m	61.2	3.95, m
		3.79, m		4.02, m
1''''	126.5		132.9	
2''''	114.1	7.04, s	122.8	7.30, s
3''''	145.4		142.5	
4''''	148.4		143.9	
5''''	115.5	6.78, m	123.8	7.15, br d
6''''	122.0	6.90, m	126.3	7.32, br d
7''''	146.1	7.56, d, 16.0	144.0	7.59, d, 16.0
8''''	114.0	6.29, d, 16.0	118.1	6.27, d, 16.0
9''''	166.4		165.0	

^aSignals of acetates resonated at δ_H 2.34, 2.27, 2.24, 2.23, 1.99, 1.97, 1.94, 1.91 and 1.89; δ_C 21.2, 21.1, 21.0, 20.9, 20.6, 20.4 (4 × CH₃), 170.6, 170.3, 170.2, 169.7 (3 × C=O), 169.4, 169.2 and 169.0.

^bNot detected

4.2.3 Structure elucidation of corchoruside B (17)

Corchoruside B (**17**) was isolated as pale yellow powder. Its molecular formula was established as $C_{28}H_{30}O_{17}$ from analysis of the HRESIMS pseudomolecular ion peak at m/z 661.1375 $[M+Na]^+$. The UV absorptions maxima at 265 and 346 were indicative of flavonoid moiety. The 1H and ^{13}C NMR spectra of **17** were also similar to those of **16**, which suggested a kaempferol type aglycone. The striking difference was the absence of characteristic signals for a 3,4-hydroxy-*trans*-cinnamoyl (caffeoyl) moiety. The glycosidic linkage was determined by HMBC correlations between glucosyl anomeric proton H-1''' (δ_H 6.52) and C-3 (δ_C 133.4) as well as a methyl gluconate anomeric proton H-1'' (δ_H 6.13) and C-3 (δ_C 161.9) of a kaempferol aglycone. The configuration of the anomeric proton was defined as β from their large coupling constants of 7.2 Hz (H-1'') and H-1'''. Therefore, the structure of **17** was established as shown (Table 4.2, Figure 4.7)

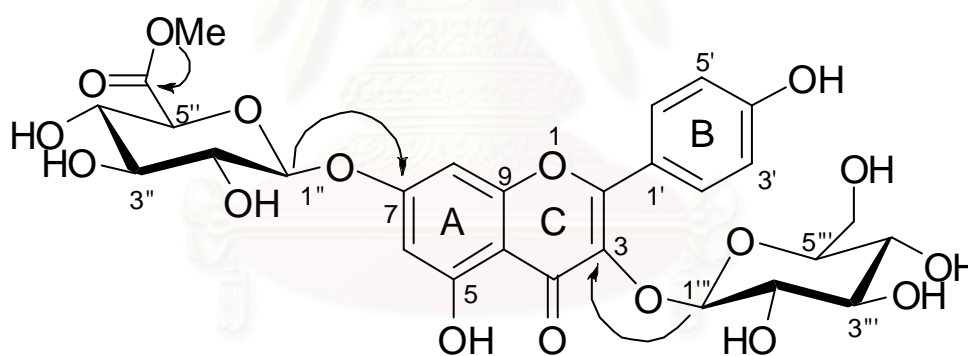


Figure 4.7 Selected HMBC correlations of **17**.

Table 4.2 ^1H , ^{13}C and HMBC NMR data of corchoruside B (**17**) in pyridine- d_5

position	δ_{C}	δ_{H} (mult, J in Hz)	HMBC correlations
2	156.4		
3	133.4		
4	<i>a</i>		
5	155.4		
6	93.5	7.13, d, 2.0	C-5, C-, C-8, C-10
7	161.9		
8	98.7	6.89, d, 2.0	C-7, C-9
9	161.3		
10	105.6		
1'	120.5		
2',6'	130.5	8.24, d, 8.8	C-2, C-4'
3',5'	114.8	7.28, d, 8.8	C-1', C-4'
4'	160.4		
Me-GlcU			
1''	100.2	4.82, d, 7.2	C-7
2''	73.1	4.52, m	C-3''
3''	76.0	4.56, m	
4''	71.5	4.71, t	C-3'', C-6''
5''	75.8	5.03, d, 9.6	C-6''
6''	168.8		
7''	50.8	3.77, s	C-6''
Glc			
1'''	102.2	5.20, d, 7.2	C-3
2'''	74.7	4.50, m	C-1''', C-3'''
3'''	77.0	4.47, m	
4'''	70.5	4.36, m	C-3'''
5'''	77.8	4.18, m	
6'''	61.2	4.38, m	
		4.52, m	

^aNot detected

สถาบันวิทยบริการ
จุฬาลงกรณ์มหาวิทยาลัย

4.2.4 α -Glucosidase inhibitory activity of the isolated compounds

The α -glucosidase inhibitory effect of isolated compounds (**16-18**) from *Corchorus olitorius* leaves and acetylated products (**18a** and **18b**) were evaluated by colorimetric method and the results are shown in Table 4.3

Table 4.3 α -Glucosidase inhibitory effect of **16-18b**

Compounds	IC ₅₀ (mM)
Corchoruside A (16)	0.18 ± 0.01
Corchoruside B (17)	0.72 ± 0.03
Capsugenin-25,30- <i>O</i> - β -diglucoopyranoside (18)	1.42 ± 0.03
Capsugenin-25,30- <i>O</i> - β -diglucoopyranoside nonaacetate (18a)	> 10
Capsugenin-25,30- <i>O</i> - β -diglucoopyranoside decaacetate (18b)	> 10
Acarbose [®] ^a	0.62 ± 0.03
1-Deoxynojirimycin(DNJ) ^a	0.17 ± 0.02

^aStandard control

This is the first report on the isolation of α -glucosidase inhibitory principles, corchorusides A (**16**) and B (**17**), the two flavonoid glycosides from leaves of *Corchorus olitorius*. Of isolated compounds, **16** was the most potent α -glucosidase inhibitor with the IC₅₀ value of 0.18 mM, which was comparable to that of DNJ (IC₅₀ 0.17 mM), while compound **17** had moderate inhibition (IC₅₀ 0.72 mM). Notably, the highly inhibitory effect of **16** over that of **17** was possibly due to the presence of caffeoyl group. The corresponding results have also been observed in other caffeoyl containing compounds (Matsui *et al.*, 2001; Matsui *et al.*, 2004; Lee *et al.*, 2008).

In case of triterpenoid glycoside, capsugenin-25,30-*O*- β -diglucoopyranoside (**18**) showed moderate α -glucosidase inhibitory activity with IC₅₀ value of 1.42 mM, whereas capsugenin-25,30-*O*- β -diglucoopyranoside nonaacetate (**18a**) and Capsugenin-25,30-*O*- β -diglucoopyranoside decaacetate (**18b**) showed weak inhibitory activity (< 30% inhibition). This results indicated that replacement of hydroxyl groups with acetate groups obviously reduced the inhibitory activity. Hence, the number of

hydroxyl groups of triterpenoid aglycone and sugar moiety were importance for enhancement in inhibitory effect.

In conclusion, **16** is the active principles inhibitors present in *C. olitorius* leaves, which may be specific structure in α -glucosidase enzyme and led to additionally enhance its inhibition activity. The structure activity relationship indicated that caffeoyl group was crucial for the activity. Moreover, **16** showed the comparable α -glucosidase inhibitory activity to a positive control DNJ. Therefore, it is concluded that **16** would be a lead compound suitable for designing new potent α -glucosidase inhibitors. In addition, *C. olitorius* may be useful as a medicinal food or as a source of natural α -glucosidase inhibitors for use in suppressing postprandial hyperglycemia in the management of type 2 diabetes.

4.3 Experiment section

4.3.1 General experimental procedures

The ^1H and ^{13}C NMR spectra were determined by Varian model Mercury+ 400 NMR spectrometer. The chemical shifts in δ (ppm) were assigned with reference to the signals from the residual protons in deuterated solvents and using TMS as an internal standard in some cases. ESIMS spectra were obtained from VG TRIO 2000 Mass spectrometer. Adsorbents used for separation were silica gel 60 Merck No. 7734 and 7729. TLC was performed on aluminium sheets precoated with silica gel (Merck Kieselgel 60 PF254). Gel filtration chromatography was performed on Sephadex LH-20. Adsorption chromatography for glycoside was performed with Diaion HP-20. UV spectra were recorded on Shimadzu UV-160A photodiode array spectrophotometer. HPLC was conducted on Water[®] 600 controllers equipped with a Water[®] 2996 photodiode array detector. Cosmosil 5C18-ARII column (10 × 250 mm) was used for separation in preparative scale.

4.3.2 Plant material

The leaves of *Corchorus olitorius* were collected in Joumtong Bangkok, Thailand in April 2008.

4.3.3 Extraction and isolation

The dried leaves of *Corchorus olitorius* (1.8 kg) were crushed into small pieces followed by extraction with 100% MeOH in a Soxhlet apparatus. The MeOH extract was partitioned between MeOH and hexane. This polarity of MeOH layer was adjusted to 1:1 MeOH-H₂O and partitioned with CH₂Cl₂. Each fraction was evaporated under reduced pressure to give hexane (76.6 g), CH₂Cl₂ (60.0 g) and 1:1 MeOH-H₂O (35.0 g) extracts. Further fractionation was carried out under a guidance of α -glucosidase inhibitory activity. The 1:1 MeOH-H₂O extract was suspended in water and applied on a Diaion HP-20 column eluted with H₂O, MeOH and acetone. The MeOH fraction was separated through vacuum column chromatography using stepwise MeOH-CH₂Cl₂ (0:100, 10:90, 30:70, 50:50 70:30 and 100:0), yielding three major fractions. The active fraction 2 was purified by Sephadex LH-20 column (MeOH) followed by silica gel column chromatography using stepwise MeOH-CH₂Cl₂ (0:100, 5:95, 10:90, 20:80, 50:50, 70:30 and 100:0). The active fraction were combined and subjected to preparative HPLC (ODS, 55:45 MeOH-H₂O, UV 254 nm) afforded a new flavonol glycoside named corchoruside A (**16**, 25 mg, 2.8x10⁻⁴ % w/w, t_R 31.2 min). The active fraction 3 was purified by Sephadex LH-20 column (MeOH) followed by silica gel repeat column chromatography using stepwise MeOH-CH₂Cl₂ (0:100, 5:95, 10:90, 20:80, 50:50, 70:30 and 100:0) to obtain two fractions (3.1 and 3.2). The active fraction 3.1 was crystallized with MeOH to afford a new flavonol glycoside named corchoruside B (**17**, 10 mg, 1.1x10⁻⁴ % w/w). The fraction 3.2 was crystallized with EtOAc to yield capsugenin-25, 30-*O*- β -diglucoopyranoside (**18**, 40 mg, 5.6x10⁻⁴ % w/w).

Corchoruside A (**16**): yellow liquid, $[\alpha]_D^{25.6} -88.7^\circ$ (c 0.05, MeOH); UV (MeOH) λ_{max} (log ϵ) 245 (3.64), 267 (3.68), 333 (3.77); HRESIMS m/z $[M+Na]^+$ 823.1715 (calcd for C₃₇H₃₆O₂₀Na, 823.1692); ¹H NMR (CD₃OD, 400 MHz) and ¹³C NMR (100 MHz) see table 4.1

Corchoruside B (**17**): yellow liquid, $[\alpha]^{25.6}_D -10.2^\circ$ (c 0.05, MeOH); UV (MeOH) λ_{\max} (log ϵ) 265 (3.53), 346 (3.64); HRESIMS m/z $[M+Na]^+$ 661.1370 (calcd for $C_{28}H_{30}O_{17}Na$, 661.1375); 1H NMR (CD_3OD , 400 MHz) and ^{13}C NMR (100 MHz) see table 4.2

Preparation of corchoruside A nonaacetate (16a)

Fraction containing corchoruside A (**16a**, 50 mg) were dissolved in pyridine (1 mL) and then treated with acetic anhydride (90 μ L) for 1 h at room temperature. After completion of reaction, the product was extracted with CH_2Cl_2 . The organic layer was washed with water and dried over anhydrous Na_2SO_4 . After evaporation to dryness, the reaction extracted was purified by column chromatography (Hexane:EtOAc) to afford corchoruside A nonaacetate (**16a**, 10 mg).

Corchoruside A nonaacetate (**16a**): white powder, $[\alpha]^{25.6}_D -94.5^\circ$ (c 0.05, MeOH); UV (MeOH) λ_{\max} (log ϵ) 255 (3.82), 284 (3.87), 357 (3.97); LRESIMS m/z $[M-H]^-$ 1177.3525 (calcd for $C_{55}H_{53}O_{29}$, 1177.2751); 1H NMR ($CDCl_3$, 400 MHz) and ^{13}C NMR (100 MHz) see table 4.1

Capsugenin-25,30-*O*- β -diglucoopyranoside (**18**): white powder; 1H NMR (CD_3OD , 400 MHz) δ_H 6.64 (1H, s, 12-OH), 4.46 (1H, d, $J = 7.6$ Hz, H-1'), 3.78 and 4.02 (2H, m, H-6'), 4.24 (1H, d, $J = 8.0$ Hz, H-1''), 3.68 and 3.84 (2H, m, H-6''), 4.56 and 4.45 (2H, d, $J = 9.6$ Hz, H-30), 4.25 (1H, dd, $J = 11.7, 6.6$ Hz, H-24), 3.80 (1H, m, H-12), 3.59 (1H, m, H-3), 0.92 (s, $2 \times CH_3$), 1.02, 1.17, 1.25 (s, $3 \times CH_3$).

Preparation of capsugenin-25, 30-*O*- β -diglucoopyranoside peracetates 18a and 18b

Fractions containing capsugenin-25, 30-*O*- β -diglucoopyranoside (**18**, 50 mg) was dissolved in pyridine (1 mL) and then treated with acetic anhydride (100 μ L) for 1 h at room temperature. After completion of reaction, the product was extracted with CH_2Cl_2 and washed with water. The aqueous layer was dried with anhydrous Na_2SO_4

and solvent was then evaporated under reduced pressure. The reaction extracted was purified by column chromatography (Hexane:EtOAc) to afford capsugenin-25, 30-*O*- β -diglucoopyranoside nanaacetate (**18a**, 7 mg) and capsugenin-25, 30-*O*- β -diglucoopyranoside decaacetate (**18b**, 7 mg).

Capsugenin-25,30-*O*- β -diglucoopyranoside nonaacetate (**18a**): colorless crystals ; ^1H NMR (CDCl_3 , 400 MHz) δ_{H} 4.49 (1H, dd, , $J = 4.8, 5.2$ Hz, H-3), 3.44 (1H, dt, $J = 4.8, 6.8$ Hz, H-12), 0.92 (1H, s, 18- CH_3), 0.88 (1H, s, 19- CH_3), 1.16 (1H, s, 21- CH_3), 3.76 (1H, dd, $J = 5.2, 5.2$ Hz, H-24), 1.05 (1H, s, 26- CH_3), 1.18 (1H, s, 27- CH_3), 0.86 (1H, s, 28- CH_3), 0.80 (1H, s, 29- CH_3), 3.32, 4.20 (2H, d, $J = 10.0$ Hz, H-30), 4.60 (1H, d, $J = 7.6$ Hz, H-1'), 4.90 (1H, d, $J = 7.6$ Hz, H-2'), 5.14 (1H, t, $J = 9.5$ Hz, H-3'), 4.92 (1H, dd, $J = 10.0, 9.5$ Hz, H-4'), 3.63 (1H, dd, $J = 10.0, 5.7$ Hz, H-5'), 4.14, 4.02 (1H, dd, $J = 12.0, 5.7$ Hz, H-6'), 4.36 (1H, d, $J = 7.6$ Hz, H-1''), 4.98 (1H, dd, $J = 9.5, 7.9$ Hz, H-2''), 5.12 (1H, t, $J = 9.5$ Hz, H-3''), 5.04 (1H, t, $J = 9.5$ Hz, H-4''), 3.67, (1H, dd, $J = 9.5, 4.5$ Hz, H-5''), 3.68, 4.14 (2H, dd, $J = 12.3, 4.5$ Hz, H-6'').

Capsugenin-25,30-*O*- β -diglucoopyranoside decaacetate (**18b**): colorless crystals ; ^1H NMR (CDCl_3 , 400 MHz) δ_{H} 4.48 (1H, dd, , $J = 4.8, 4.4$ Hz, H-3), 3.45 (1H, dt, $J = 4.4, 6.4$ Hz, H-12), 0.92 (1H, s, 18- CH_3), 0.88 (1H, s, 19- CH_3), 1.16 (1H, s, 21- CH_3), 3.69 (1H, dd, $J = 5.2, 5.2$ Hz, H-24), 1.05 (1H, s, 26- CH_3), 1.18 (1H, s, 27- CH_3), 0.86 (1H, s, 28- CH_3), 0.80 (1H, s, 29- CH_3), 3.34, 4.21 (2H, d, $J = 9.9$ Hz, H-30), 4.63 (1H, d, $J = 7.9$ Hz, H-1'), 4.92 (1H, dd, $J = 7.6$ Hz, H-2'), 5.15 (1H, t, $J = 9.5$ Hz, H-3'), 4.98 (1H, dd, $J = 10.0, 9.5$ Hz, H-4'), 3.63 (1H, dd, $J = 10.0, 5.7$ Hz, H-5'), 4.16, 4.02 (1H, dd, $J = 12.0, 5.7$ Hz, H-6'), 4.35 (1H, d, $J = 7.9$ Hz, H-1''), 5.00 (1H, dd, $J = 9.5, 7.9$ Hz, H-2''), 5.12 (1H, t, $J = 9.5$ Hz, H-3''), 5.08 (1H, t, $J = 9.0$ Hz, H-4''), 3.66 (1H, dd, $J = 9.2, 4.3$ Hz, H-5''), 3.65, 4.13 (2H, dd, $J = 12.3, 4.5$ Hz, H-6'').

4.3.4 α -Glucosidase inhibitory assay

The α -glucosidase inhibitory effects of isolated compounds were evaluated by the same procedure previously described in Chapter II.



Supporting information

สถาบันวิทยบริการ
จุฬาลงกรณ์มหาวิทยาลัย

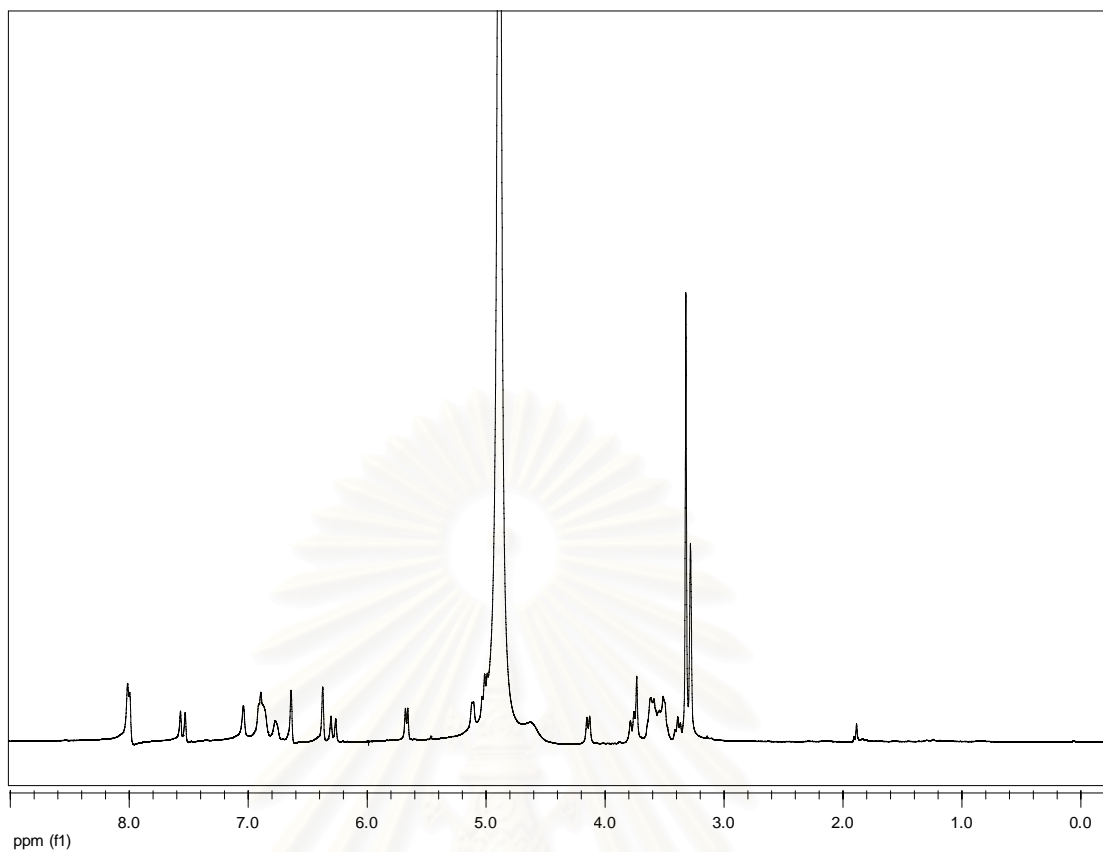


Figure S-4.1 The ^1H NMR (CD_3OD) spectrum of corchoruside A (**16**).

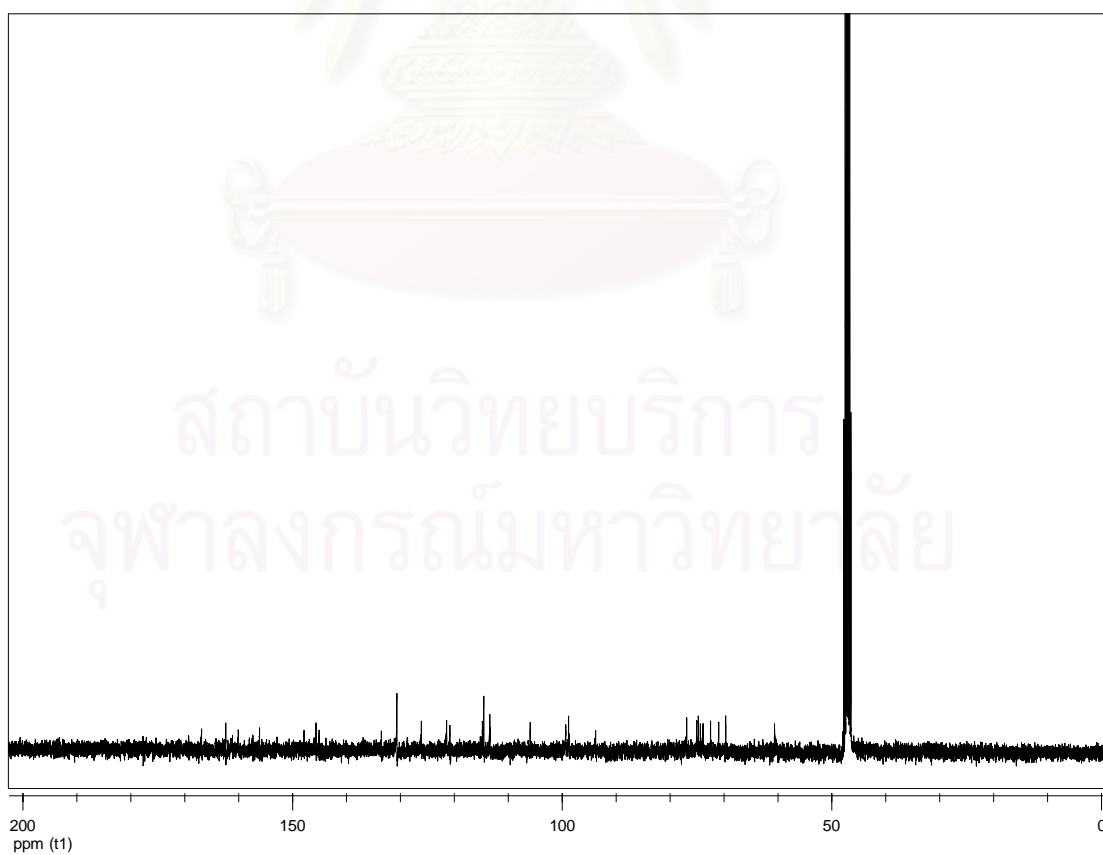


Figure S-4.2 The ^{13}C NMR (CD_3OD) spectrum of corchoruside A (**16**).

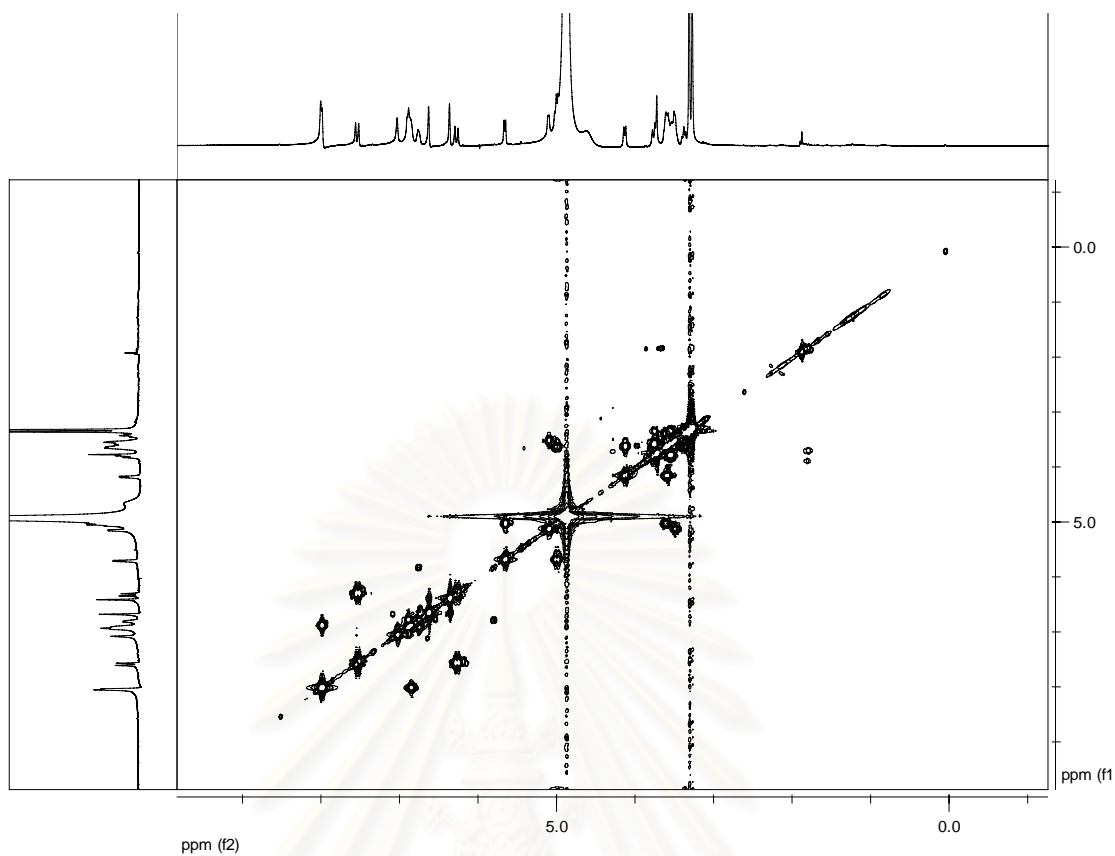


Figure S-4.3 The COSY (CD₃OD) spectrum of corchoruside A (**16**).

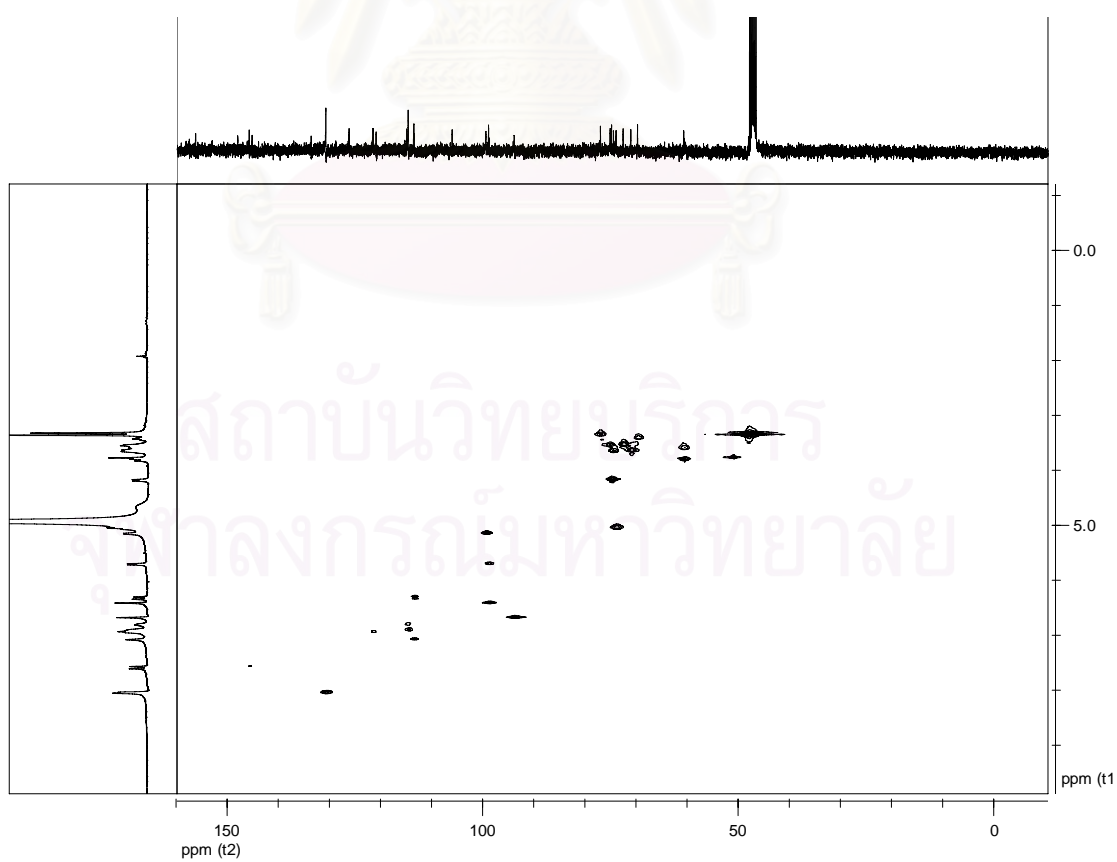


Figure S-4.4 The HSQC (CD₃OD) spectrum of corchoruside A (**16**).

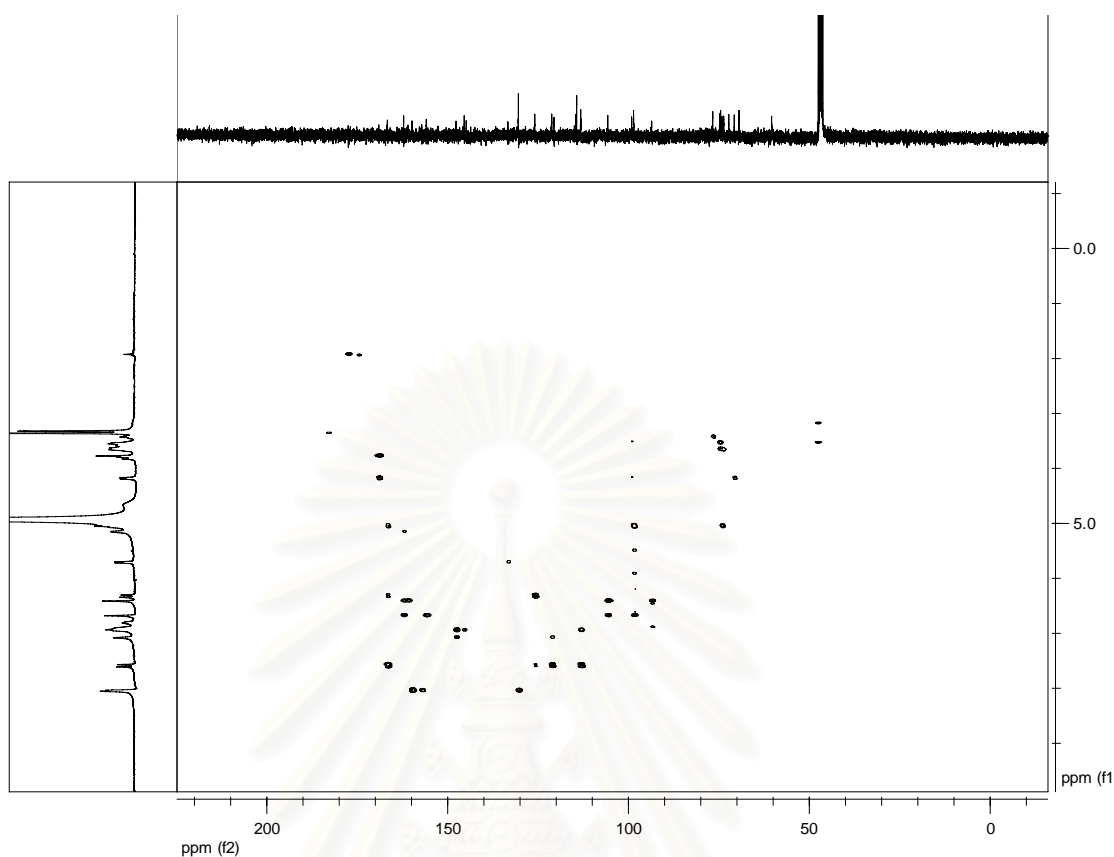


Figure S-4.5 The HMBC (CD₃OD) spectrum of corchoruside A (16).

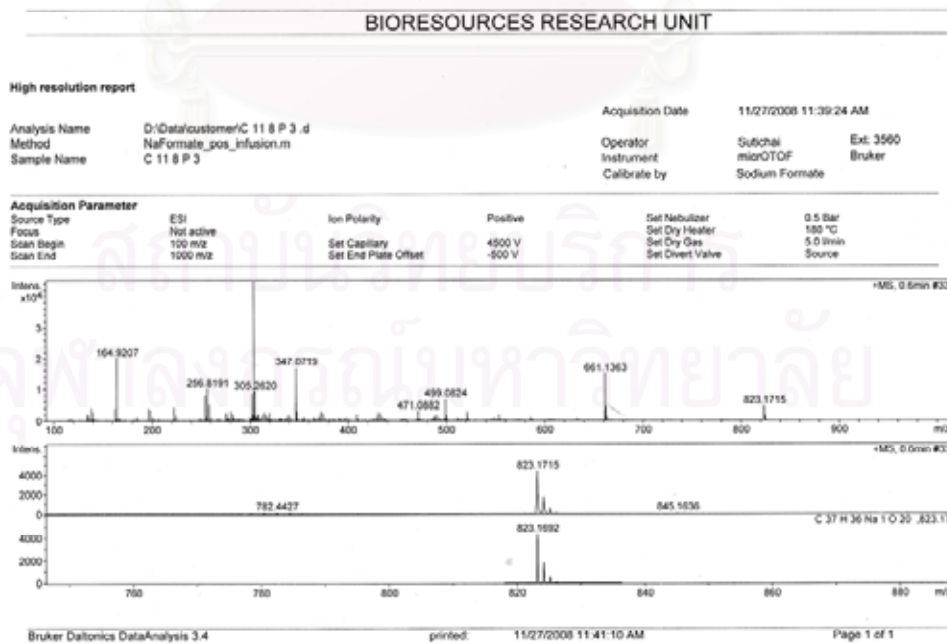


Figure S-4.6 Mass spectrum of corchoruside A (16).

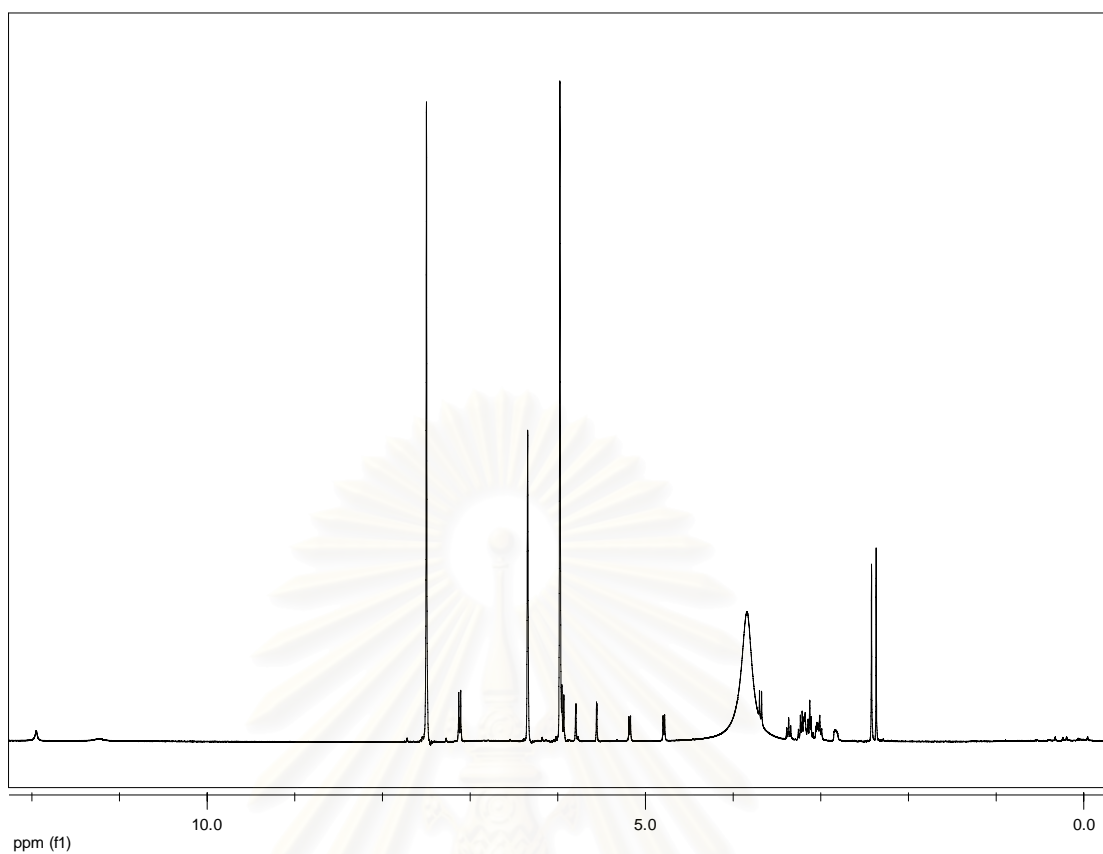


Figure S-4.7 The ^1H NMR ($\text{pyridine-}d_5$) spectrum of corchoruside B (17).

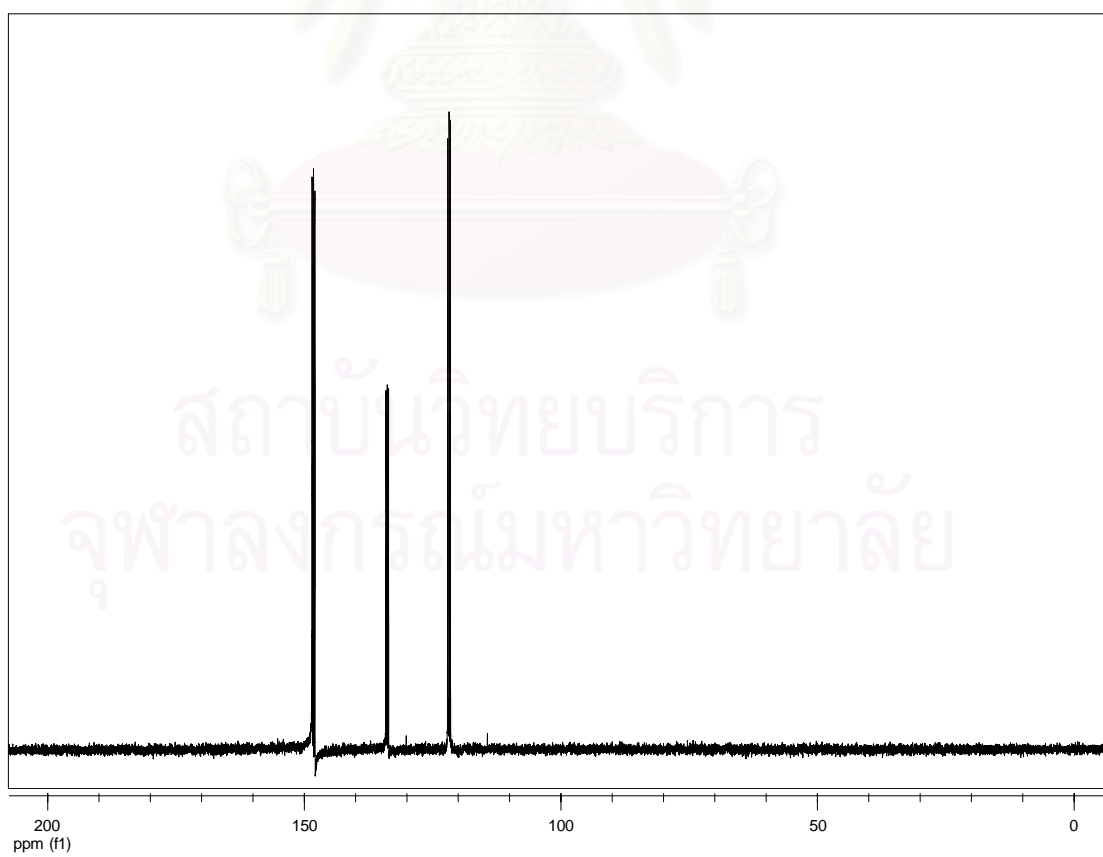


Figure S-4.8 The ^{13}C NMR ($\text{pyridine-}d_5$) spectrum of corchoruside B (17).

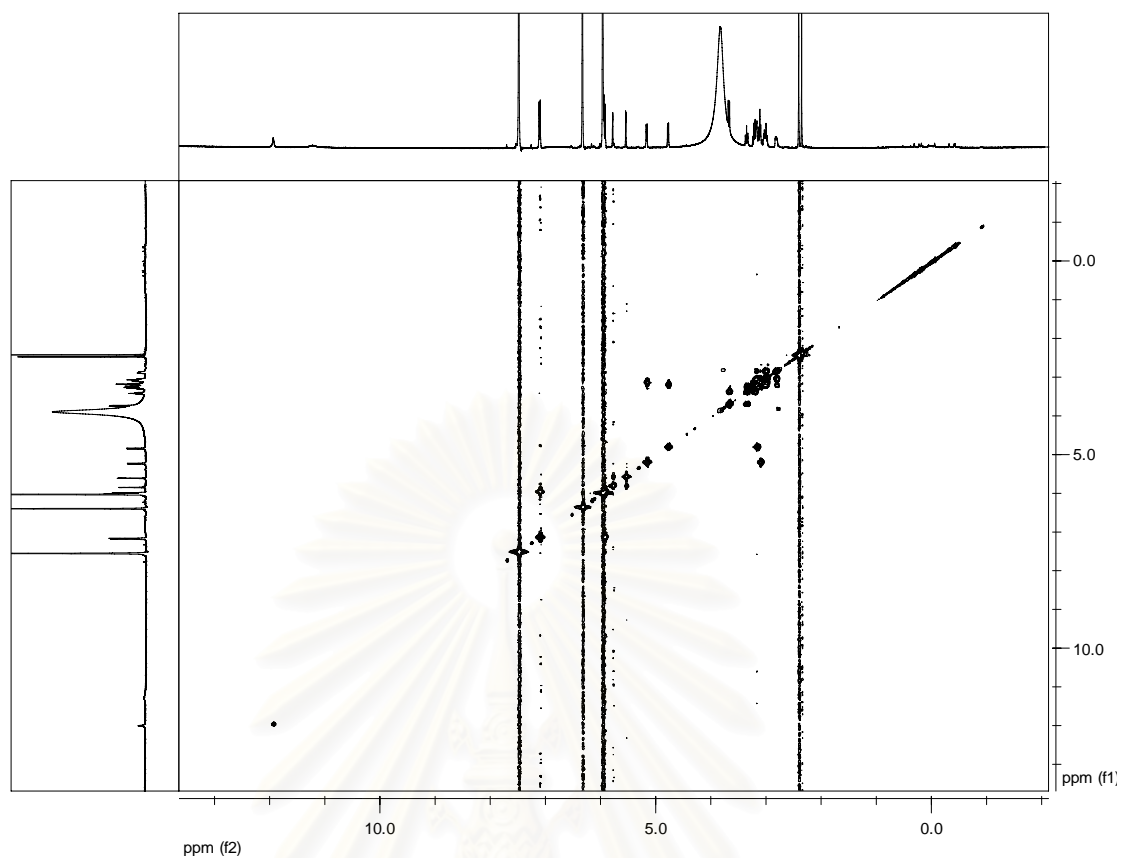


Figure S-4.9 The COSY (pyridine- d_5) spectrum of corchoruside B (17).

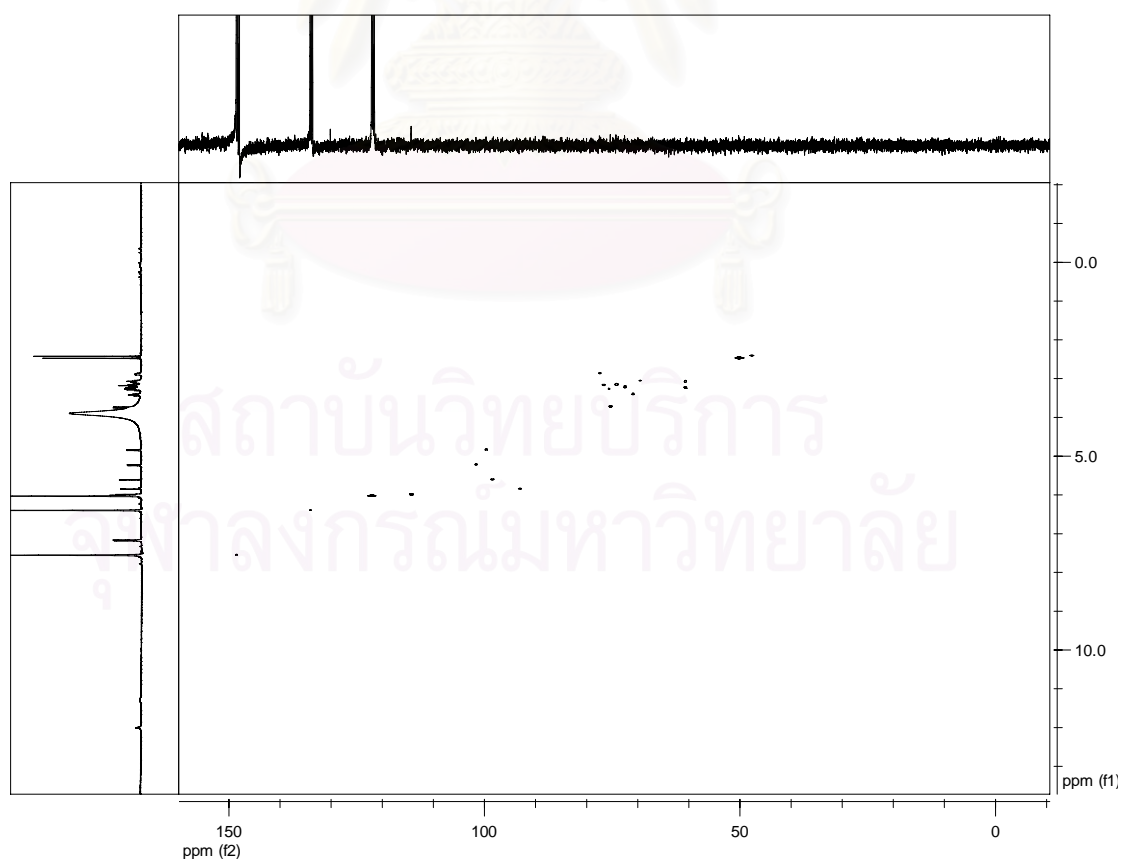


Figure S-4.10 The HSQC (pyridine- d_5) spectrum of corchoruside B (17).

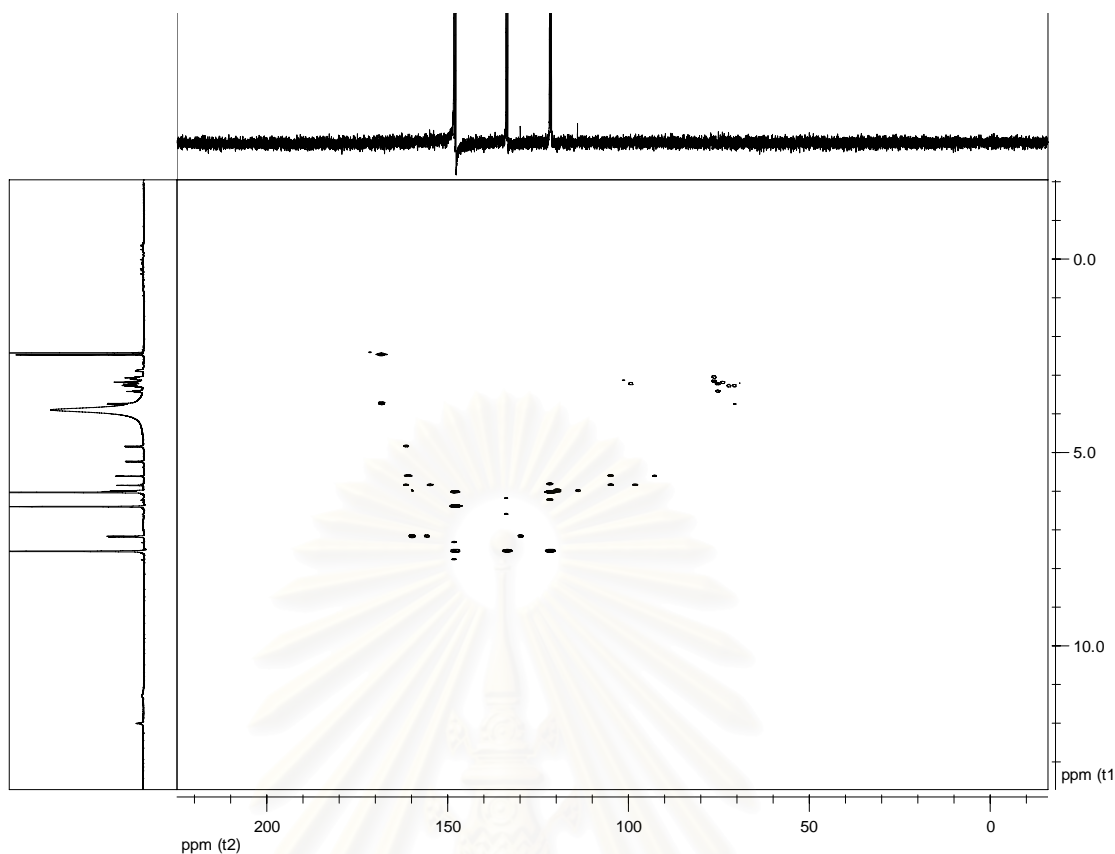


Figure S-4.11 The HMBC (pyridine- d_5) spectrum of corchoruside B (17).

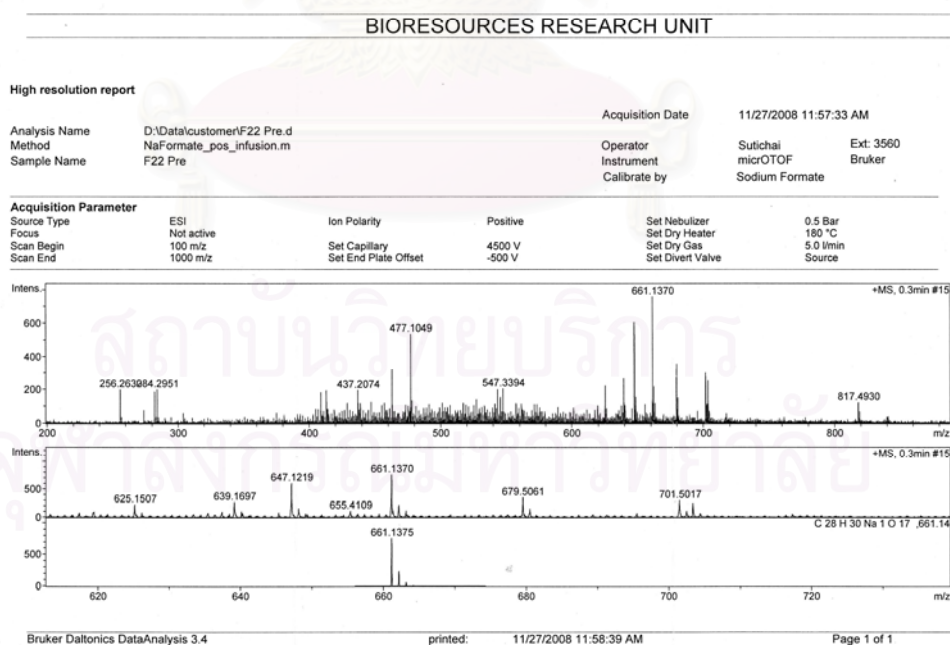


Figure S-4.12 Mass spectrum of corchoruside B (17).

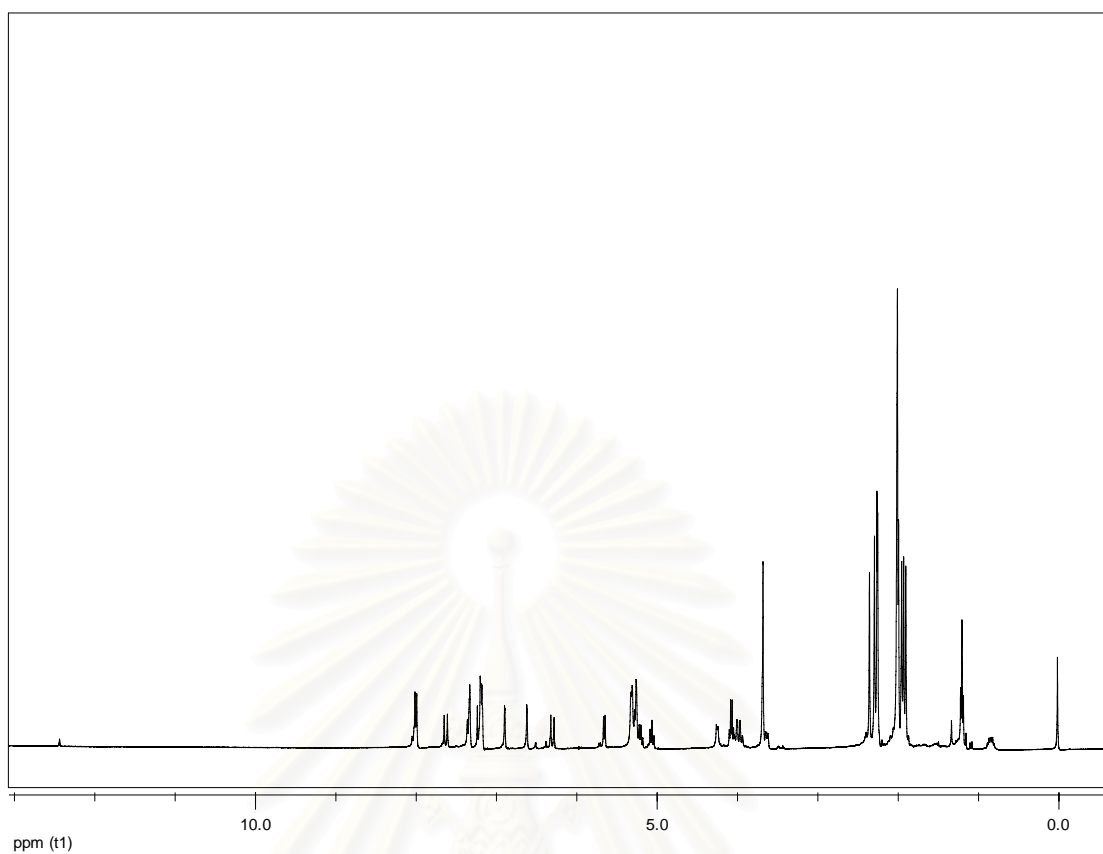


Figure S-4.13 The ^1H NMR (CDCl_3) spectrum of corchoruside A nonaacetate (**16a**).

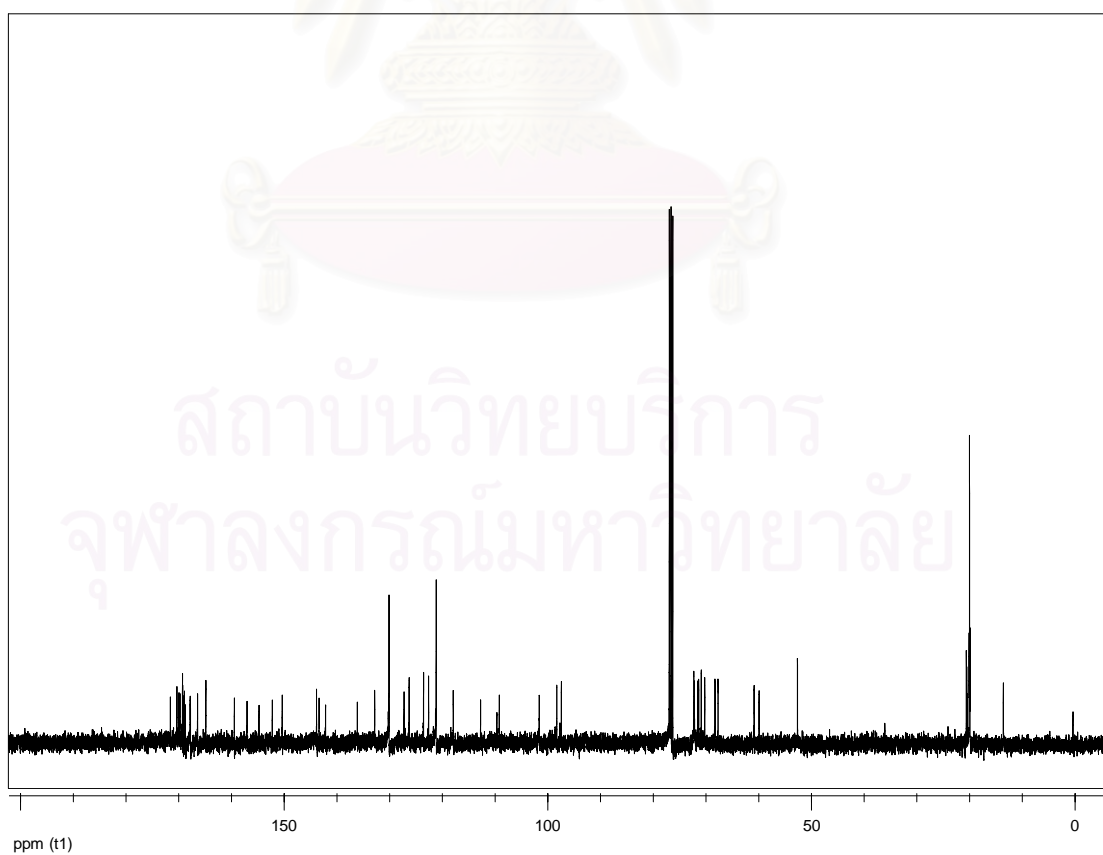


Figure S-4.14 The ^{13}C NMR (CDCl_3) spectrum of corchoruside A nonaacetate (**16a**).

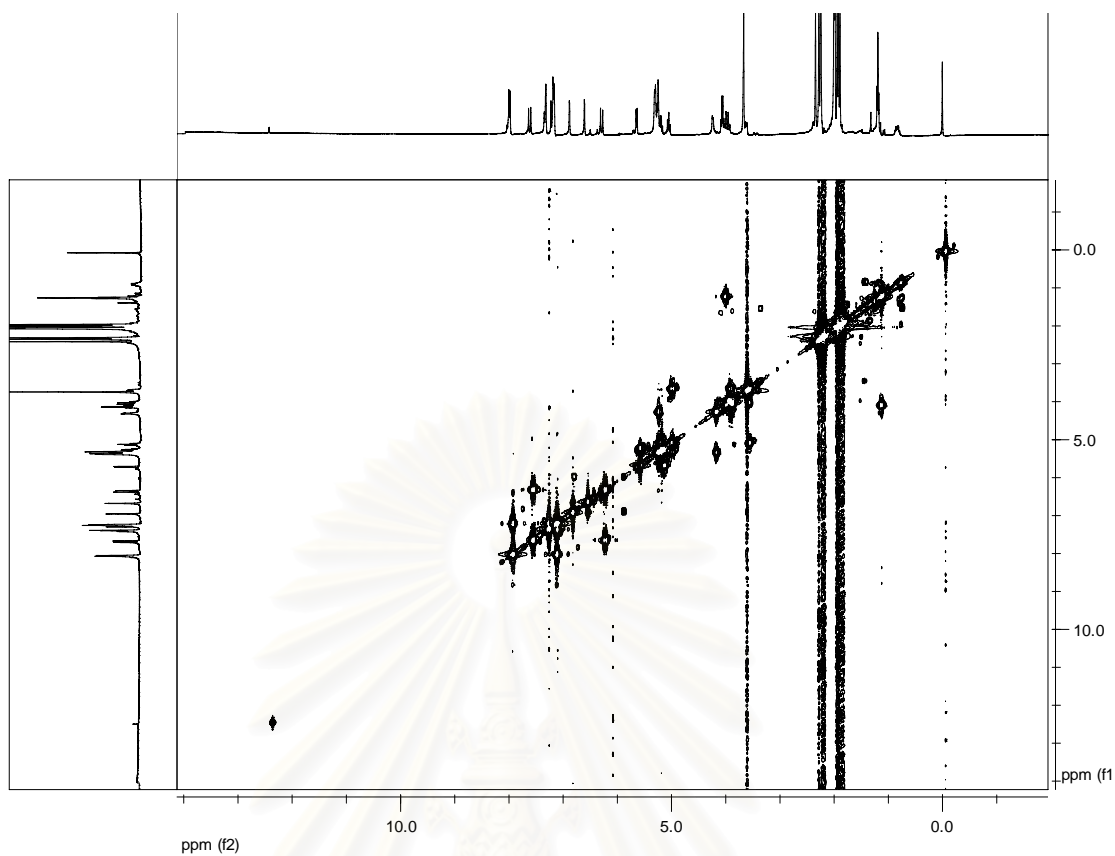


Figure S-4.15 The COSY (CDCl₃) spectrum of corchoruside A nonaacetate (**16a**).

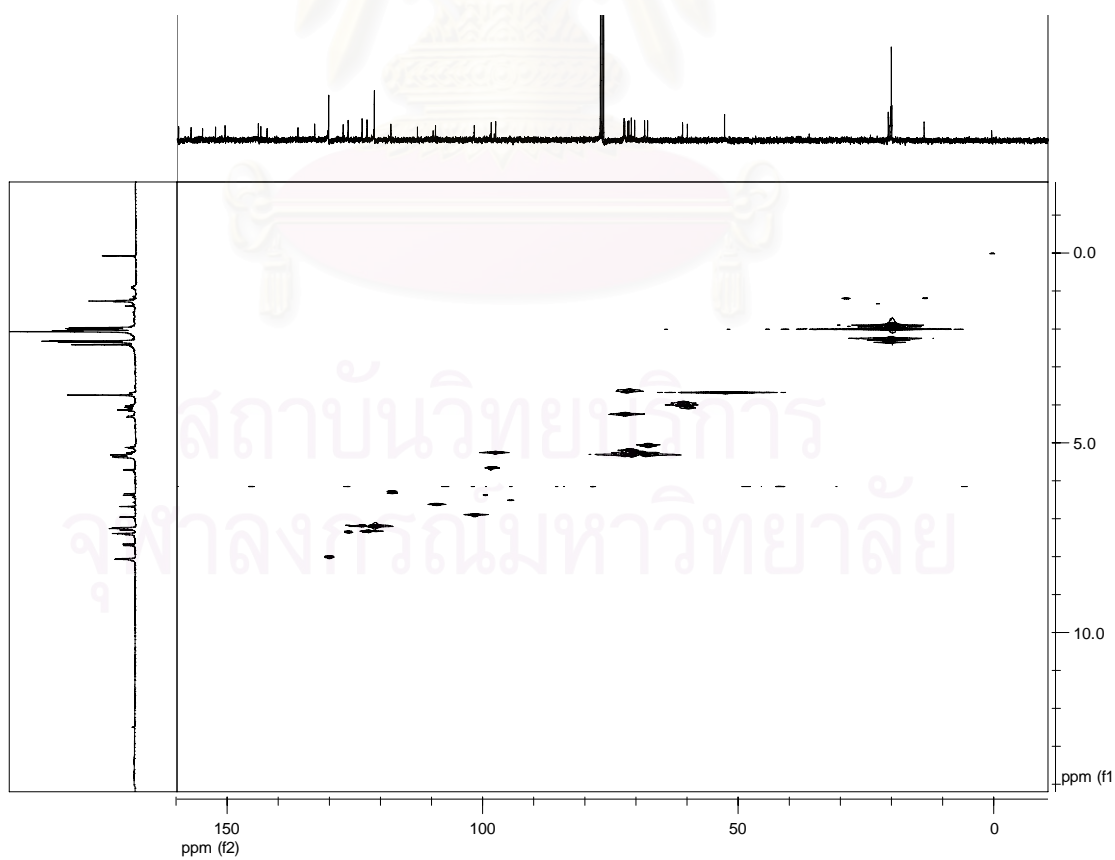


Figure S-4.16 The HSQC (CDCl₃) spectrum of corchoruside A nonaacetate (**16a**).

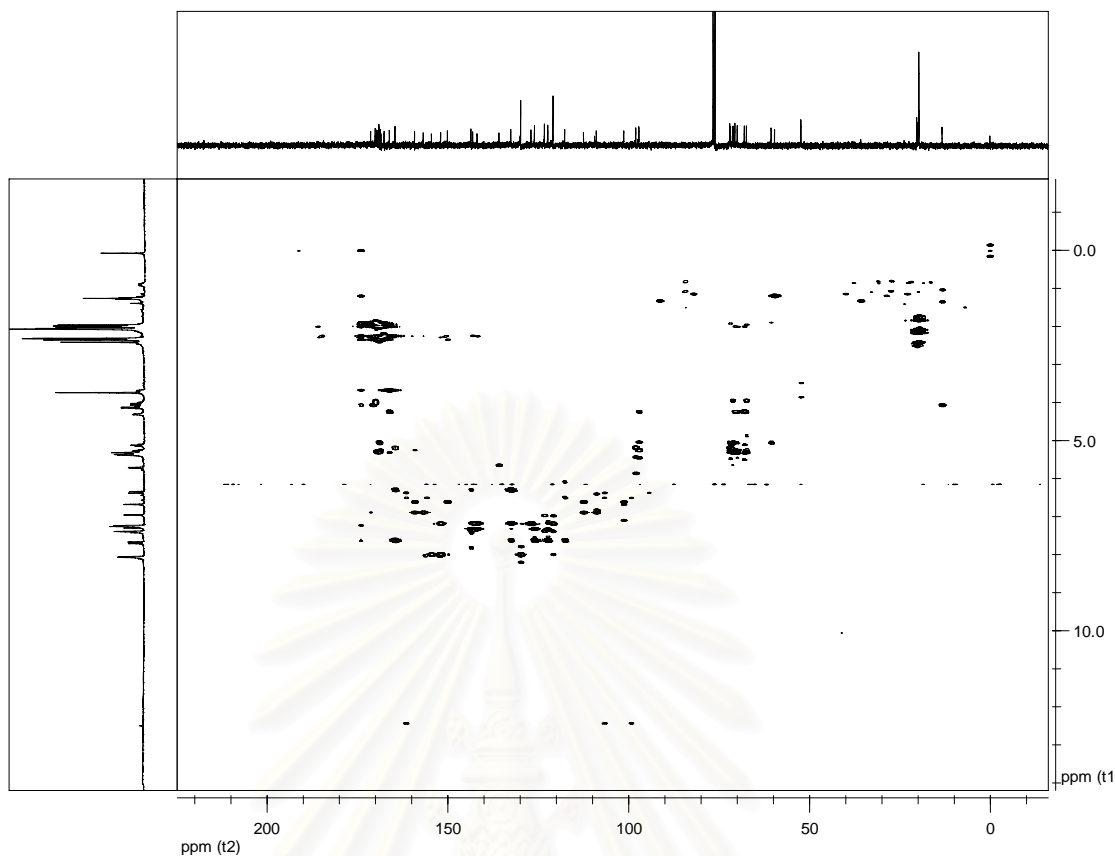


Figure S-4.17 The HMBC (CDCl_3) spectrum of corchoruside A nonacetate (**16a**).

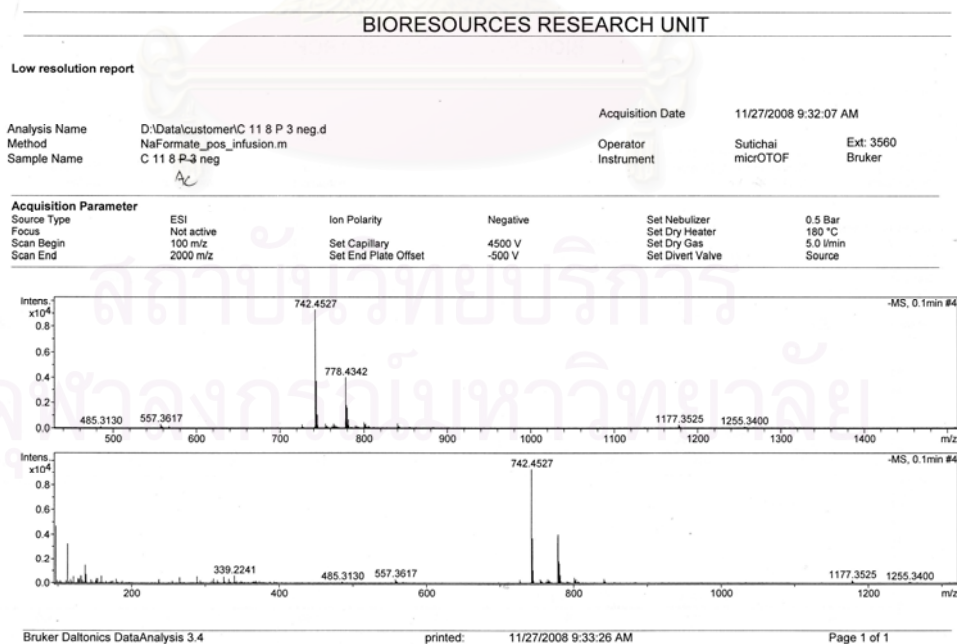
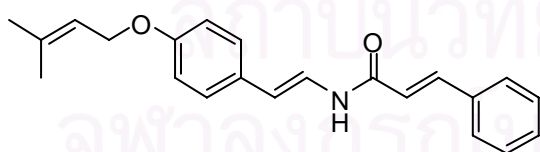


Figure S-4.18 Mass spectrum of corchoruside A nonacetate (**16a**).

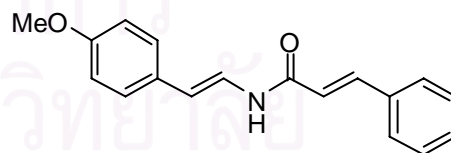
CHAPTER V

CONCLUSION

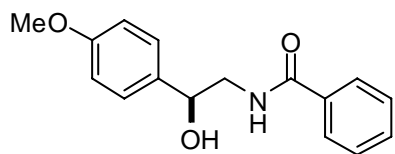
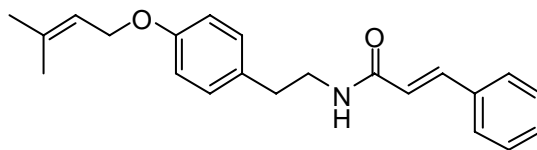
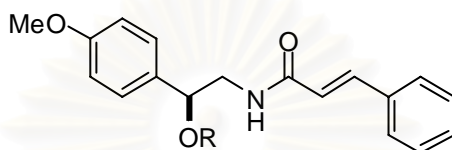
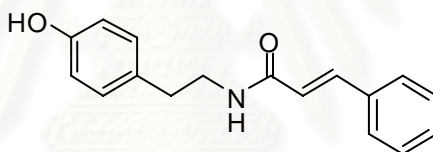
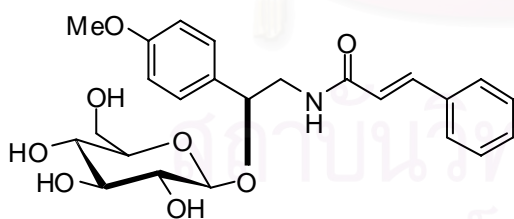
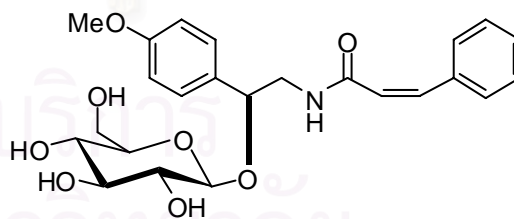
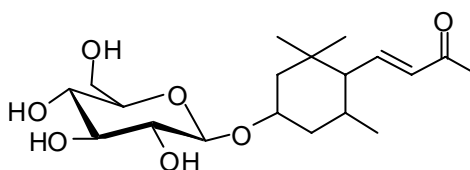
In search of α -glucosidase inhibitors from medicinal plants, bioactive principles from leaves of *Aegle marmelos* and *Corchorus olitorius* were identified. The isolation of the CH_2Cl_2 extract and MeOH extracts from the leaves of *Aegle marmelos* afforded fifteen compounds, which consisted of alkaloids and flavonoids. Three novel phenylethyl cinnamiades named anhydromarmeline (**1**), aegelinosides A (**7**) and aegelinosides B (**8**) were identified, along with eight known compounds anhydroaegeline (**2**), (-)-tembamide (**3**) dehydroaegeline (**4**), (-)-aegeline (**5**), (-)-*O*-methylether aegeline (**6**), alangionosides L (**9**), *N*-2-ethoxy-2-(4-methoxyphenyl)ethyl-cinnamide (**10**) and *N*-(2-(4-Hydroxyphenyl) ethyl)-cinnamide (**11**). In addition, four known flavonoids such as kaempferol-3-*O*-(6''-*O*- α -rhamosyl)- β -glucoside (**12**), kaempferol-3,7-*O*- α -dirhamnopyranoside (**13**), quercetin-3-*O*-(6''-*O*- α -rhamosyl)- β -glucoside (**14**) and quercetin-3,7-*O*- α -dirhamnopyranoside (**15**) were also isolated (Figure 5.1). The isolation of MeOH extract from the leaves of *Corchorus olitorius*, yielded two new flavonoids named corchorusides A (**16**) and B (**17**) together with a known triterpenoid named capsugenin-25,30-*O*- β -diglucoopyranoside (**18**). The structures of all isolated substances from leaves of *A. marmelos* and *C. olitorius* were summarized in Figure 5.1 and 5.2, respectively.

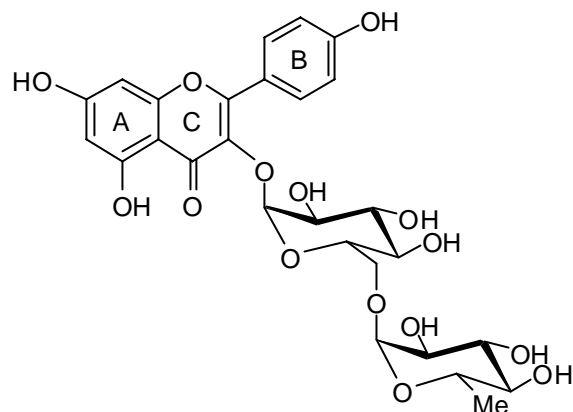


Anhydromarmeline (**1**, new compound)

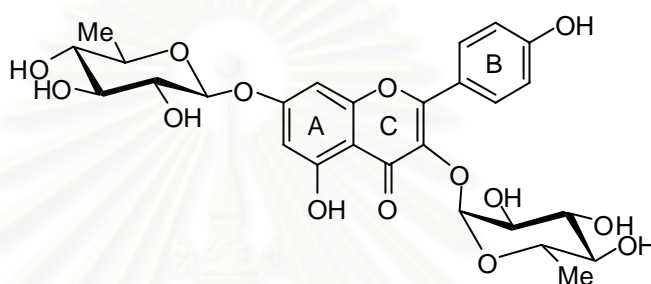


Anhydroaegeline (**2**)

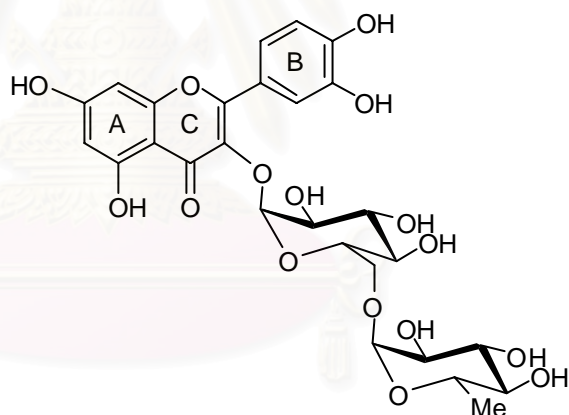
(-)-Tembamide (**3**)Dehydroaegeline (**4**)(-)-Aegeline (**5**); R = H(-)-*O*-Methylether aegeline (**6**); R = Me*N*-2-Ethoxy-2-(4-methoxyphenyl)ethyl-cinnamide (**10**); R = Et*N*-(2-(4-Hydroxyphenyl)ethyl)-cinnamide (**11**)Aegelinosides A (**7**, new compound)Aegelinosides B (**8**, new compound)Alangionosides L (**9**)



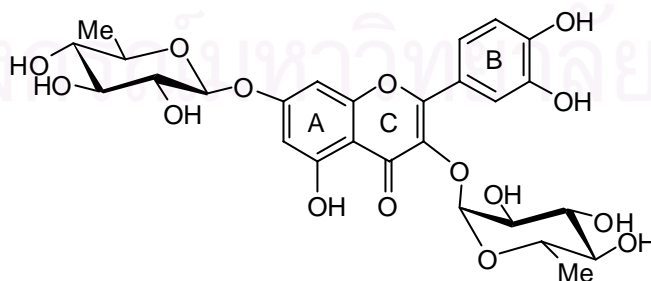
Kaempferol-3-*O*-(6''-*O*- α -rhamosyl)- β -glucoside (**12**)



Kaempferol-3,7-*O*- α -dirhamnopyranoside (**13**)



Quercetin-3-*O*-(6''-*O*- α -rhamosyl)- β -glucoside (**14**)



Quercetin-3,7-*O*- α -dirhamnopyranoside (**15**)

Figure 5.1 The chemical structures of isolated compounds from *Aegle marmelos* leaves.

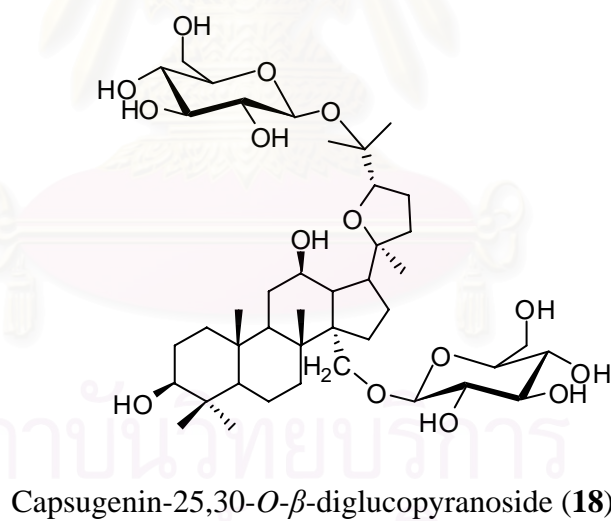
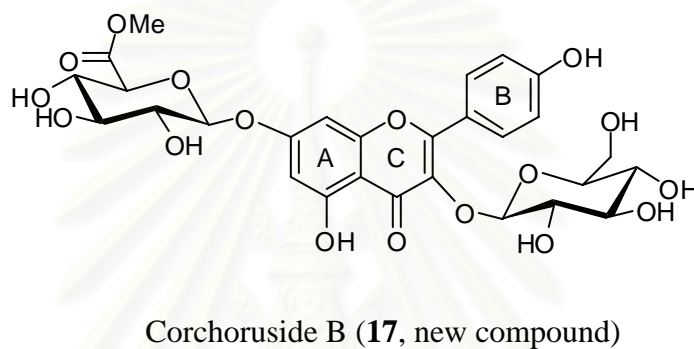
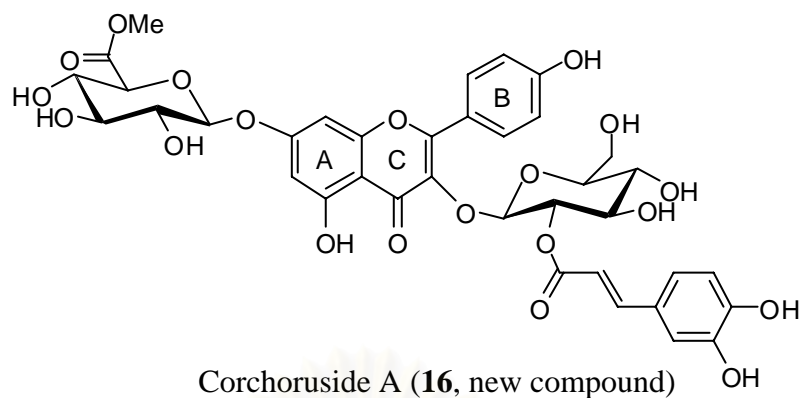


Figure 5.2 The chemical structures of isolated compounds from *Corchorus olitorius* leaves.

The inhibitory activity against α -glucosidase enzyme of compounds isolated from *Aegle marmelaos* leaves was evaluated using colorimetric method. Quercetin-3-*O*-(6''-*O*- α -rhamosyl)- β -glucoside (**14**), and quercetin-3,7-*O*- α -dirhamnopyranoside (**15**) exhibited the most effective activity with IC_{50} values of 0.34 and 0.46 mM, respectively. Although compound **15** was slightly less activity than compound **14**, this compound was found to have higher inhibitory effect than acarbose[®] (IC_{50} 0.62 mM) but showed slightly less than DNJ (IC_{50} 0.17 mM). On the other hand, kaempferol-3-*O*-(6''-*O*- α -rhamosyl)- β -glucoside (**12**) and kaempferol-3,7-*O*- α -dirhamnopyranoside (**13**) revealed moderate inhibition with IC_{50} values of 0.62 and 0.77 mM, respectively. Of phenylethyl cinnamides, *N*-(2-(4-hydroxyphenyl) ethyl)-cinnamide (**11**) showed the strongest activity with IC_{50} value of 2.41 mM.

Investigation of α -glucosidase inhibitors from *C. olitorius* leaves yielded corchoruside A (**16**) as the most active inhibitor (IC_{50} 0.18 mM) , which was as potent as a positive control DNJ (IC_{50} 0.17 mM) . Obviously, corchoruside B (**17**), a congener of **16** consisting no caffeoyl moiety, displayed reduced inhibition; however **17** and acarbose[®] had the same level of inhibition. Of isolated compounds, triterpenoid glycosides including **18** showed weak inhibitory effect or were inactive toward α -glucosidase.

REFERENCES

- Adisakwattana, S.; Sookkongwaree, K.; Roengsumran, S.; Petsom, A.;
Ngamrojnavanich, N.; Chavasiri, W.; Deesamer, S. and Yibchok-anun, S.
Structure-activity relationships of *trans*-cinnamic acid derivatives on
 α -glucosidase inhibition. Bioorg. Med. Chem. Lett. 14 (2004): 2893-2896.
- Aoyama, Y. Baicalein, an α -glucosidase inhibitors from *Scutellaria baicalensis*.
J. Nat. Prod. 61 (1998): 1413-1415.
- Azuma, K.; Nakayama, M.; Koshioka, M.; Ippoushi, K.; Yamaguchi, Y. Kohata, K.
Yamaychi, Y.; Ito, H. and Higashio, H. Phenolic antioxidants from leaves of
Corchorus olitorius L. J. Agric. Food Chem. 47 (1999): 3963-3966.
- Basu, D. and Sen, R. Alkaloids and coumarins from root-bark of *Aegle marmelos*.
Phytochemistry 13 (1974): 2329-2330.
- Bhattacharai, N. K. Folk medicinal use of plants for respiratory complaints in central
Nepal. Fitoterapia 64 (1993): 163-169.
- Bischoff, H. Pharmacology of alpha-glucosidase inhibition. Eur. J. Clin. Invest. 24
(1994): 3-10.
- Bridges, C. G.; Brennan, T. M.; Taylor, D. L.; McPherson, M. and Tyms, A. S.
The prevention of cell adhesion and the cell-to-cell spread
castanospermine (MDL 28574). Antivir. Res. 25 (1994): 169-175.
- Chatterjee, A.; Sen, R. and Ganguly, D. Aegelinol, a minor lactonic constituent of
Aegle marmelos. Phytochemistry 17 (1978): 328-329.
- Chen, H.; Feng, R.; Guo, Y.; Sun, L. and Jiang, J. Hypoglycemic effect of aqueous
extracts of *Rhizoma polygonati odorati* in mice and rats. J. Ethnopharmacol.
74 (2001): 225-229.
- Das, A.V.; Padayatti, P. S. and Paulose, C. S. Effect of leaf extract of *Aegle*
marmelose (L) Correa ex Roxb. on histological and ultrastructural changes in
tissues of streptozotocin induced diabetic rats. Indian J. Exp. Biol. 34 (1996):
341-345.
- Fico, G.; Braca, A.; Morelli, I. and Tome, F. Flavonol glycosides from *Aconitum*
vulparia. Fitoterapia 74 (2003): 420-422.

- Fischer, P. B.; Karlsson, G. B., Dwek, R. A. and Platt, F. M. Butyleoxynojirimycin mediated inhibition of HIV entry correlates with impairment of gp 120 shedding and gp41 exposure. J. Virol. 70 (1996): 7153-7160.
- Florence, J.A. and Yeager, B.F. Treatment of type 2 diabetes. Am. Fam. Physician. 59 (1999): 2835-2925.
- Gao, H.; Huang, Y. N.; Xu, P. Y. and Kawabata, J. Inhibitory effect on α -glucosidase by the fruits of *Terminalia chebula* Retz. Food Chem. 105 (2007): 628-634.
- Govindachari, T. R. and Premila, M. S. Some alkaloids from *Aegle marmelos*. Phytochemistry 22 (1983): 755-757.
- Grover, J. K.; Yadav, S. and Vats, V. Medicinal plants of India with antidiabetic potential. J. Ethnopharmacol. 81 (2002): 81-100.
- Hasan, C. M.; Islam, A.; Ahmed, M.; Ahmed, M. D. and G, P. Capsugenin, a dammarane triterpene from *Corchorus capsularis*. Phytochemistry 23 (1984): 2583-2587.
- Heacock, P. M. Effects of a medical food containing anherbal alpha-glucosidase inhibitor on post-prandial glycemia and insulinemia in healthy adults. J. Am. Dietetic Assoc. 105 (2005): 65-71.
- Innami, S.; Ishida, H.; Nakamura, K.; Kondo, M.; Tabata, K.; Koguchi, T.; Shimizu, J. and Furusho, T. Jew's Mellow (*Corchorus olitorius*) suppress elevation of postprandial blood glucose levels in rats and humans. Int. J. Vitam. Nutr. 75 (2005): 39-46.
- Jagetia, G. C.; Venkatesh, P. and Baliga, M. S. Fruit extract of *Aegle marmelos* protects mice against radiation-induced lethality. Integrat. Cancer Ther. 3 (2004): 323-332.
- Kamalakkannan, N. and Prince, S. M. Hypoglycaemic effect of water extracts of *Aegle marmelos* fruits in streptozotocin diabetic rats. J. Ethnopharmacol. 87 (2003): 207-210.
- Kawabata, J.; Mizuhata, K.; Sato, E.; Nishioka, T., Aoyama, Y. and Kasai, T. 6-Hydroxyflavonoids as α -glucosidase inhibitors from marjoram (*Origanum majorana*) leaves. Biosci. Biotechnol. Biochem. 67 (2003): 445-447.
- Kawaguchi, M.; Tanabe, H. and Nagamine, K. Isolation and characterization of a novel flavonoid possessing a 4, 2"-glycosidic linkage from green mature acerola (*Malpighia emarginata* DC.) fruit. Biosci. Biotechnol. Biochem. 71 (2007): 1130-1135.

- Lee, S. S.; Lin, H. C. and Chen, C. K. Acylated flavonol monorhamnosides, α -glucosidase inhibitors from *Machilus philippinensis*. Phytochemistry 69 (2008): 2347-2353.
- Li, W. L.; Zheng, H. C.; Bukuru, J. and De Kimpe, N. Natural medicines used in the traditional Chinese medicinal system of therapy of diabetes mellitus. J. Ethnopharmacol. 92 (2004): 1-21.
- Liu, X.; Wei, J.; Tan, F.; Zhou, S.; Wurthwein, G. and Rohdewald, P. Antidiabetic effect of Pycnogenol French maritime pine bark extract in patients with diabetes type II. Life Sci. 75 (2004a): 2505-2513.
- Liu, X.; Zhou, H. J. and Rohdewald, P. French maritime pine bark extract Pycnogenol dose-dependently lowers glucose in type 2 diabetic patients. Diab. Care. 27 (2004b): 839.
- Manandhar, M. D.; Shoeb, A.; Kapil, R. S. and Popli, S. P. New alkaloids from *Aegle marmelos*. Phytochemistry 17 (1978): 1814-1815.
- Manandham, N. P. A survey of medicinal plants of Jaarkot district, Nepal. J. Ethnopharmacol. 48 (1995): 1-6.
- Matsui, T.; Ebuchi, S.; Matsugano, K.; Terahara, N. and Matsumoto, K. Caffeoylsophorose, a new natural α -glucosidase inhibitor, from red vinegar by fermented purple-fleshed sweet potato. Biosci. Biotechnol. Biochem. 68 (2004): 2239-2246.
- Matsui, T.; Ueda, T.; Oki, T.; Sugita, K.; Terahara, N. and Matsumoto, K. α -Glucosidase inhibitory action of natural acylated anthocyanins. 2. α -glucosidase inhibition by isolated acylated anthocyanins. J. Agric. Food Chem. 49 (2001): 1952-1956.
- Matsunoto, M.; Matsukawa, N.; Mineo, H.; Chiji, H. and Hara, H. A soluble flavonoid-glycoside, α -g-rutin, is absorbed as glycosides in the isolated gastric and intestinal mucosa. Biosci. Biotechnol. Biochem. 68 (2004): 1929-1934.
- Melo, E. B.; Gomes, A. S. and Carvalho, I. α and β -Glucosidase inhibitors: chemical structure and biological activity. Tetrahedron 62 (2006): 10277-10302.
- Mulinaacci, N.; Vincieri, F. F.; Baldi, A.; Bambagiotti-Alberti, M.; Sendl, A. and Wagner, H. Flavonol glycosides from *Sedum telephium* subspecies Maximum leaves. Phytochemistry 38 (1995): 531-533.

- Muruganandan, S. Mangiferin protects the streptozotocin induced oxidative damage cardiac and renal tissues in rats. Toxicology 176 (2002): 165-173.
- Nakamura, T.; Goda, Y.; Sakai, S.; Kondo, K.; Akiyama, H. and Toyoda, M. Cardenolide glycosides from seeds of *Corchorus olitorius*. Phytochemistry 49 (1998): 2097-2101.
- Nishioka, T.; Kawabata, J. and Aoyama, Y. Baicalein, an α -glucosidase inhibitor from *Scutellaria baicalensis*. J. Nat. Prod. 61 (1998): 1413-1415.
- Ponnachan, P. T. C.; Paulose, C. S. and Panikkar, K. R. Hypoglycaemic effect of alkaloid preparation from leaves of *Aegle marmelos*. Amala. Res. Bull. 13 (1993a): 37-41.
- Ponnachan, P. T. C.; Paulose, C. S. and Panikkar, K. R. Effect of leaf extract of *Aegle marmelos* in diabetic rats. Ind. J. Exp. Biol. 31 (1993b): 345-347.
- Rhabasa-Lhoret, R. and Chiasson, J., 3rd ed. Alpha-glucosidase inhibitors. In R. A. Defronzo, E.; Ferrannini, H.; Keen and P. Zimmet (eds.). International textbook of diabetes mellitus (vol. 1). UK: John Wiley, 2004.
- Samarasekera, J. K. R. R.; Khambay, B. P. S. and Hemalal, K. P. A new insecticidal protolimonooid from *Aegle marmelos*. Nat. Prod. Res. 18 (2004): 117-122.
- Sharma, B. R.; Rattan, R. K. and Sharma, P. Marmeline, an alkaloid, and other components of unripe fruits of *Aegle marmelos*. Phytochemistry 20 (1981): 2606-2607.
- Schäfer, A and Högger, P. Oligomeric procyanidins of French maritime pine bark extract (Pycnogenol[®]) effectively inhibit α -glucosidase. Diabetes Research and Clinical Practice 77 (2007): 41-46.
- Seo, E. J.; Curtis-Long, M. J.; Lee, B. W.; Kim, H. Y.; Ryu, Y. B.; Jeong, T. S.; Lee, W. S. and Park, K. H. Xanthenes from *Cudrania tricuspidata* displaying potent α -glucosidase inhibition. Bioorg. Med. Chem. Lett. 17 (2007): 6421-6424.
- Shoeb, A.; Kapil, R. S. and Popli, S. P. Coumarins and alkaloids of *Aegle marmelos*. Phytochemistry 12 (1973): 2071-2072.
- Shibano, M.; Kakutani, K.; Taniguchi, M.; Yasuda, M. and Baba, K. Antioxidant constituents in the dayflower (*Commelina communis* L.) and their α -glucosidase-inhibitory activity. J. Nat. Med. 62 (2008): 349-353.
- Shoba, F. G. and Thomas, M. Study of antidiarrhoeal activity of four medicinal plants in castor-oil induced diarrhea. J. Ethnopharmacol. 76 (2001): 73-76.

- Shrestha, I. and Joshi, N. Medicinal plants of the Lete village of Lalitpur district, Nepal. Int. J. Pharm. 31 (1993): 130-134.
- Singab, A. N. B.; El-Beshbishy, H. A.; Yonekawa, M.; Nomura, T. and Fukai, T. Hypoglycemic effect of Egyptian *Morus alba* root bark extract: Effect on diabetes and lipid peroxidation of streptozotocin-induced diabetic rats. J. Ethnopharmacol. 100 (2005): 333-338.
- Wang, M.; Kikuzaki, H.; Csiszar, K.; Boyd, C. D. Maunakea, A.; Fong, S. F. T.; Ghai, G.; Rosen, R. T.; Nakatani, N. and Ho, C. T. Novel trisaccharide fatty acid ester identified from the fruits of *Morinda citrifolia* (Noni). J. Agric. Food Chem. 47 (1999): 4880-4882.
- Wild, S.; Roglic, G.; Green, A.; Sicree, P. and King, H. Global prevalence of diabetes. Estimates for the year 2000 and projections 2030. Diab. Care. 27 (2004): 1047-1053.
- World Health Organization. Available from: [http:// www.who.org](http://www.who.org). (2006, April).
- Yasuda, K.; Shimowada, K.; Uno, M; Odaka, H.; Adachi, T.; Shihara, N.; Suzuki, N.; Tamon, A.; Nagashima, K.; Hosokawa, M.; Tsuda, K. and Seino, Y. Long-term therapeutic effects of voglibose, a potent intestinal alpha-glucosidase inhibitor, in spontaneous diabetic GK rats Diabetes Res. Clin. Pract. 59 (2003): 113-122.
- Yoshikawa, M.; Murakami, T.; Shimada, H.; Matsuda, H.; Yamahara, J. and Tanabe, G. and Muraoka, O. Salacinol, potent antidiabetic principle with unique thiosugar sulfonium sulfate structure from the Ayurvedic traditional medicine *Salacia reticulata* in Sri Lanka and India. Tetrahedron Lett. 38 (1997): 8367-8370.
- Yoshikawa, M.; Murakami, T.; Yashiro, K. and Matsuda, H. Kotalanol, a potent α -glucosidase inhibitor with thiosugar sulfonium sulfate structure, from antidiabetic medicine *Salacia reticulata*. Chem. Pharm. Bull. 46 (1998): 1339-1340.
- Zakaria, Z. A.; Somchit, M. N.; Zaiton, H.; Mat-Jais, A. M., Sulaiman, M. R.; Farah, W. O.; Nazratulmawarina, R. and Fatimah, C. A. The in vitro antibacterial activity of *Corchorus olitorius* extracts. Int. J. Pharm. 2 (2006): 213-215.

VITA

Ms. Thanchanok Puksasook was born on June 20, 1983 in Nakhon Pathom province, Thailand. She graduated with Bachelor's Degree of Science in Biology (second class honors) from Faculty of Science, Silpakorn University, in 2005. During studying in Master Degree in Biotechnology program, she received the 90th Anniversary of Chulalongkorn University Fund and TRF-Master (MAG Window II) Research Grants of Thailand Research Fund.



สถาบันวิทยบริการ
จุฬาลงกรณ์มหาวิทยาลัย